KINETIC, BIOCHEMICAL, AND GENETIC ANALYSIS OF THE PARTICULATE METHANE MONOOXYGENASE

Thesis by

Jeremy D. Semrau

In Partial Fulfillment of the Requirements

for the Degree of

Doctor of Philosophy

California Institute of Technology

Pasadena, California

1995

(Submitted June 28, 1994)

ACKNOWLEDGEMENTS

There are a great number of people that I must thank, none so important as my advisor, Dr. Mary E. Lidstrom. Without her guidance my thesis wouldn't be half of what is presented here. Thanks, Mary, I owe you a Sprecher. I also must thank Dr. Sunney I. Chan. Without his assistance and willingness to teach an engineer biochemistry, I would not have figured out what the hell copper does in the methane monooxygenase.

Beyond the obvious people I must acknowledge, I now have the difficult task of sorting through all the people who have helped me enjoy myself at Caltech. I have to start by mentioning my housemates at 1170 Steuben - Don, Dave, Bryan, Bob, and Laszlo. It was always fun to have a party to go home to when you really needed it. Although the trips to the emergency room were a bit much...

Speaking of emergency rooms, I have to thank all the medical personnel who kept my body in one piece the past 6 years. Dr. Cathleen Godzik and Dr. Richard Lis tried their best to keep my wrist whole, but they weren't dealing with just any patient. I also have to thank the folks at Huntington Memorial Hospital for bandaging and stitching my injuries, of which there were too many. For those students who may read this and not know what I speak, let me just say it is possible to have too good a time at Caltech. Strange, but true.

As for the people who helped me wreck my body, I have to start with Eric Belz. Dude, the midnight monster mountain bike rides up to Mt. Wilson were fun, but a little tough on my wrist, especially when you go up without a headlight. Scott May was an excellent rock climbing partner and it was hilarious to jump out of a plane with Brent.

Who knew falling two miles could be so much fun? Ron Siefert showed me how to ride in the desert at night, although I wish he hadn't used my unsuspecting body as a launch pad to (unsuccessfully) jump over a fire pit, complete with fire. Mike Hannigan was a excellent drinking buddy and a good friend. Hang tough, you'll get out next.

I can't complete this without mentioning all those women in my life. Mila, Tina, Karin, Kelly G., Andria, and Christine among all the others were great friends and generally kept me sane while I was here. Linda was especially nice in keeping me fed and filled with beer.

Penultimately I'd like to thank those who showed me how it's done. Steve Rogak, Mark Schlautman, Mike Scott, Rob Harley, and Anne Marie Eldering were all great inspirations. See you on the outside.

And finally, I want to mention my family. I have to thank Jeff for being the ideal evil twin, Jim for always reminding me how good Texas cuisine is, and Sis for putting up with three brothers for so long. Of course, I can't forget my mom. She had the patience of a saint (up until Jeff and I started learning how to get into trouble). Lastly, I want to dedicate my thesis to my father:

James E. Semrau, Sr.

1937-1988.

'Nuff said.

ABSTRACT

The partiuculate methane monooxygenase (pMMO) is expressed by all known methanotrophs and may be very useful for the degradation of small halogenated hydrocarbons such as trichloroethylene (TCE). The pMMO, however, is poorly understood and much work is needed to determine the usefulness of this enzyme for the degradation of wastes both in-situ and in above-ground treatment reactors. In this thesis, the kinetics, biochemistry, and genetics of the pMMO are examined. The research indicates that copper plays a major role in the kinetics of both TCE and methane oxidation by the pMMO. Furthermore, by correlating activity assays, metal analysis, and electron paramagnetic resonance spectroscopy, we have concluded that copper makes up the active site of the pMMO, and that multiple active sites may exist on the pMMO. Finally, genetic analysis of chromosomal DNA from several methanotrophs indicates that two copies of the pMMO exist. Data suggest the products of these gene copies may be different, and that they might be affected by the amount of bioavailable copper.

Table of Contents

List of Figures

List of Tables

Chapter 1

Introduction to Biodegradation of Trichloroethylene

Humans have continually tried to increase their standard of living through innovative technologies and practices. Due to the industrial complex created during World War II, compounds such as organic solvents, pesticides, plastics, and dyes have been mass-produced. Their extensive utilization, however has produced wide-spread pollution problems in the environment due to inadequate storage, improper disposal, and accidental spills. For example, Figure 1.1 shows the location of industrial sites with at least one liquid-waste disposal site in the United States. Many of these sites, although built and maintained according to then-existing regulations, inadequately contain the waste(s). As these sites are frequently near urban areas, contamination of groundwater can occur. In a random survey conducted in 1984, 21% of drinking water obtained from groundwater was found to be contaminated with organic, xenobiotic pollutants (1). This is a serious problem as approximately 50% of the US population relies on aquifers for their drinking water (2).

One of the most commonly reported contaminants in the United States is trichloroethylene (TCE) (1). Like many organic contaminants, TCE sorbs onto the soil matrix, making it unfeasible to remove using current pump-and-treat remediation methods. It is estimated that the time scales for pump-and-treat remediation for an ideal homogeneous aquifer are on the order of 100 years to decrease pollutant concentrations by a factor of 100 (3, 4, 5). Any treatment scheme involving removal of the waste for above-ground remediation can be both financially prohibitive and lengthy. Therefore, the most economical treatment may be in situ treatment. In situ treatment would necessitate the introduction of a chemical or biological catalyst that could transform the waste(s) into less harmful products. For TCE degradation, biodegradation has been examined using a variety of systems (6). It is the objective of this report to examine the parameters affecting the ability of a select group of bacteria, methane-oxidizing bacteria, methanotrophs, to consume TCE.

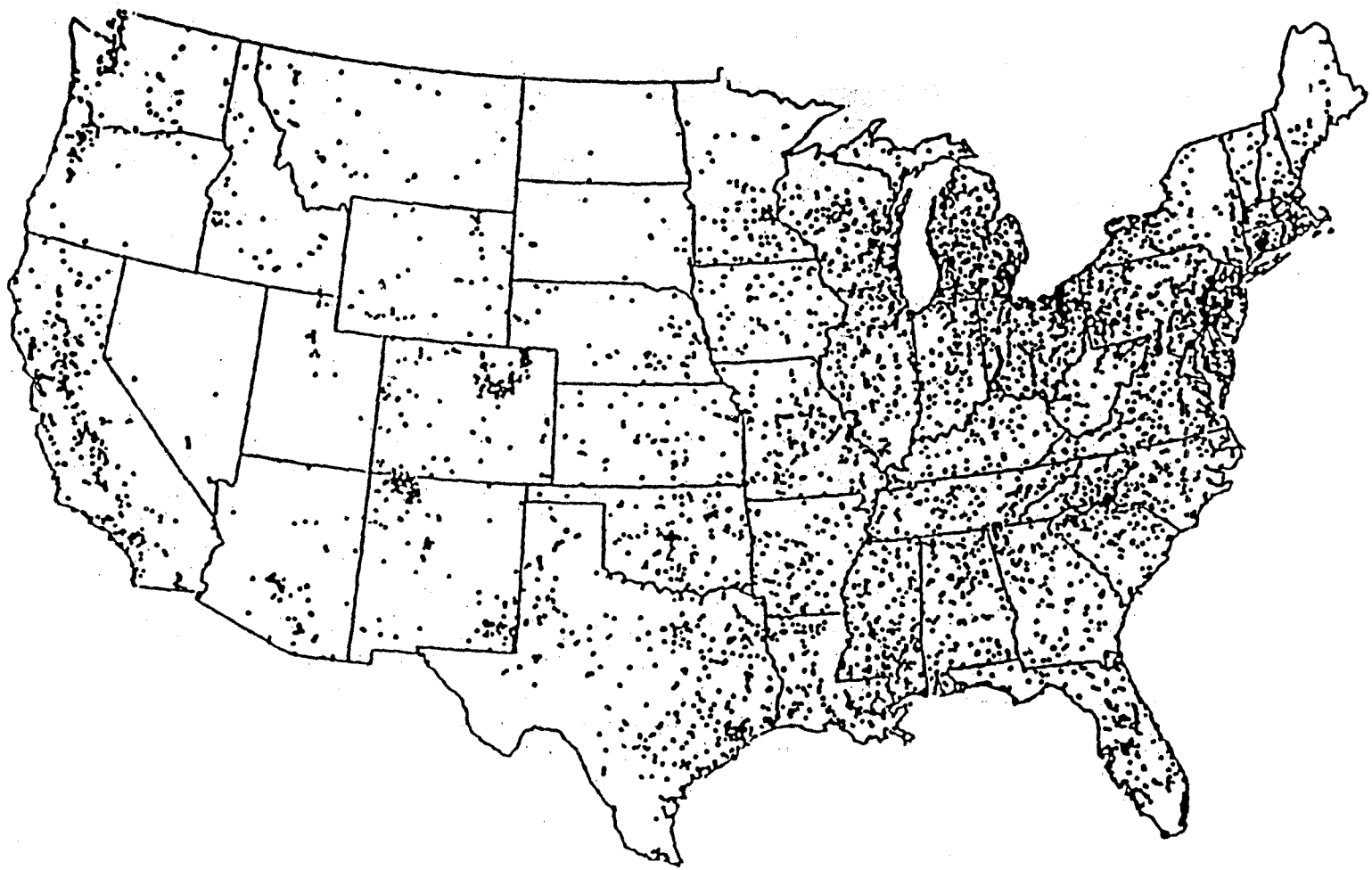

Figure 1.1. Industrial sites with at least one liquid disposal area (From USEPA. Office of Drinking Water, 1980).

1.1 HISTORY OF BIOREMEDIATION

Bioremediation, the use of biological systems for the removal of undesirable substances has been used for many years, most significantly in the treatment of wastewater. The utilization of naturally occurring microorganisms including both prokaryotic and eukaryotic cells has been quite useful in the removal of organic wastes generated by humans. As the industrial capacity of many nations increased, however, the wastes generated by these societies soon overtaxed the capacity of ecosystems to remove them. The persistence of many of the new, synthetic compounds used to develop a better standard of living created both human and environmental health hazards.

Historically, accidental spills and improper storage of crude oil and its refined products have been among the most prevalent hazardous substances found in the environment. Bioremediation has been successfully applied for the removal of these compounds (7). Many schemes ranging from the introduction of genetically engineered microorganisms to enhance the range and extent of degradation to addition of fertilizer to increase natural populations have been attempted. Although with the introduction of non-native microorganisms it is difficult to prove whether the released cells are the catalysts for hydrocarbon degradation or are simply an indirect source of nitrogen and phosphorous, the attempts still show an enhanced decrease in the concentration of hydrocarbons.

With the success of bioremediation for hydrocarbon removal, attention has focused on the feasibility of using microbial systems for the degradation of more recalcitrant compounds such as pesticides and chlorinated solvents. Unlike the degradation of the hydrocarbons comprising crude oil and its refined products, these compounds often cannot be used as the sole source of carbon or energy, i.e., an alternative source of carbon and energy must be provided to maintain microbial

populations if these compounds are to be significantly degraded microbially. This process of *co-metabolism* has become very interesting as many bacterial strains will often fortuitously transform hazardous substances into less harmful compounds.

1.2 TRICHLOROETHYLENE BIODEGRADATION

Trichloroethylene (TCE) is an example of a ubiquitous contaminant that can be co-metabolized both anaerobically and aerobically. As shown in Figure 1.2, under anaerobic conditions TCE is reductively dechlorinated by methanogenic consortia. Anaerobic transformation, however, is undesirable as vinyl chloride, a known carcinogen, is the major end product. Although vinyl chloride has been shown to be further dechlorinated to ethylene, the rate of dechlorination decreases as the extent of dechlorination increases, and the production of ethylene is a very slow process (8).

Aerobic degradation is typically much faster than anaerobic degradation. A variety of microorganisms including toluene oxidizers, propane oxidizers, phenol oxidizers, ammonia oxidizers, and methane oxidizers have been shown to oxidize TCE (6). No aerobic or anaerobic strain, however, has been isolated that can grow using TCE as its sole source of carbon and energy. Continued TCE degradation must be carried out in the presence of a primary substrate, the process of co-metabolism. In the case of TCE co-metabolism, the enzyme that transforms TCE is the same enzyme responsible for the initial oxidation of the growth substrate, e.g., toluene, propane, and methane. To understand and describe the kinetics of TCE degradation it is necessary to also assess the kinetics of consumption of the primary substrate, as it will compete with TCE for binding sites on the enzyme responsible for TCE transformation.

The biodegradation of TCE is further complicated by both substrate and product toxicity. It has been shown for many biological systems that TCE degradation is inhibited above some critical concentration of TCE, possibly due to partitioning of TCE

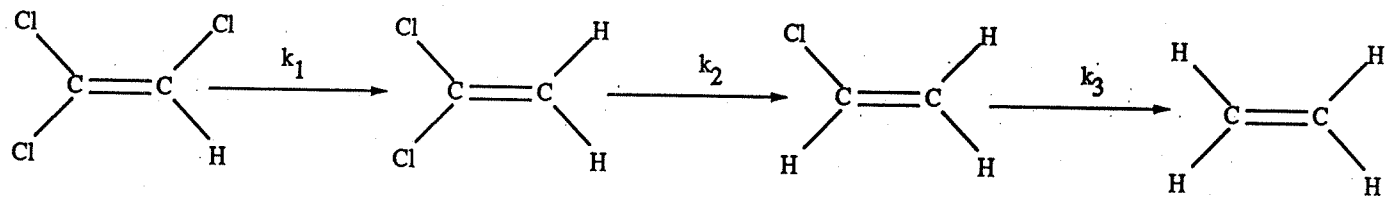

$$k_1 > k_2 > k_3$$

Figure 1.2. Reductive dechlorination of trichloroethylene by methanogenic consortia.

within cell membranes or competition with the primary substrate for enzymatic binding sites. The products of TCE oxidation can also be toxic (9, 10, 11). Cells expressing the soluble form of the methane monooxygenase (sMMO) have been shown to transform TCE into chloral and TCE-epoxide (12). TCE-epoxide is quite unstable in water and has a half-life of 10-20 seconds. When the epoxide ring opens up, it may covalently bind to any nearby electron donor, including cell material such as proteins or lipids. If the amount of covalent binding is sufficient, enzymes are inactivated and biodegradation can be inhibited (11). To understand how TCE and its transformation products can be toxic, it is necessary to consider the physical and chemical properties of TCE.

1.3 PROPERTIES OF TRICHLOROETHYLENE

Trichloroethylene is a colorless, heavy, stable, chlorinated solvent that was first manufactured in Germany at the turn of the century (13). Table 1.1 summarizes the physical and chemical properties of TCE. As shown in the table, TCE is a stable liquid at room temperature, with a boiling temperature of 86.7° C at a pressure of 760 mm mercury. TCE is much denser than water, with a specific gravity of 1.465 at 20° C. The carbon-carbon double bond confers a great deal of stability, making it an ideal solvent with a long shelf life. TCE is also practically insoluble in water, with solubility of 1100 ppm at 25° C.

Despite the attractive properties of TCE, its initial use as a degreaser was later supplanted by carbon tetrachloride. During World War II, however, TCE use increased dramatically as a degreaser of machinery parts. TCE is an ideal degreaser as it has high solvency for oils, greases, and tars found in the metal-processing industry but will not corrode steel, copper, or zinc (14). Furthermore, TCE is non-flammable and non-explosive at room temperature. Its use continued to increase when the main stabilizer, an alkaline reacting amine, was replaced with a neutral one and its use

Table 1.1. Properties of trichloroethylene

Molecular weight	131.40
Density at 20 °C (g/cm3)	1.4649
Melting point (°C)	-84.8
Boiling point at 760 mm Hg (°C)	86.7
Solubility in water at 25 °C (mg/l)	1100
Vapor pressure at 25°C (mm Hg)	69.0
Log octanol/water partition coefficient	2.42
EPA drinking water standard (ppb)	5 (38 nM)
Priority pollutant (EPA)	
Hazardous substance and waste (EPA)	
Suspected carcinogen (IARC)	

expanded to the manufacture of semiconductors, paints, and inks. Over 155,000 pounds of TCE are used annually in the United States (15). Although the stability of TCE makes it an excellent degreaser and solvent, its stability also makes it very refractory and difficult to remove from the environment. Due to its persistence, TCE can be transported great distances in aquifers over time. In a random survey TCE has been detected in 6% of drinking water supplies obtained from groundwater in the US (1).

The problem of TCE pollution is acerbated by the severe toxicological effects of chronic and acute exposure. In 1976, TCE was discovered to cause cancerous tumors by the National Cancer Institute (16). TCE has also been found to affect the heart, liver, skin and kidneys. Due to the health effects of TCE, it is considered by the US Environmental Protection Agency (EPA) to be a hazardous waste and a priority toxic pollutant. It is unclear how much of the toxicity of TCE is intrinsic and how much is due to its transformation products. The high solvency of TCE for oils, waxes and fats can cause skin irritations (17). The products of TCE oxidation can be more hazardous, however. Cytochrome-P-450, an oxygenase found in mammalian systems may form products similar to the sMMO, TCE-epoxide and chloral. As in the bacterial system, after the epoxide ring is opened, TCE-epoxide may bind covalently to cell proteins, leading to cell damage. Chloral can also have deleterious effects and is known to produce skin tumors and decrease kidney and liver function.

Because TCE is a refractory, hazardous waste that is a suspected carcinogen, the drinking water standard has been established at 5 ppb, or approximately 38 nM. This low standard can be very difficult to achieve, particularly in contaminated aquifers. TCE is very hydrophobic and will adsorb strongly to the groundwater matrix, making above-ground treatment unfeasible. Because of their ubiquity in nature and ability to

degrade chlorinated solvents, methanotrophs have been proposed as one possibility for degrading TCE in situ.

1.4 METHANOTROPHS

Methanotrophs are a group of Gram-negative bacteria that utilize methane as their sole source of carbon and energy. Two general categories of methanotrophs, Type I and II have been identified based on the pattern of internal membranes, carbon assimilation pathway, 16s rRNA sequences, mol% G+C, and predominant fatty acid chain length as outlined in Table 1.2 (18). Type I methanotrophs have stacks of membranes throughout the cytoplasm, while Type II strains have intracytoplasmic membranes in rings throughout the periphery of the cell membrane.

By oxidizing methane to carbon dioxide, methanotrophs obtain energy and reducing equivalents in the form of NADH as shown in Figure 1.3. The first step is the conversion of methane into methanol by the methane monooxygenase (MMO). Two forms of the MMO have been shown to exist, a membrane bound or particulate form (pMMO) and a cytoplasmic or soluble form (sMMO) (19). All known methanotrophs can express the pMMO, which appears to contain copper and can only degrade short-chain aliphatic compounds but most of these do not contain the sMMO (20). The sMMO appears to be restricted mainly to the *Methylococcus* and *Methylosinus* strains, although one example each of a *Methylocystis* and a *Methylomonas* strain containing sMMO have been reported (18, 21, 22, 23, 24, 25, 26). The sMMO contains iron and has a broad substrate range that includes long chain aliphatic compounds and aromatic substances (20). The sMMO has been purified and the genes cloned from *M.capsulatus* Bath and *Methylosinus trichosporium* OB3b (27). The crystal structure of the hydroxylase component of the sMMO has been recently published (28). The pMMO has never been reproducibly purified and little is known

Table 1.2 Characteristics of type I and type II methanotrophs (adapted from 18)

Characteristic	Type I	Type II
Cell Shape	Short rods and cocci	Rod or pear shaped
GC content of DNA (mol%)	50-64	62.5
Membrane arrangement		
Bundles of vesicular disks	Yes	No
Paired membranes aligned to periphery of cell	No	Yes
Resting stages		
Azotobacter-like cysts	Yes	No
Exospore or "lipid" cysts	No	Yes
Rosettes formed	No	Yes
HMP pathway - 3-hexulose phosphate synthase	Present	Absent
Serine cycle - hydroxypyruvate reductase[1]	Absent	Present
Ketoglutarate dehydrogenase and a complete tricarboxylic acid cycle	Absent	Present
Predominant phospholipid fatty acid chain length	16	18

[1]Some portions present in *M. capsulatus* Bath

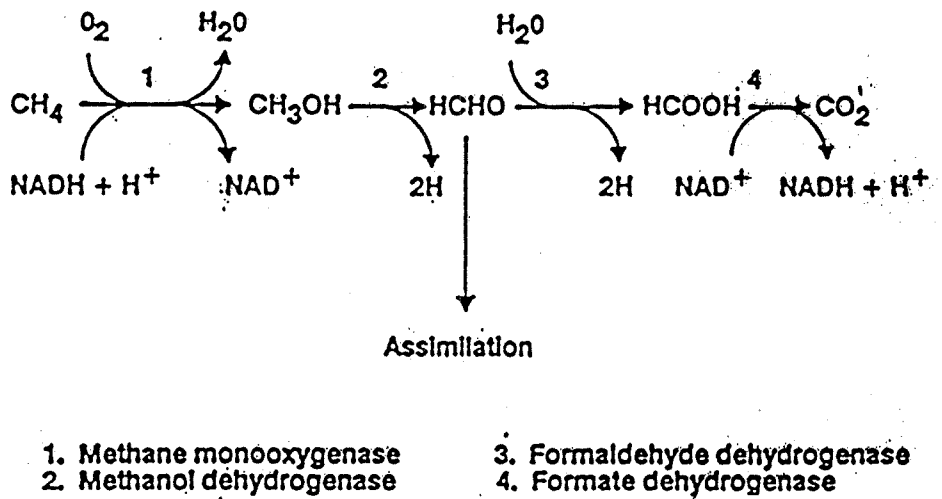

Figure 1.3 Oxidation of methane by methanotrophs.

about its crystal structure (29). Table 2.2 summarizes the different properties of the sMMO and pMMO.

From the detailed studies performed on the sMMO, it has been clearly shown that it can degrade TCE. The proposed transformation pathway is shown in Figure 1.4. As noted previously, the initial products are believed to be the TCE-epoxide and chloral. Both products can inhibit further TCE oxidation due to their toxicity. Furthermore, TCE oxidation requires a source of reducing equivalents in the form of NADH, but only a small amount of NADH is reformed per TCE oxidized (Figure 1.3). Therefore TCE oxidation may decrease in the absence of a primary substrate even if product toxicity is not significant.

TCE is also oxidized by the pMMO, but at much lower rates than the sMMO (11, 23, 30, 31, 32). Although TCE oxidation by the purified pMMO has not been studied, the same products are made as when TCE is oxidized by the sMMO. This conclusion is based on consumption studies using ^{14}C-TCE and GC/MS analysis for chlorinated compounds. TCE oxidation by the pMMO has been observed using purified membranes, but in this case the rates of TCE oxidation were not measured (30). To effectively utilize methanotrophs for the degradation of TCE, it is necessary to provide both methane and TCE to the cell. This creates competition for binding sites on the pMMO. To fully understand TCE oxidation, the affinity of methane uptake must first be examined.

Another important factor in understanding co-metabolism of TCE is copper availability. It is well-known that copper plays a key role in the expression of the MMO (19). The strains that can express both forms of the MMO produce the pMMO predominantly under high copper/biomass ratios while the sMMO is formed under low copper/biomass ratios. What has not been previously observed is the effect of copper on cells expressing the pMMO. In this study, the effect of copper on the ability of

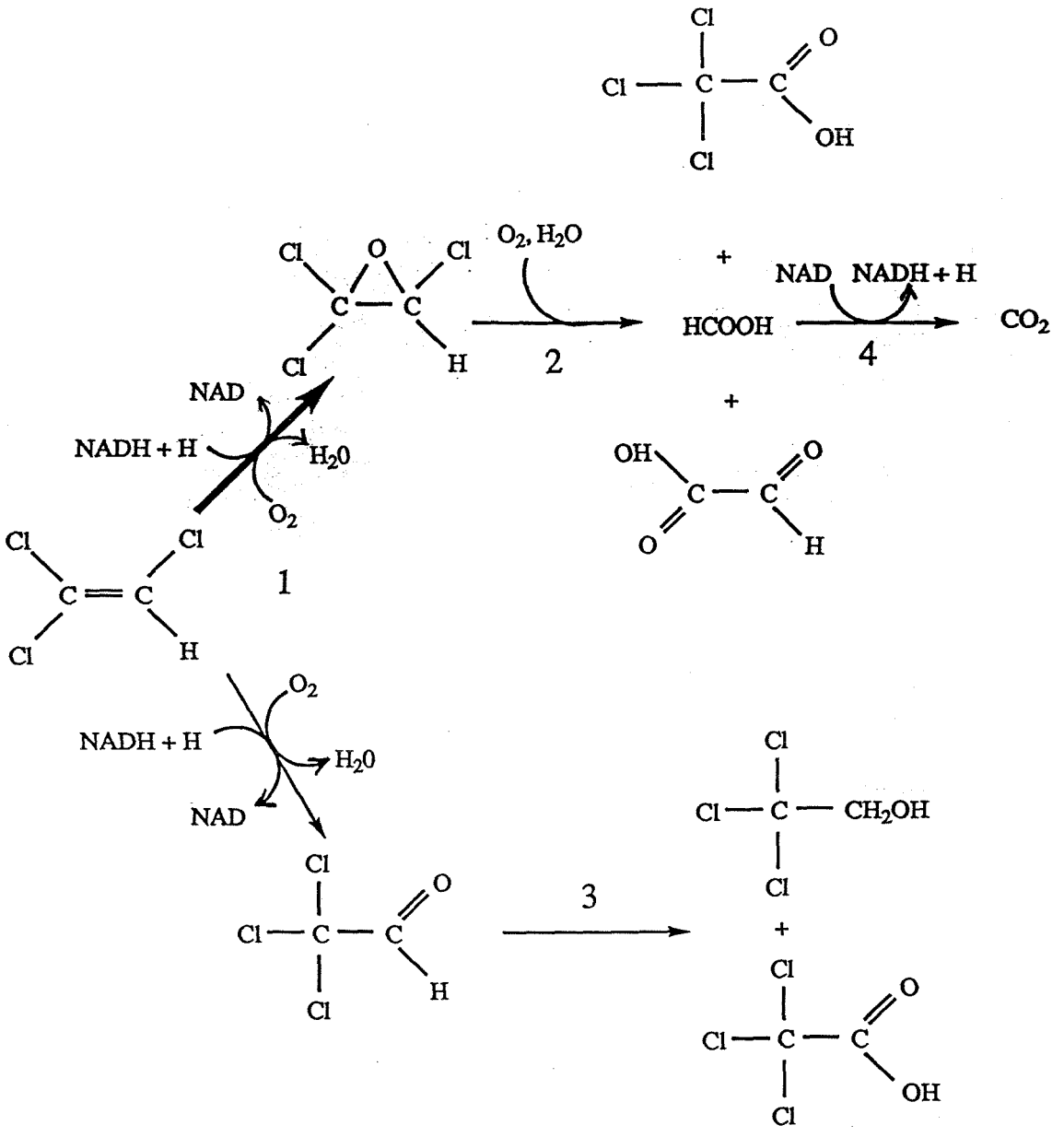

1. Soluble methane monooxygenase
2. Spontaneous abiotic hydrolysis and oxidation reactions
3. Unknown biotic transformations
4. Formate dehydrogenase

Figure 1.4. Aerobic transformation of trichloroethylene by the sMMO in whole cells. Approximately 6-16% of TCE is converted to chloral and 84-94% is converted into TCE-epoxide.

methanotrophs to oxidize methane and TCE using the pMMO is examined at the whole-cell level. First the consumption of each substrate is examined individually to determine the kinetic parameters of substrate uptake. Second, since TCE oxidation can be limited not only by binding site competition but also by competition for reducing equivalents, the effect of adding an external source of reducing equivalents on TCE oxidation has been examined. Third, membrane preparations have been used to determine the effect of copper on pMMO activity and on the electron paramagnetic resonance spectra and copper/protein ratio. Finally, the gene encoding one of the polypeptides of the pMMO was isolated and sequenced. The information obtained by examining the pMMO at the whole-cell, molecular, and genetic levels is important for the future use of the pMMO both in situ and in above-ground reactors for the removal of trichloroethylene as well as other halogenated hydrocarbons.

1.5 REFERENCES

1. Westrick, J. J., J. W. Mello, and R. F. Thomas. 1984. The groundwater supply survey. J. AWWA. **5**:52-59.

2. Patrick, R., E. Ford, J. Quarles. 1987. Groundwater contamination in the United States, 2nd edition. University of Pennsylvannia Press, Philadelphia.

3. Travis, C. C. 1992. Toxic waste in groundwater: can it be removed? J. NIH Res. **4**:49-51.

4. Travis, C. C. and C. B. Doty. 1990. Can contaminated aquifers at Superfund sites be remediated?. Environ. Sci. Technol. **24**:1464-1466.

5. Olsen, R. L. and M. C. Kavanaugh. 1993. Can groundwater restoration be achieved? Wat. Environ. Technol. March:42-47.

6. Ensley, B. D. 1991. Biochemical diversity of trichloroethylene metabolism. Ann. Rev. Microbiol.. **45**:283-299.

7. Bragg, J. R., R. C. Prince, E. J. Harner, and R. M. Atlas. 1994. Effectiveness of bioremediation from the Exxon Valdez oil spill. Nature. **368**:413-418.

8. Vogel, T. M. and P. L. McCarty. 1985. Biotransformation of tetrachloroethylene to trichloroethylene, dichloroethylene, vinyl chloride, and carbon dioxide under methanogenic conditions. Appl. Environ. Microbiol. **49**:1080-1083.

9. Alvarez-Cohen, L. and P. L. McCarty. 1991. Product toxicity and cometabolic competitive inhibition modeling of chloroform and trichloroethylene transformation by methanotrophic resting cells. Appl. Environ. Microbiol. **57**:1031-1037.

10. Henry, S. M. and D. Grbic-Galic. 1991. Influence of endogenous and exogenous electron donors and trichloroethylene oxidation toxicity on trichloroethylene oxidation by methanotrophic cultures from a groundwater aquifer. Appl. Environ. Microbiol. **57**:236-244.

11. Oldenhuis, R., J. Y. Oedzes, J. J. van der Waarde, and D. B. Janssen. 1991. KInetics of chlorinated hydrocarbon degradation by *Methylosinus trichosporium* OB3b and toxicity of trichloroethylene. Appl. Environ. Microbiol. **57**:7-14.

12. Fox, B. G., J. G. Borneman, L. P. Wackett, and J. D. Lipscomb. 1990. Haloalkene oxidation by the soluble methane monooxygenase from

OB3b: mechanistic and environmental implications. Biochemistry. **29**:6419-6427.

13. The Merck Index, Centennial Edition. 1989. Merck and Co., Inc. Rahway, N. J.

14. Lowenheim, F. A. and M. K. Moran. 1975. Faith, Keyes, and Clark's Industrial Chemicals, 4th Edition. John Wiley and Sons. New York.

15. Handbook of environmental fate and exposure data for organic chemicals. 1990. Edited by P. H. Howard. Lewis Publishers Inc., Chelsea, Michigan.

16. Carcinogenesis bioassay of trichloroethylene. National Cancer Institute. Washington D.C. 1976. CAS No. 79-01-6. NC-CG-TR-2.

17. Sittig, M. (1991), Handbook of toxic and hazardous chemicals and carcinogens, Third edition. Noyes Publications, Park Ridge, N. J.

18. Hanson, R. S., A. I. Netrusov, and K. Tsuji. 1992. Chapter 118, The obligate methanotrophic bacteria *Methylococcus, Methylomonas,* and *Methylosinus. In* A. Balows, H. G Truper, M. Dworkin, W. Harder, and K-H. Schleifer (eds.), The Prokaryotes, 2nd ed. Springer Verlag, New York.

19. Prior, S. D. and H. Dalton. 1985. The effect of copper ions on membrane content and methane monooxygenase activity in methanol-grown cells of *Methylococcus capsulatus* (Bath). J. Gen. Microbiol. **131**:155-163.

20. Burrows,. K. J., A. Cornish, D. Scott, and I. J. Higgins. 1984. Substrate specificities of the soluble and particulate methane monooxygenases of *Methylosinus trichosporium* OB3b. J. Gen. Microbiol. **130**:3327-3333.

21. Colby, J. and H. Dalton. 1976. Some properties of a soluble methane monooxygenase from *Methylococcus capsulatus* strain Bath. Biochem J. **157**:495-497.

22. Fox, B. G., W. A. Froland, J. E. Dege, and J. D. Lipscomb. 1989. Methane monooxygenase from *Methylosinus trichosporium* OB3b. Purification and properties of a three-component system with high specific activity from a type II methanotroph. J. Biol. Chem. **264**:10023-10033.

23. Koh, S-C., J. P. Bowman, and G. S. Sayler. 1993. Soluble methane monooxygenase production and trichloroethylene degradation by a type I methanotroph, *Methylomonas methanica* 68-1. Appl. Environ. Microbiol. **59**:960-967.

24. Nakajima, T., H. Uchiyama, O. Yagi, and T. Nakahara. 1992. Purification and properties of a soluble methane monooxygenase from *Methylocystis* sp. M. Biosci. Biotechnol. Biochem. **56**:736-740.

25. Pilkington, S. J, and H. Dalton. 1991. Purification and characterisation of the soluble methane monooxygenase from *Methylosinus sporium* 5 demonstrates the highly conserved nature of this enzyme in methanotrophs. FEMS Microbiol. Lett. **78**:103-108.

26. Stainthorpe, A. C., G. P. C. Salmond, H. Dalton and J. C. Murrell. 1990. Screening of obligate methanotrophs for sMMO genes. FEMS Microbiol Lett. **70:**211-216.

27. Murrell, J. C. 1992. Genetics and microbiology of methanotrophs. FEMS Microbiol. Rev. **88**:233-248.

28. Rosenzweig, A. C., C. A. Frederick, S. J. Lippard, and P. Nordlund. 1993. Crystal structure of a bacterial nonheme iron hydroxylase that catalyzes the biological oxidation of methane. Nature. **366**:537-543.

29. Tonge, G. M., D. E. F. Harrison, and I. J. Higgins. 1977. Purification and properties of the methane mono-oxigenase enzyme system from M*ethylosinus trichosporium* OB3b. Biocehm J. **161**:333-344.

30. DiSpirito, A. A., J. Gulledge, J. C. Murrell, A. K. Shiemke, M. E. Lidstrom, and C. L. Krema. 1992. Trichloroethylene oxidation by the membrane associated methane monooxygenase in type I, type II, and type X methanotrophs. Biodeg. **2**:151-164.

31. Brusseau, G. A., H-C. Tsien, R. S. Hanson, and L. P. Wackett. 1990. Optimization of trichloroethylene oxidation by methanotrophs and the use of a colorimetric assay to detect soluble methane monooxygenase activity. Biodeg. **1**:19-29.

32. Hanson, R. S., H. C. Tsien, K. Tsuji, G. A. Brusseau, and L. P. Wackett. 1990. Biodegradation of low-molecular weight halogenated hydrocarbons by methanotrophic bacteria. FEMS Microbiol. Rev. **87**:273-278.

Chapter 2

Whole-Cell Consumption of Methane

(To be submitted to *Applied and Environmental Microbiology*)

2.1 ABSTRACT

The use of bioremediation for the degradation of hazardous wastes such as trichloroethylene (TCE) has been proposed as an efficient and economic alternative to landfilling and incineration. One group of bacteria, methanotrophs, are ubiquitous in the environment, occurring in almost all instances where an air:methane interface is found. Methanotrophs have been shown to degrade TCE, but the primary function of the enzyme responsible for TCE degradation, the methane monooxygenase (MMO), is to oxidize methane into methanol, which then can then be further oxidized for the production of energy or for the assimilation of carbon into biomass. The MMO exists in two forms, a membrane-bound or particulate methane monooxygenase (pMMO), or a cytoplasmic or soluble form (sMMO). The pMMO is the predominant form of the MMO, therefore methane oxidation must be understood to effectivley utilize methanatrophs for the degradation of TCE. In this chapter, whole-cell assays of methane consumption were performed on four methanotrophs from both phylogenetic categories. From these assays it is apparent that varying the growth concentration of copper causes the kinetics of methane consumption to change. For *Methylobacter albus* BG8, *Methylosinus trichosporium* OB3b and *Methylocystis parvus* OBBP, increasing the copper growth concentration caused a decrease in the methane concentration at half-maximal uptake rate. Furthermore, for *M. parvus* OBBP and *Methylococcus capsulatus* Bath, as the concentration of copper in the growth medium increased, the kinetics of methane consumption changed from hyperbolic to sigmoidal kinetics. With this information, the ability of methanatrophs to degrade TCE in both in situ and above-ground treatment reactors can be more accurately modeled and optimized.

2.2 INTRODUCTION

Copper has long been known to regulate the relative expression of the sMMO and pMMO in methanotrophs that can express both forms of the MMO (1, 2). Recent information, however, suggests that copper may also affect cells producing only the pMMO (2, 3). In cell-free extracts additional copper has been shown to increase the activity of the pMMO in *Methylococcus capsulatus* Bath (2). Further physiological studies on the effect of copper on methanotrophs has shown that increasing copper in the growth medium increases cell yield and pMMO activity in *Methylobacter albus* BG8 (4). These researchers have suggested that this particular methanotroph may produce two forms of the pMMO or have one form whose activity may be regulated by the amount of bioavailable copper. The phospholipid content of the membranes of *M. capsulatus* Bath also has been seen to change as the amount of bioavailable copper increases. The mol-% of phosphatidylcholine increased from 10 to 16% as copper was increased from 0 to 9.6 μM $CuSO_4$ (5). A recent study has also shown that varying the amount of several nutrients including copper, iron, manganese, and ammonia affect the ability of an uncharacterized mixed culture of methanotrophs to oxidize methane (6). It is not possible, however, to conclude from this study if the varying nutrient concentrations are causing fundamental physiological changes or altering the population diversity.

Both the pMMO and sMMO have also been shown to oxidize a wide range of substrates (7-12) including TCE. The ability of these cells to degrade hazardous wastes has generated a great deal of research focusing on the sMMO because of the high rate of turnover of TCE (7, 9-12). Because the majority of known methanotrophs express only the pMMO and under typical environmental conditions, the copper/biomass ratio can be expected to be high, it is important to characterize the ability of the pMMO to oxidize TCE. Before one can adequately describe TCE degradation by the pMMO,

however, the kinetic characteristics of the pMMO for its primary substrate, methane, must be determined.

In this chapter, the effects of available copper on the expression of the pMMO are examined. It appears that increasing the amount of available copper not only causes a switch from sMMO expression to pMMO expression, it also causes a change in the uptake of methane by methanotrophs expressing the pMMO. Four methanotrophs representing all known phylogenetic categories were assayed for their ability to consume methane under conditions in which only the pMMO was expressed.

2.3 METHANOTROPHS SELECTED FOR METHANE OXIDATION STUDIES

To examine the effect of copper on the ability of methanotrophs to oxidize methane, it is crucial that any survey include representatives from both phylogenetic categories. It is not known *a priori* what the consequence of varying the copper concentration provided in the growth medium will be on methane oxidation. Therefore, to determine if copper is an important factor in the ability of the pMMO to transform methane, the pMMO from different cells must be examined. This information is also important for the utilization of *in situ* methanotrophic populations for the degradation of TCE. If the composition of the population is known and the kinetic parameters of methane and TCE oxidation of each physiological category are also known, then the capacity of the population to degrade TCE can be determined *a priori*. Furthermore, the population composition can be theoretically altered to optimize the rate and extent of TCE removal.

The methanotrophs selected are shown in Table 2.1.

Table 2.1. Methanotrophs used in methane uptake assays

Strain	Phylogenetic Category	sMMO
Methylobacter albus BG8	I	No
Methylococcus capsulatus Bath	I	Yes
Methylocystis parvus OBBP	II	No
Methylosinus trichosporium OB3b	II	Yes

Methylobacter albus BG8 is a Type I methanotroph that can only express the pMMO. Likewise, *Methylocystis parvus* OBBP does not contain the sMMO, but is a Type II methanotroph. The last two strains, *Methylococcus capsulatus* Bath (Type I) and *Methylosinus trichosporium* OB3b (Type II) can express both the sMMO and the pMMO. It is imperative that the sMMO not be expressed in these experiments to show that any copper effects on methane oxidation are due to changes in the pMMO activity, rather than to a switchover from the sMMO to the pMMO. In these experiments expression of the sMMO was avoided by keeping the copper:biomass ratio above that required for sMMO expression.

2.4 MATERIALS AND METHODS

2.4.1. Materials

All chemicals used in media preparation were of reagent grade. Highest purity methane (>99.99%) was obtained from Matheson Gas Company. Distilled - deionized water from a Corning Megapure D2 system was used for all experiments. The level of copper in this water was measured to be 0.45 ppb using an Inductively Conducted Plasma- Mass Spectrometer (ICP-MS).

2.4.2 Removal of Trace Metal Ions

All glassware was washed with detergent and then acid-washed in 1N HCl overnight to remove trace metals. The hydrochloric acid was subsequently removed by repeated rinses with distilled-deionized water.

2.4.3 Strains and Growth Conditions

All four methanotrophs were grown on nitrate mineral salts medium (NMS) (13) at 30 °C with shaking at 200 rpm under a methane-air atmosphere (1:3 vol/vol) at one atmosphere. Copper was added aseptically after autoclaving as $CuSO_4 \cdot (H_2O)_5$ to vary the copper concentration from 0 to 20 μM. In all flasks, the culture medium was no more than 15% of the total flask volume to insure adequate gas transfer of oxygen and methane. The cells were grown to the late-exponential phase and then harvested for all experiments. For *M. trichosporium* OB3b and *M. capsulatus* Bath, the minimum concentration of $CuSO_4 \cdot (H_2O)_5$ used was 2.5 μM to prevent expression of the sMMO.

2.4.4 Soluble Methane Monooxygenase Activity

To insure that the pMMO was the only enzyme present in the cells that is capable of oxidizing methane, an assay specific for the sMMO developed by Brusseau, et al. (7) was used. The sMMO has a broader substrate range than the pMMO and is able to oxidize long-chain and aromatic hydrocarbons. The pMMO can only oxidize short-chain hydrocarbons. In this assay, cell samples were taken and methane was removed by degassing. The samples were added to 10 ml serum bottles and crushed crystalline naphthalene was then added to provide a saturated aqueous solution. The samples were then shaken at 200 rpm at room temperature. If the sMMO is present, naphthalene will be oxidized to 1- and/or 2-napthol. The presence of napthol can then be detected by adding 4.21 mM of tetrazotized-o-dianisidine. If napthol is present,

Brusseau et al. (7) state that it will form a violet-colored adduct that is readily visible to the naked eye and measurable with a UV/VIS spectrophotometer. In all cases, the assay did not detect any sMMO activity.

2.4.5 Biorad® Protein Assay

To reference consumption results to the amount of cells present, the Biorad® protein assay was used. Standards were made using bovine plasma albumin. The cells were digested at 90°C for 30 minutes in 0.5N NaOH. Serial dilutions were prepared to achieve final protein concentrations within the linear range of the assay. The amount of protein is determined by measuring the absorbance at 595 nm after the Biorad® assay dye (an acidic solution of methanol, phosphoric acid and Coomassie Brilliant Blue G-250) has been added.

2.4.6 Determination of Methane Consumption

Cell cultures at the late-exponential phase were used for the methane consumption experiments. Any residual methane was removed by evacuating the flasks three times and allowing air to re-equilibrate after each evacuation. 5 ml aliquots were then transferred aseptically to 30 ml serum vials. These vials were then capped with butyl rubber stoppers (Bellco) and sealed with aluminum crimp seals. To obtain a range of methane concentrations in solution, a dimensionless Henry's Constant of 27.2 was used to calculate the amount of methane to add to the headspace using A-2 gas-tight syringes from Dynatech Precision Sampling Corporation. The vials were re-shaken at 200 rpm at room temperature. At pre-determined time points, the cells were killed by adding 20 µl of a 50% NaOH solution (w/v). Headspace samples (100 µl) were then injected into a Hach-Carle Gas Chromatograph with a flame-ionization detector and a Haysep 80/100 analytical column (EG & G Engineering) and compared to methane standards. Controls killed with either a 5% (v/v) solution of formaldehyde

or 50% (w/v) NaOH solution were made to monitor any volatilization or adsorption losses over the time course of the experiment. The amount remaining in solution was then recalculated using Henry's Law. To calculate the velocities of uptake the amount of methane consumed was taken to be the difference between what was measured in the sample vial versus the concentration at t = 0 hours. The amount was then divided by the volume of the sample vial, the total cell protein as measured by the Biorad protein assay and the time of consumption. The typical time course for an individual experiment was 4 hours.

2.5 RESULTS

The results of the effect of copper on methane oxidation are shown in Figures 2.1-2.4. In these figures the rate of methane uptake by the cells (V) normalized to the maximum uptake rate (V_{max}) is plotted against the initial methane concentration. Only the high and low copper concentrations are shown here, but individual methane uptake plots for each copper concentration are shown in Appendix A. The kinetic parameters for all copper concentrations are compiled in Table 2.2 and Table 2.3.

The simplest model that can be used to describe the kinetics of substrate disappearance is the Michaelis-Menten model. In this model, an enzyme is assumed to bind the substrate, forming an enzyme-substrate complex that can either reform the enzyme and unchanged substrate or the enzyme can convert the substrate into a product:

$$E + S \underset{k_2}{\overset{k_1}{\rightleftharpoons}} ES$$

$$ES \xrightarrow{k_3} E + P$$

If one assumes the enzyme-substrate complex, ES, is in pseudo-steady state, the amount of enzyme is much less than the amount of substrate present, and that the

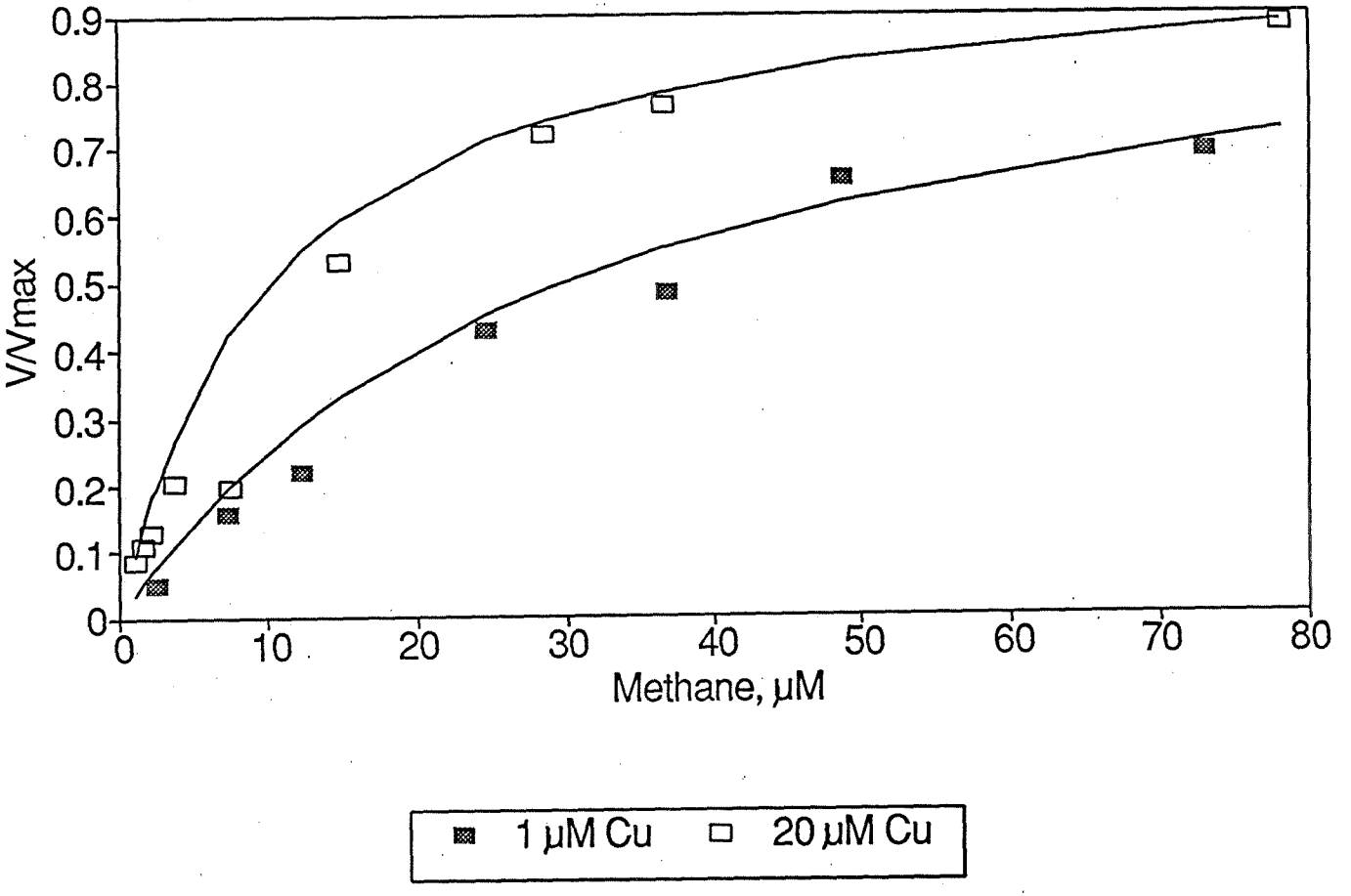

Figure 2.1. Effect of copper on methane uptake by *Methylobacter albus* BG8 expressing the pMMO.
V_{max} for 1 µM copper = 0.041 µmol methane/(hr•µg protein)
V_{max} for 20 µM copper = 0.050 µmol methane/(hr•µg protein)
——— = Michaelis-Menten model

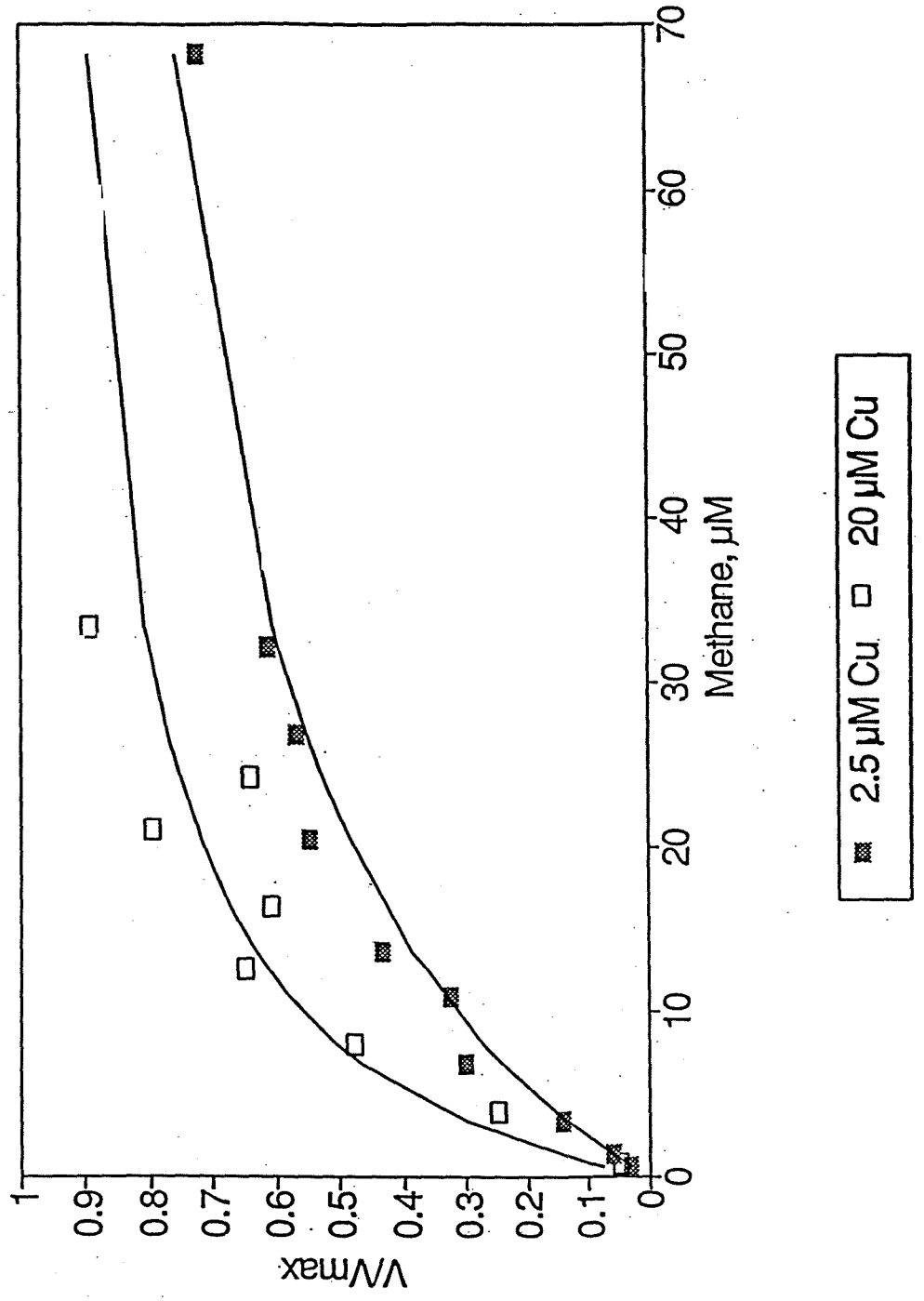

Figure 2.2. Effect of copper on methane uptake by *Methylosinus trichosporium* OB3b expressing the pMMO.
V max for 2.5 µM copper = 0.035 µmol methane/(hr•µg protein)
V max for 20 µM copper = 0.036 µmol methane/(hr•µg protein)
_____ = Michaelis-Menten model

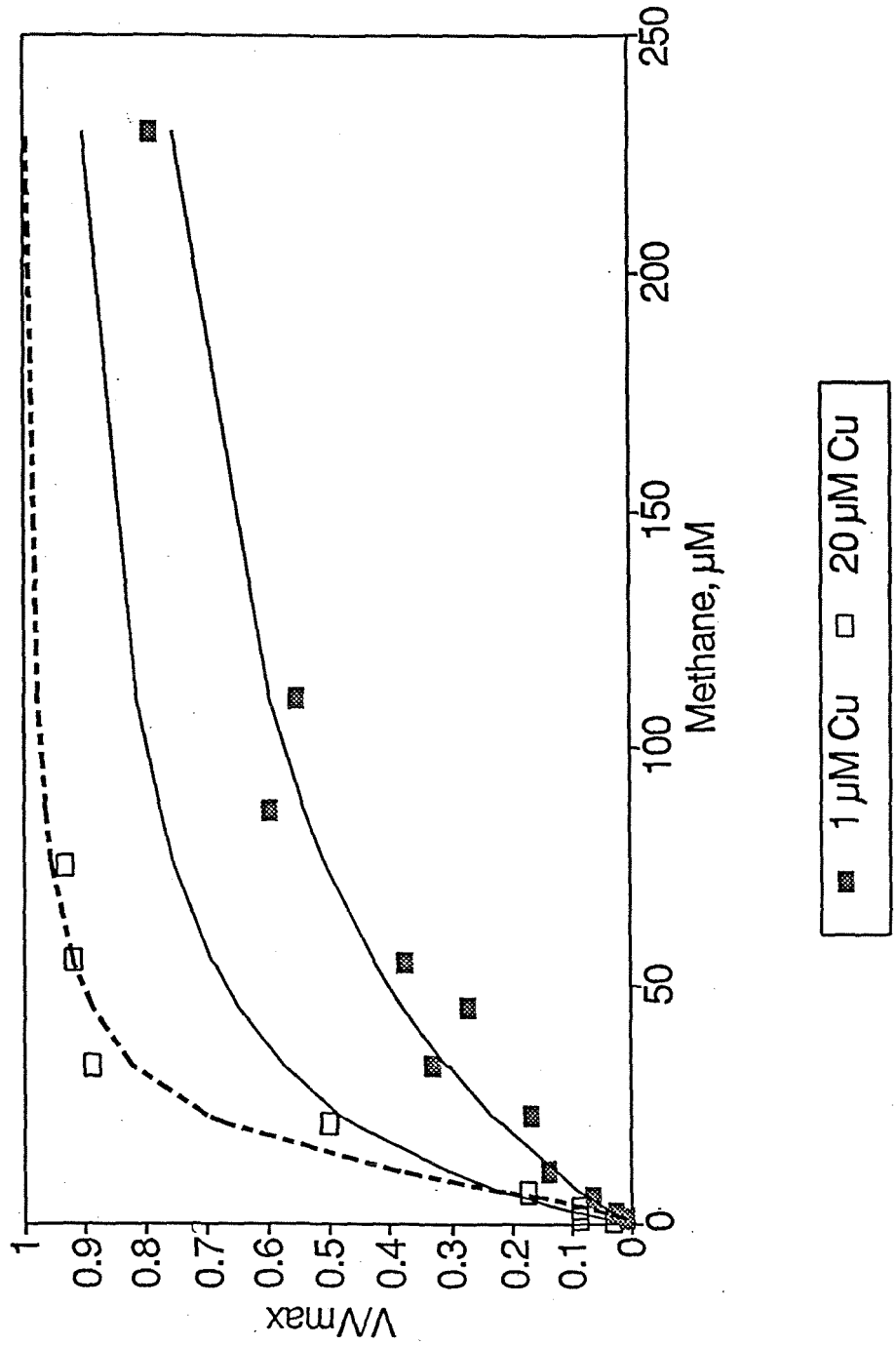

Figure 2.3. Effect of copper on methane uptake by *Methylocystis parvus* OBBP expressing the pMMO.
V_{max} for 1 µM copper = 0.065 µmol methane/(hr•µg protein)
V_{max} for 20 µM copper = 0.035 µmol methane/(hr•µg protein)
——— = Michaelis-Menten model
---------- = Hill model

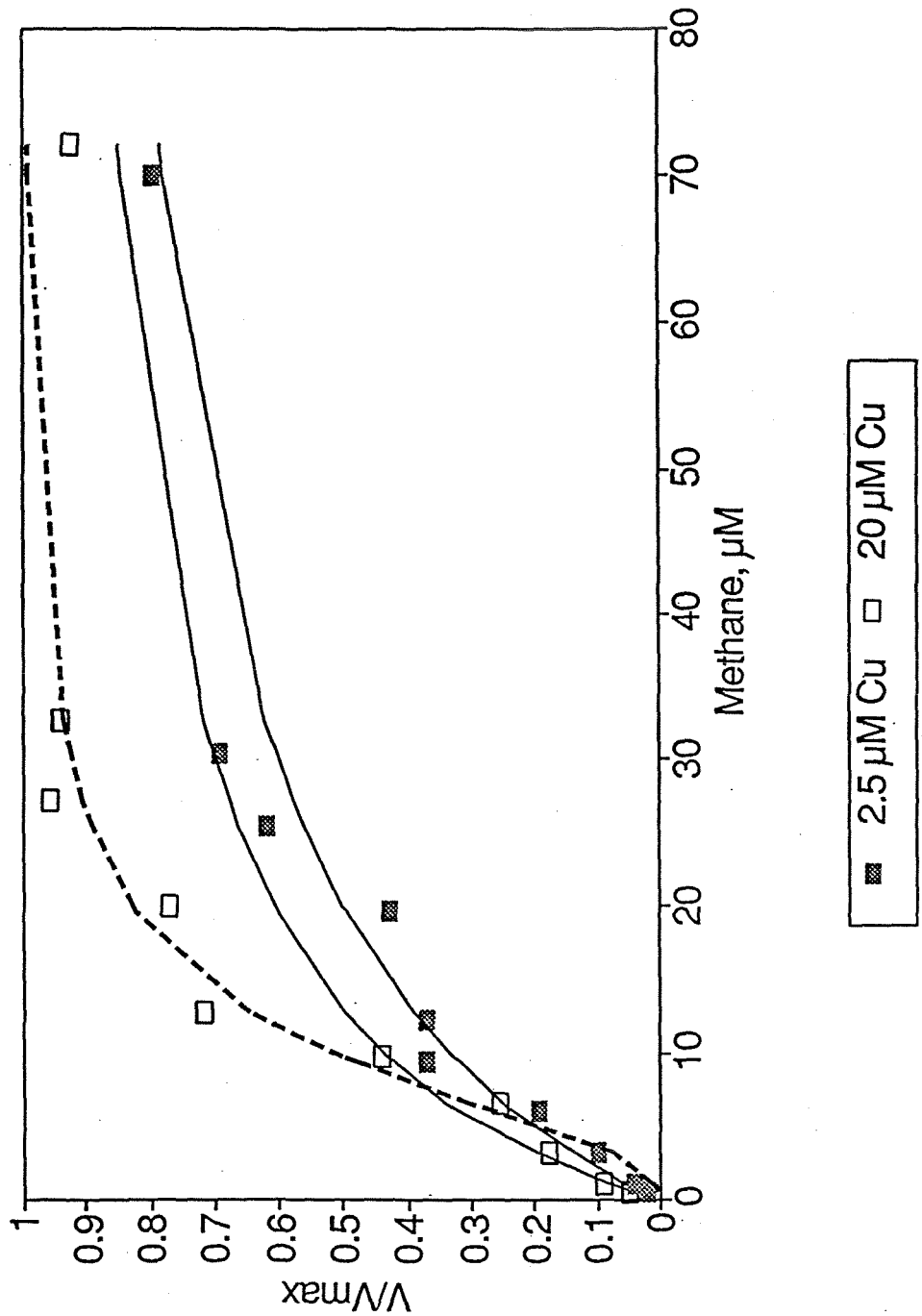

Figure 2.4. Effect of copper on methane uptake by *Methylococcus capsulatus* Bath expressing the pMMO.
V max for 2.5 µM copper = 0.050 µmol methane/(hr•µg protein)
V max for 20 µM copper = 0.022 µmol methane/(hr•µg protein)
——— = Michaelis-Menten model
---------- = Hill model

Table 2.2. Kinetic parameters for strains showing Michaelis-Menten kinetics.

Copper μM	*Methylobacter albus* BG8 V_{max}	K_s	*Methylosinus trichosporium* OB3b V_{max}	K_s
1.0	0.041	30	ND	ND
2.5	ND	ND	0.035	22
5.0	0.040	15	0.025	18
10.0	0.014	7	0.027	10
20.0	0.050	10	0.036	8

ND = Not Determined
V_{max} = μmol methane/(hr•μg protein)
K_S = μM

Table 2.3. Kinetic parameters for strains showing sigmoidal kinetics at high copper concentrations.

Copper, μM	*Methylocystis parvus* OBBP			*Methylococcus capsulatus* Bath		
	V_{max}	K_h	n	V_{max}	K_h	n
1.0	0.065	75	1	ND	ND	ND
2.5	ND	ND	ND	0.050	22	1.2
5.0	0.037	13	1.3	0.038	70	2.0
10.0	0.017	200	1.8	0.030	120	1.9
20.0	0.035	120	1.8	0.022	130	2.1

ND = Not Determined
V_{max} = μmol methane/(hr•μg protein)
$K_h = \mu M^n$

conversion of substrate to product is irreversible, one can obtain the familiar Michealis-Menten expression (14):

$$\frac{-dS}{dt} = V = \frac{k_3 E_0 \times S}{\left(\frac{k_2 + k_3}{k_1}\right) + S}$$

where: V = rate of substrate disappearance
E_O = total amount of enzyme present

If one defines V_{max}, the maximal uptake rate, as k_3E_O and K_S as the ratio of rate constants, one can then write:

$$\frac{-dS}{dt} = V = \frac{V_{max} \times S}{K_S + S}$$

If the rate of substrate disappearance is plotted vs. the initial substrate concentration, one obtains a hyperbolic plot. K_S is taken to be the substrate concentration at half-maximal uptake rate. To determine the kinetic parameters, K_S and V_{max}, the data are often linearized by plotting a Lineweaver-Burke plot, 1/V vs. 1/S. If the Michaelis-Menten model accurately reflects the kinetics of substrate disappearance, a linear plot should be obtained with a y-intercept equivalent to $1/V_{max}$. It is common to take the X-intercept to be equivalent to $1/K_S$. Bailey, however, advises the use of the Lineweaver-Burke plot only for calculating V_{max} (14). He recommends that the standard plot of V vs. S should then be used to determine K_S by calculating the substrate concentration at half-maximal uptake rate. With this method, the two parameters are more accurately ascertained than from using the Lineweaver-Burke plot alone. This method has been used throughout this study to determine the kinetic parameters for both methane and trichloroethylene.

Figure 2.1 shows the effect of growth in the presence of 1.0 and 20 μM $CuSO_4 \cdot (H_2O)_5$ on methane uptake in *M. albus* BG8. As can be seen in this figure and in Table 2.2, as the copper concentration in the growth medium increased, the affinity for methane increased (K_S decreased) by approximately a factor of 3. The maximum rate of methane uptake (V_{max}), however, did not change significantly as the amount of copper added to the growth medium was increased. This indicates that *M. albus* BG8 is able to consume methane at lower concentrations as the amount of available copper increases, but copper does not increase the rate of methane oxidation to methanol.

A similar effect is seen with *M. trichosporium* OB3b as shown in Figure 2.2 and Table 2.2. Again as the concentration of copper in the growth medium increased the whole-cell affinity for methane increased while the rate of uptake did not show any significant trend. The response is the same as with *M. albus* BG8. Furthermore, these data show that copper also affects the pMMO in a cell that can express both the sMMO and pMMO.

For two other strains, *M. parvus* OBBP and *M. capsulatus* Bath, increasing the amount of copper in the growth medium also caused the kinetics of methane consumption by the pMMO to change. The change in kinetics, however, is more complicated than that for *M. albus* BG8 and *M. trichosporium* OB3b. For the latter strains, the Michaelis-Menten model of substrate utilization fit the data well at all copper concentrations. As shown in Figure 2.3 and 2.4, methane uptake appears to change from hyperbolic kinetics to sigmoidal kinetics for *M. parvus* OBBP and *M. capsulatus* Bath at higher growth medium copper concentrations. The Michaelis-Menten model does not fit the methane uptake data from these cells grown at high copper concentration without a large amount of error. Some enzyme systems have been noted to exhibit sigmoidal kinetics, for example, hemoglobin. In the case of hemoglobin, the sigmoidicity is due to multiple sites of oxygen binding that are cooperative, i.e.,

binding of oxygen to one site enhances the binding of oxygen to a second site. Based on these observations, Hill formulated the empirical equation (15):

$$Y = \frac{K_h \times S^n}{1 + K_h S^n}$$

where: Y = fractional saturation of sites

K_h is the equilibrium constant of substrate binding by the enzyme:

$$E_n + nS \leftrightarrow E_n S_n$$

$$K_h = \frac{[E_n S_n]}{[E_n][S]^n}$$

Since Y is defined as the fraction of sites occupied by the substrate, it can be considered to be:

$$Y = \frac{V}{V_{max}}$$

With rearranging terms and substituting the above expression for Y, one gets:

$$V = \frac{V_{max} \times S^n}{K_h + S^n}$$

This expression can also be obtained from an equilibrium model similar to that used for the derivation of the Michaelis-Menten equation (eqns 2.1 - 2.2):

$$E_n + nS \underset{k_2}{\overset{k_1}{\rightleftharpoons}} E_n S_n$$

$$E_n S_n \xrightarrow{k_3} E_n + nP$$

If one assumes as in the case for Michaelis-Menten kinetics that the enzyme-substrate complex, E_nS_n is pseudo-steady-state, one can then obtain:

$$\frac{-dS}{dt} = V = \frac{k_3E_0 \times S^n}{\left(\frac{k_2 + k_3}{k_1}\right) + S^n}$$

If k_3E_0 is defined as the maximal uptake velocity, V_{max}, and the ratio of rate constants as K_h, we then get an expression similar to the Michaelis-Menten equation:

$$\frac{-dS}{dt} = V = \frac{V_{max} \times S^n}{K_h + S^n}$$

In this equation, there are three unknowns: V_{max}, K_h, and n. V_{max} is determined by plotting 1/V vs 1/S and noting where the curve intersects the abscissa. The value of n is calculated by using a linear form of equation 2.13, called the Hill equation:

$$\log\left(\frac{V}{V_{max} - V}\right) = n\log[S] - \log K_h$$

If the logarithm of $(V/V_{max} - V)$ is plotted vs. the logarithm of S, one ideally gets a line with slope n. This is only true, however, if the binding of each substrate occurs with the same affinity. If this is not the case, and should not be expected due to cooperativity, a curved line is seen (16). At substrate concentrations near the half-maximal uptake rate, the curve is linear with a slope that can be used to approximate n. With this value of n, K_h is calculated by raising the substrate at half-maximal uptake to the nth power. The uptake data for *M. parvus* OBBP and *M. capsulatus* Bath at 20 μM copper have been replotted according to equation 2.14 and are shown in Figures 2.5 and 2.6. The results for all copper concentrations are presented in Table 2.2. As can

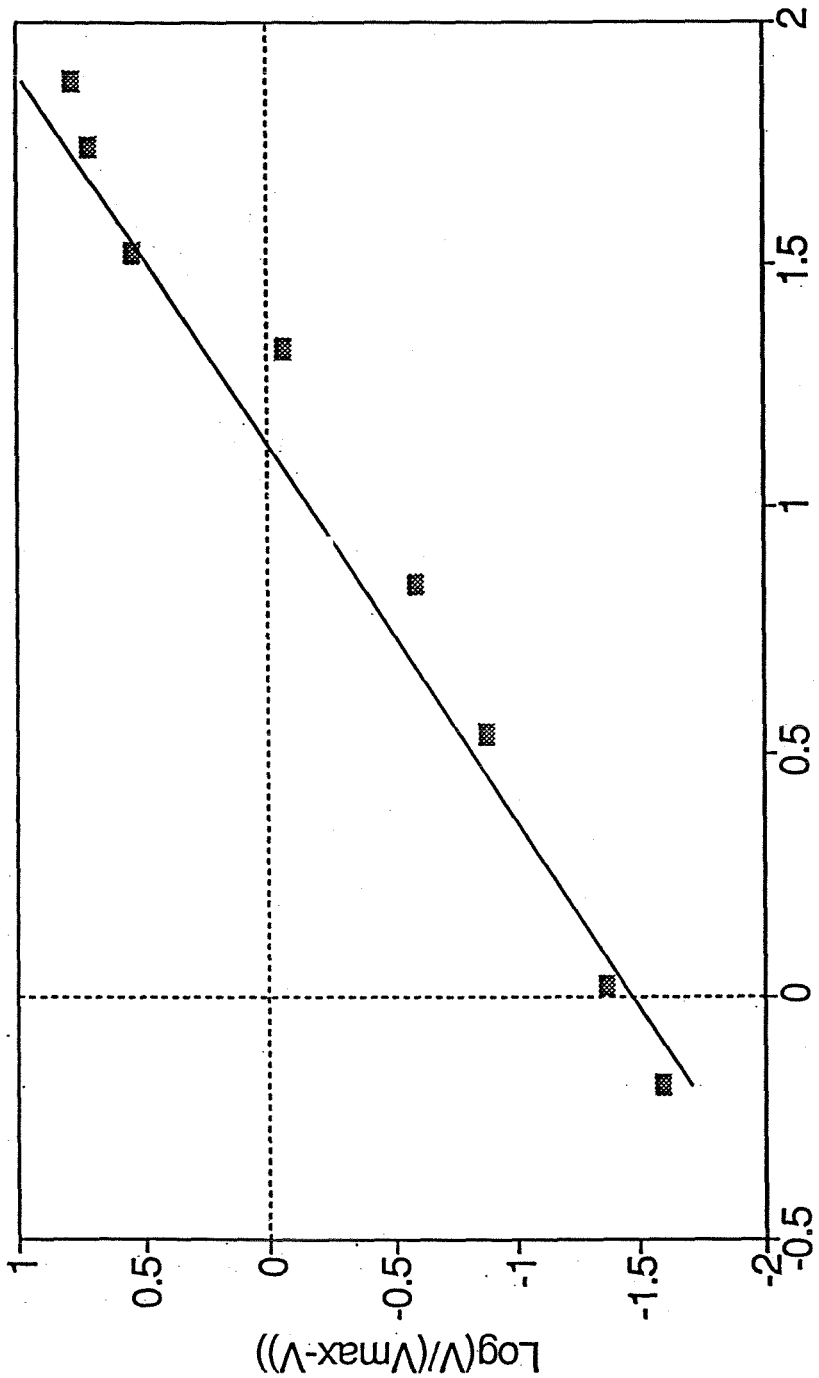

Figure 2.5. Hill plot of methane uptake by *M. parvus* OBBP with 20 µM copper.
n = 1.8
r^2 = .96

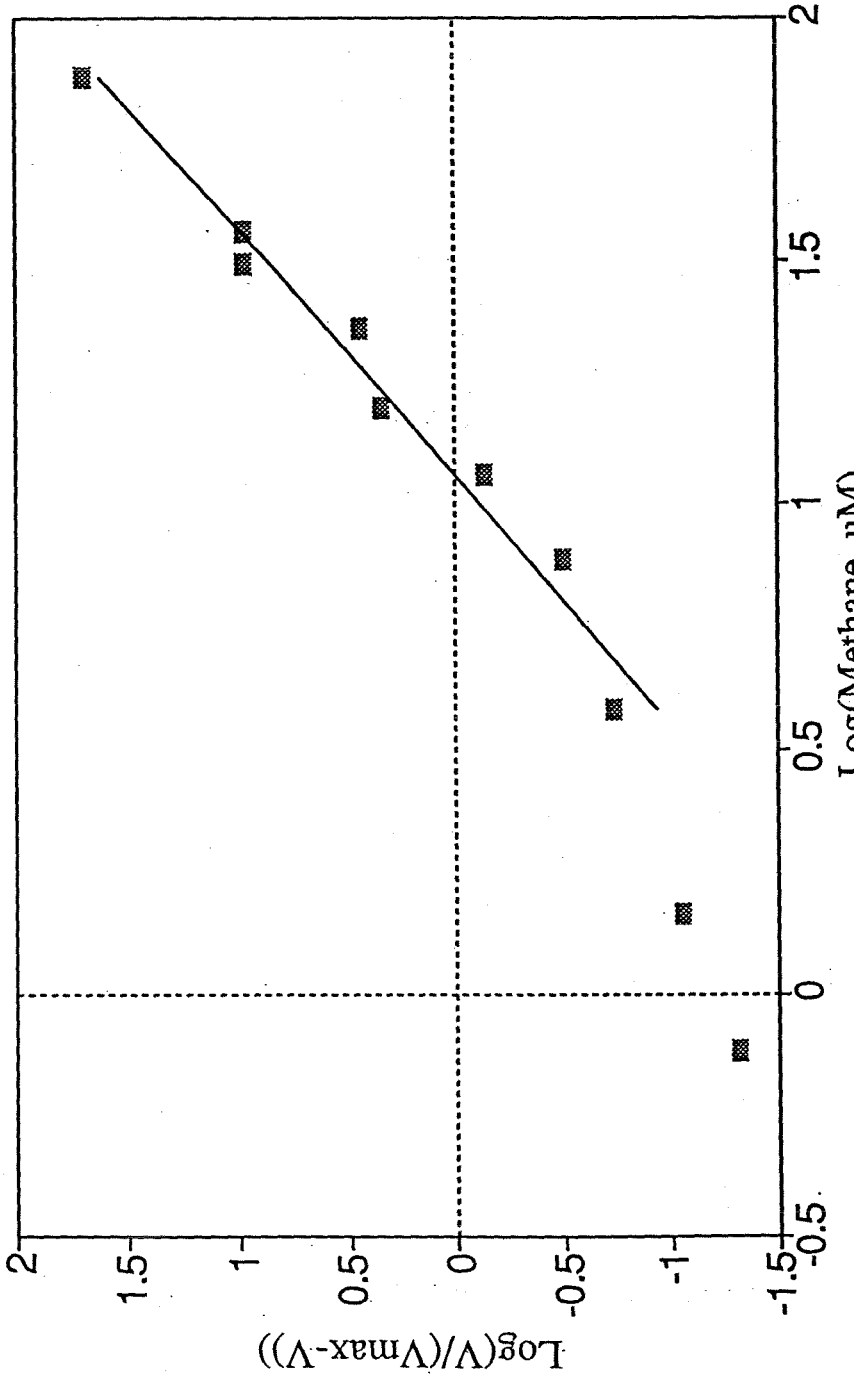

Figure 2.6. Hill plot of methane uptake by *M. capsulatus* Bath with 20 µM copper.
n = 2.1
r^2 = .97

be seen in this table, the predicted n value increased directly as the amount of copper added to the medium increased. One explanantion for these results is that in these cells multiple active sites may exist that may be deficient at low growth concentrations of copper, and are filled as more copper is provided to the cells. A similar copper enzyme, the ammonia monooxygenase (AMO), has also been shown to exhibit sigmoidal kinrtics (17). Therefore, multiple active sites may exist in some forms of the pMMO that are cooperative, i.e., the binding of one substrate affects the binding of substrate to other sites, possibly due to conformational change of the enzyme.

Also shown in Table 2.2 are the K_h values. It is difficult, however, to ascertain the change in the cells' affinity for methane with changing growth copper concentrations because K_h has units of μM^n. If we examine the substrate concentration at half-maximal uptake rate, we can ascertain whether the affinity for methane changes significantly. These values are reported in Table 2.4:

Table 2.4 Methane concentrations at half-maximal uptake rate, μM

Copper, μM	*Methylocystis parvus* OBBP	*Methylococcus capsulatus* Bath
1.0	75	-
2.5	-	13
5.0	7.2	8.4
10.0	19	12
20.0	14	10

It is evident that for *M. parvus* OBBP the affinity for methane changes, but not for *M. capsulatus* Bath. Therefore, copper has an effect on the pMMO for all strains tested, but the effect is not consistent for all strains.

2.6 DISCUSSION

From the data presented here, it is clear that copper affects the ability of cells expressing the pMMO to oxidize methane. Specifically, increasing the growth concentration of copper increases the whole-cell affinity for methane in cells expressing only the pMMO. The colorimetric assay developed by Brusseau, et al (7) specific for sMMO activity was used to determine whether the sMMO was present in the strains capable of expressing the sMMO (*M. trichosporium* OB3b and *M. capsulatus* Bath). In all cases, the sMMO was not detected with this assay. Therefore the effect of copper in these experiments on methane uptake is not due to differential expression of the sMMO and pMMO.

The effect of copper on the cells' ability to take up methane, however, varied between cells. For two of the strains examined, *M. albus* BG8 and *M. trichosporium* OB3b, the affinity for methane of the whole cells increased as measured by a decrease in the K_S values determined from Michaelis-Menten kinetics. For *M. capsulatus* Bath and *M. parvus* OBBP, however, the data suggest that the number of active sites on the pMMO increases from 1 to 2 as copper levels increase. Furthermore, the kinetics of methane uptake in these strains became sigmoidal at high growth concentrations of copper, indicating that these sites may be cooperative in binding methane. These data are interesting in relation to field populations of methanotrophs, since the substrate concentrations at half-maximal uptake rate are similar to K_S values obtained from field studies. This indicates that in situ populations of methanotrophs may be predominantly expressing the pMMO (18). What is not clear, however, is the mechanism whereby the increase in the amount of copper present in the growth medium changes the kinetics of methane oxidation. In this section, alternatives are discussed with respect to the possible role of copper in the pMMO, with some possibilities examined more closely in later chapters.

Two broad categories exist that could explain the data obtained. First, the cells may have only one pMMO, which changes its kinetics in response to copper. In that case, copper may either play a role in the structure of the pMMO by changing its conformation or a direct role in catalysis by creating multiple active sites on each pMMO. Alternatively, the cell may have two (or more) pMMO's, which have different kinetics. In that case, copper may act by regulating the expression of similar, but not identical pMMO's. If only one pMMO exists, then additional copper may bind to the pMMO in vacant sites, thereby changing the structure and/or activity of the pMMO. Alternatively, copper may fill unsaturated new active sites on the pMMO that are cooperative. If multiple pMMO's exist, copper may regulate the expression of the genes encoding the pMMO, and the gene products may have different kinetic characteristics. Either hypothesis may explain why methane oxidation by the pMMO is affected by copper, but its role cannot be accurately determined by whole-cell studies. At this level of experimentation, it can be only stated that two kinetically different forms of the pMMO exist and the relative amounts of these two forms is at least partially regulated by the amount of bioavailable copper present in the growth medium.

The problem of determining the mechanism by which copper affects whole-cell oxidation of methane is also complicated by the problem of which species of copper are bioavailable to these cells (19). It is unclear whether only free copper is available or if some complexed forms of copper in the medium are also bioavailable. Although the scope of this research is to examine the kinetics of substrate oxidation, the bioavailablility of copper must be examined if methanotrophs are to be used for in situ degradation of hazardous wastes.

2.7 SUMMARY AND CONCLUSIONS

Whole-cell studies of methane uptake by methanotrophs grown under varying copper concentrations indicate that the kinetics of methane consumption changes. The

effect of copper was observed in all four strains tested, regardless of their phylogenetic category and regardless of whether they have only the pMMO or both forms of the MMO. Increasing copper generally caused an enhanced ability to bind methane at low concentrations, as indicated by the decrease in the substrate concentrations at the half-maximal uptake rate. In two cases, the kinetics of methane uptake changed from hyperbolic to sigmoidal kinetics at higher copper levels, with both the K_h and n values changing with the copper. With this information the competition between methane and TCE for binding sites on the pMMO can be more accurately determined. TCE oxidation must next be measured in the absence of methane to obtain similar kinetic parameters and also to determine if copper has a similar effect on the uptake of TCE by the pMMO.

2.8 REFERENCES

1. Prior, S. D. and H. Dalton. 1985. The effect of copper ions on membrane content and methane monooxygenase activity in methanol-grown cells of *Methylococcus capsulatus* (Bath). J. Gen. Microbiol. **131**:155-163.

2. Stanley, S. H., S. D. Prior, D. J. Leak, and H. Dalton. 1983. Copper stress underlies the fundamental change in intracellular location of methane monooxygenase methane-oxidizing organisms: studies in batch and continuous culture. Biotechnol. Lett. **5**:487-492.

3. Nguyen, H-H., A. K. Shiemke, S. J. Jacobs, B. J. Hales, M. E. Lidstrom, and S. I. Chan. 1994. The nature of copper ions in the membranes containing the particulate methane monooxygenase from *Methylococcus capaulstus* (Bath). J. Biol. Chem. (in press).

4. Collins, M. L. P., L. A. Bulchholz, and C. C. Remsen. 1991. Effect of copper on *Methylomonas albus* BG8. Appl. Environ. Microbiol. **57**:1261-1264.

5. Peltola, P., P. Priha, and S. Laakso. 1993. Effect of copper on membrane lipids and on methane monooxygenase activity of *Methylococcus capsulatus* (Bath). Arch. Microbiol. **159**:521-525.

6. Boisen, A., E. Arvin, and K. Broholm. 1993. Effect of mineral nutrients on the kinetics of methane utilization by methanotrophs. Biodeg. **4**:163-170.

7. Brusseau, G. A., H-C. Tsien, R. S. Hanson, and L. P. Wackett. 1990. Optimization of trichloroethylene oxidation by methanotrophs and the use of a colorimetric assay to detect soluble methane monooxygenase activity. Biodeg. **1**:19-29.

8. Dipirito, A. A., J. Gulledge, A. K. Shiemke, J. C. Murrell, M. E. Lidstrom, and C. L. Krema. 1992. Trichloroethylene oxidation by the membrane-associated methane monooxygenase in type I, type II, and type X methanotrophs. Biodeg. **2**:151-164.

9. Fox, B. G., J. G. Borneman, L. P. Wackett, and J. D. Lipscomb. 1990. Haloalkene oxidation by the soluble methane monooxygenase from *M. trichosporium* OB3b: mechanistic and environmental implications. Biochemistry. **29**:6419-6427.

10. Oldenhuis, R., J. Y. Oedzes, J. J. van der Waarde,and D. B. Janssen. 1991. Kinetics of chlorinated hydrocarbon degradation by *Methylosinus trichosporium* OB3b and toxicity of trichloroethylene. Appl. Environ. Microbiol. **57**:7-14.

11. Alvarez-Cohen, L., P. L. McCarty, E. Boulygina, R. S. Hanson, G. A. Brusseau, and H. C. Tsien. 1992. Characterization of a methane-utilizing bacterium from a bacterial consortium that rapidly degrades trichloroethylene and chloroform. Appl. Environ. Microbiol. **58**:1886-1893.

12. Koh, S-C., J. P. Bowman, and G. S. Sayler. 1993. Soluble methane monooxygenase production and trichloroethylene degradation by a type I methanotroph, *Methylomonas methanica* 68-1. Appl. Environ. Microbiol. **59**:960-967.

13. Whittenbury, R., K. D. Philips, and J. F. Wilkinson. 1970. Enrichment, isolation and some properties of methane-utilizing bacteria. J. Gen. Microbiol. **61**:205-218.

14. Bailey, J. E. and D. F. Ollis. 1986. Biochemical engineering fundamentals. McGraw-Hill. New York.

15. Segel, I. H., Enzyme Kinetics: behavior and analysis of rapid equilibrium and steady-state enzyme systems. John Wiley & Sons, Inc., New York. 1975.

16. Cornish-Bowden, A. and D. E. Koshland, Jr. 1975. Diagnostic uses of the Hill (Logit and Nernst) plots. J. Mol. Biol. **95**:201-212.

17. Ward, B. B. 1990. Kinetics of ammonia oxidation by a marine nitrifying bacterium: methane as a substrate analogue. Microb. Ecol. **19**:211-225.

18. Lidstrom, M. E. and L. Somers. 1984. Seasonal study of methane oxidation in Lake Washington. Appl. Environ. Microbiol. **47**:1255-1260.

19. Trevors, J. T. and C. M Cotter. 1990. Copper toxicity and uptake in microorganisms. J. Ind. Microbiol. **6**:77-84.

Chapter 3

Whole-Cell Degradation of Trichloroethylene

(To be submitted to *Environmental Science and Technology*)

3.1 ABSTRACT

Trichloroethylene (TCE) oxidation by the methane monooxygenase (MMO) has been proposed as an effective and economic alternative to decontaminate polluted areas. Much of the work has focused on the sMMO due to its high rate of TCE oxidation. The sMMO, however, is only expressed by 6 known methanotrophs while all methanotrophs express the pMMO. In this chapter, the effect of copper and exogenous reducing equivalents in the form of formate on the whole-cell oxidation of TCE is examined for one methanotroph, *Methylobacter albus* BG8. From these experiments, it is apparent that the concentration of copper in the growth medium not only affects methane oxidation, it also affects TCE oxidation. The V_{max} of TCE oxidation determined here is approximately one order of magnitude less than the V_{max} commonly reported for the sMMO. The whole-cell half-saturation constant (K_S) of *M. albus* BG8 expressing the pMMO, however, is 5-9x less than the K_S of cells expressing the sMMO. Therefore it may be advantageous to use the pMMO for TCE degradation even though its degradation rate is slower than the sMMO because of the ability of the pMMO to remove TCE to lower levels than for the sMMO. It appears that as cells are grown in higher copper, the pMMO becomes more specific for its primary substrate, methane. This would indicate that copper plays a role in changing the conformation of the pMMO to make it more selective for methane. When reducing equivalents were added in the form of formate, however, TCE oxidation was stimulated regardless of the copper concentration. Biochemical and genetic analyses are necessary to clarify the role of copper in the pMMO.

3.2 INTRODUCTION

TCE is a widely used solvent for the degreasing of metal parts and production of organic chemicals and pharmaceuticals (1). The widespread use of TCE, however, has caused extensive pollution of groundwater (2). It may be very difficult to remove TCE from contaminated soils and aquifers with conventional pump-and-treat methods because of adsorption onto the soil matrix, low soil permeability, and the presence of non-aqueous phase liquids that may be onerous to locate (3, 4). It has been suggested that it may take on the order of 100 years to remove pollutants such as TCE from contaminated areas using current pump-and-treat techniques (3,4). Furthermore, methods such as air-stripping, landfilling, and incineration are undesirable as these procedures merely transfer pollution from one medium to another. A "holistic" approach to environmental remediation is being advocated whereby the polluted area is decontaminated without polluting another part of the environment (5). Biodegradation may achieve this goal as the waste(s) can be completely mineralized to CO_2 and H_2O.

Methanotrophs have been extensively studied for their ability to oxidize TCE (6-26). As discussed in Chapter 1, the methane monooxygenase (MMO) expressed by these cells can degrade TCE through the process of co-metabolism. Much of the work carried out on TCE degradation by methanotrophs has examined uncharacterized mixed cultures in which the predominant form of the MMO is unknown and the effect of varying nutrient concentrations on TCE uptake is difficult to ascertain (6, 7, 9, 13, 15, 16, 21, 26). Those studies that have examined well-characterized or pure cultures of methanotrophs have almost exclusively involved the sMMO due to the high rate of TCE turnover by cells expressing this enzyme (8, 10, 12, 14, 17, 18, 20, 22, 23). Other studies have examined pure cultures of methanotrophs, but the form of the MMO expressed was not determined (19, 24-26).

One study by DiSpirito et al. (11) has shown that the pMMO can also degrade TCE. Table 3.1 compiles the current reported kinetic values for TCE degradation by methanotrophs.

Table 3.1 Reported kinetic values for the degradation of TCE by methanotrophs known to be expressing either the sMMO or pMMO.

Strain	Enzyme	V_{max} (nmol/min/mg protein)	K_S (μM)	Reference
A45	pMMO	0.296	ND	11
MN	pMMO	0.233	ND	11
OBBP	pMMO	0.677	ND	11
MC	pMMO	0.202	ND	11
OB3b	pMMO	0.58	ND	11
OB3b	sMMO	456	138	10
OB3b	sMMO	995	126	17
OB3b	sMMO	290	145	20
68-1	sMMO	2235	225	17

(ND = Not Determined)

A45 - *Methylobacter marinus* A45
MN - *Methylomonas* MN
OBBP - *Methylocystis parvus* OBBP
MC - *Methylococcus capsulatus* Bath
OB3b - *Methylosinus trichosporium* OB3b
68-1 - *Methylomonas methanica* 68-1

As can be seen in Table 3.1, the maximal rate of oxidation of TCE by whole cells of methanotrophs expressing the sMMO is 1000-fold greater than cells expressing the pMMO, with *M. methanica* 68-1having the highest V_{max}. This is perhaps not surprising as *M. methanica* 68-1 was isolated from a TCE-contaminated aquifer. From these studies, the affinity of the pMMO for methane was not determined, nor

was the effect of additional copper on the oxidation of TCE by the pMMO assessed. It is possible that TCE degradation is affected by the growth concentration of copper similar to methane consumption.

TCE oxidation by whole cells is more complicated than methane oxidation. First, TCE itself may be toxic to cells above a certain concentration due to its ability to partition into cellular membranes and disrupt them. Second, the products of TCE oxidation may also be toxic. As shown in Figure 3.1 the primary products of oxidation of TCE by the sMMO are TCE-epoxide and trichloroacetaldehyde, or chloral (27, 28). The TCE-epoxide has a half-life in water of approximately 10-20 seconds (29). When the epoxide ring opens, it can undergo a variety of hydrolysis and oxidation reactions that are uncontrolled by the cell. After opening, the ring can bind nucleophilically to nearby cellular material including proteins and nucleic acids (20). If this occurs frequently, cellular inhibition can result, leading to decreased TCE oxidation. It is unknown if chloral is toxic to bacterial cells. It is known to have adverse effects on the kidneys, liver, and blood pressure of laboratory animals (30). Therefore, it is unclear if chloral is more toxic than TCE, but its formation is cause for concern. Current data suggest that cells expressing the pMMO do not produce significant amounts of chloral (28), another reason for favoring the pMMO over the sMMO for biodegradation of TCE.

Finally, as discussed in Chapter 1, TCE oxidation is a co-metabolic reaction in which TCE competes with methane for binding sites and reducing equivalents believed to be in the form of NADH. Studies have shown that the addition of an exogenous substrate that can supply reducing equivalents can enhance the degradation of TCE (6, 15, 16). These studies, however, have examined uncharacterized mixed cultures. It is unclear if methanotrophs expressing the pMMO will have increased TCE oxidation if exogenous supplies of reducing equivalents such as formate are

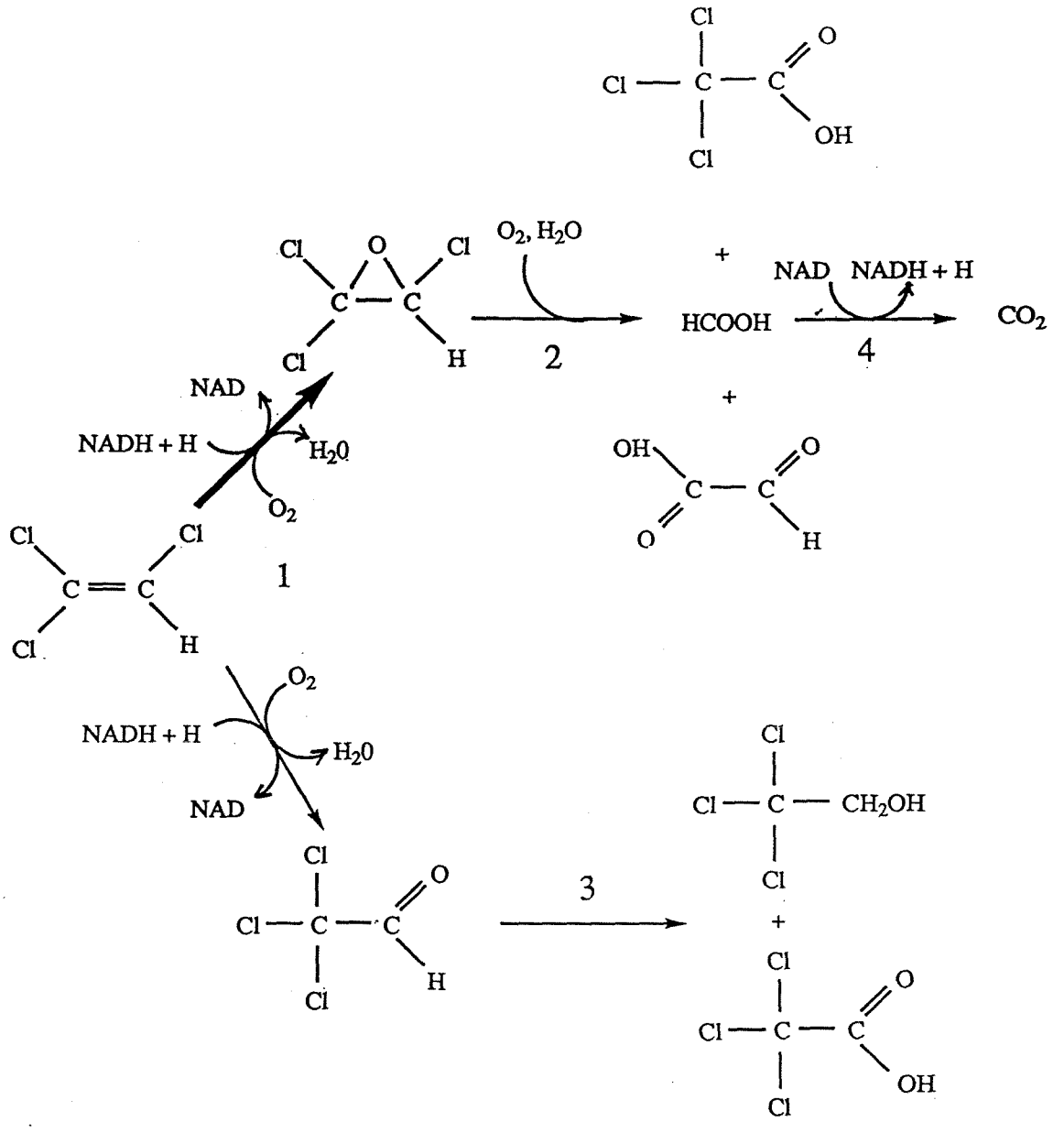

1. Soluble methane monooxygenase
2. Spontaneous abiotic hydrolysis and oxidation reactions
3. Unknown biotic transformations
4. Formate dehydrogenase

Figure 3.1. Aerobic transformation of trichloroethylene by the sMMO in whole cells. Approximately 6-16% of TCE is converted to chloral and 84-94% is converted into TCE-epoxide.

added to the assay mixture. The effect of added reducing equivalents on the uptake of TCE by cells expressing the pMMO is examined and reported here for the first time.

In this chapter, the effects of varying copper and formate concentrations on TCE degradation are examined for one methanotroph, *Methylobacter albus* BG8. This strain was selected because as mentioned in Chapter 2 it can only express the pMMO and varying the growth concentrations of copper caused the kinetics of methane uptake to change. In addition it represents a group of methanotrophs that appear to be common in natural populations. As in the methane uptake experiments, copper was provided to the growth medium in concentrations up to 20 μM for the TCE degradation experiments. To examine the effect of an external source of reducing equivalents on TCE degrading experiments were carried out either in the absence or in the presence of 20 mM formate.

3.3 METHODS AND MATERIALS

3.3.1 Materials

As in the methane consumption assays, all chemicals used in media preparation were of reagent grade. *M. albus* was grown with highest purity methane (>99.99%) from Matheson gas company. Distilled-deionized water from a Corning Megapure D2 system was used for all media and stock solutions. The level of copper in this water was measured to be 0.45 ppb (7.1 nM) using an Inductively Coupled Plasma Mass Spectrometer (ICP-MS). Spectrophotometric grade TCE was obtained from the Aldrich Chemical Company.

3.3.2 Removal of Trace Metal Ions

All glassware was washed with detergent and then soaked in 1N HCl overnight to remove trace metals. The hydrochloric acid was subsequently removed by repeated rinses with distilled-deionized water until the conductivity of the rinse

water as measured with a conductivity meter from Yellow Springs Instruments Company (Yellow Springs, Ohio) was the same conductivity as the distilled-deionized water.

3.3.3 Growth Conditions of *M. albus* BG8

M. albus BG8 was grown on nitrate mineral salts medium (NMS) (Whittenbury) (31) with trace elements and vitamins at 30°C. Copper was added aseptically to sterilized medium as $CuSO4 \cdot (H2O)5$. The cells were grown in 2l flasks in which the culture medium was no more than 15% of the total flask volume to insure adequate gas transfer of methane and oxygen. The flasks were placed on a platform shaker at 200 rpm. The cells were grown to late-exponential phase and then harvested for TCE degradation assays.

3.3.4 Biorad® Protein Assay

To reference TCE uptake to the amount of cells present, the Biorad® protein assay was used to measure total cell protein. Standards were made using bovine serum albumin. The cells were digested at 90°C for 30 minutes in 0.5N NaOH. Serial dilutions were prepared to achieve final protein concentrations within the linear range of the assay. The amount of protein was determined by measuring the absorbance at 595 nm after the Biorad® assay was added and comparing to a standard curve.

3.3.5 Determination of TCE Biodegradation

Any residual methane remaining in the growth flasks was removed by evacuating the flasks three times and allowing air to re-equilibrate after each evacuation. Formate was added at this point in some cases as noted as a sterile stock of sodium formate. 5 ml aliquots were then aseptically transferred to 30 ml serum

vials. These vials were then capped with teflon coated rubber butyl stoppers and sealed with aluminum crimp seals. To obtain a range of TCE concentrations in solution, TCE was added to the vials from a saturated solution of TCE prepared by adding 20 ml of TCE to a 150 ml serum bottle with 130 ml distilled-deionized water. The stock solution was sealed with a teflon-coated rubber septum, wrapped in aluminum foil and shaken for at least two days. Prior to the experiment, the non-aqueous TCE phase was allowed to settle and the TCE-saturated water was added to the experimental vials making sure to exclude non-aqueous phase TCE. The TCE-saturated water was transferred using gas-tight syringes to minimize loss of TCE by volatilization. The serum vials were then shaken at 23°C at 200 rpm. At pre-determined time points, the cells were killed by adding 20 µl of 50% NaOH (w/v). The amount of TCE remaining was determined by headspace analysis. 50 µl of the headspace was removed with an A-2 gas-tight syringe from Dynatech Precision Sampling Corporation. The headspace samples were then injected into a Shimadzu GC-14A equipped with an electron capture detector and a 60 m capillary column, 0.32 mm inner diameter, packed with phenylmethyl polysiloxane. The injector, oven, and detector temperatures were set at 100°C, 150°C, and 300°C, respectively. The amount of TCE in the headspace was determined by comparing the GC results to those obtained from TCE standards made in methanol. The amount of TCE in solution was then calculated using a dimensionless Henry's constant of 0.35 (32). The amount of TCE degraded by the cells was considered to be the difference in total TCE mass between the sample vial and the concentration measured at t = 0 hours. The velocity of degradation was considered to be the total amount degraded divided by the total amount of cell protein and the time of degradation. All TCE degradation experiments were performed over a period of 2 hours to obtain the initial degradation rates. Killed controls received 20 µl of 50% NaOH (w/v) prior to addition of TCE, and were used to assess biological TCE degradation. For the experiments reported

here, each experiment was performed twice, with duplicate samples for each concentration and time point in all assays. The amount of TCE in each sample was measured twice using the Shimadzu GC-14A.

3.4 RESULTS

The disappearance of TCE was assumed to be due to co-metabolism by the pMMO. Volatilization losses were minimized using gas-tight syringes and the amount of TCE degraded biologically was determined by comparing the amount of TCE remaining after the cells were exposed to TCE to the amount remaining for the killed controls. The degradation of TCE by *M. albus* BG8 grown at 2 μM copper with and without formate added to the assay mixtures is shown in Figures 3.2 and 3.3. As can be seen in Figure 3.2, TCE was not degraded to any significant extent by the cells grown at 2 μM copper in the two hour time course of the experiment in the absence of formate. Therefore no kinetic parameters can be determined from this set of conditions. When formate was added to the assay mixture, TCE degradation was observed for cells grown with 2 μM copper. It may be possible that the cells grown with low copper have low endogenous reservoirs of reducing equivalents that can be augmented by providing formate. As shown in Figure 3.3, the initial rates of TCE degradation (V) were a function of TCE concentration. The data in Figure 3.3 have been fitted with a Michaelis-Menten model, with V_{max} predicted from the double-reciprocal plot in Figure 3.4 to be 35 nmol/(min•mg protein). With this value for V_{max}, K_S was then found to be 25 μM by determining the TCE concentration at $V_{max}/2$.

For the second set of conditions, *M. albus* BG8 was grown with 20 μM copper with and without extra formate in the assay. TCE degradation by *M. albus* BG8 with no added formate is shown in Figure 3.5. The data do not exhibit the expected asymptotic behavior. Instead the degradation velocity increased approximately

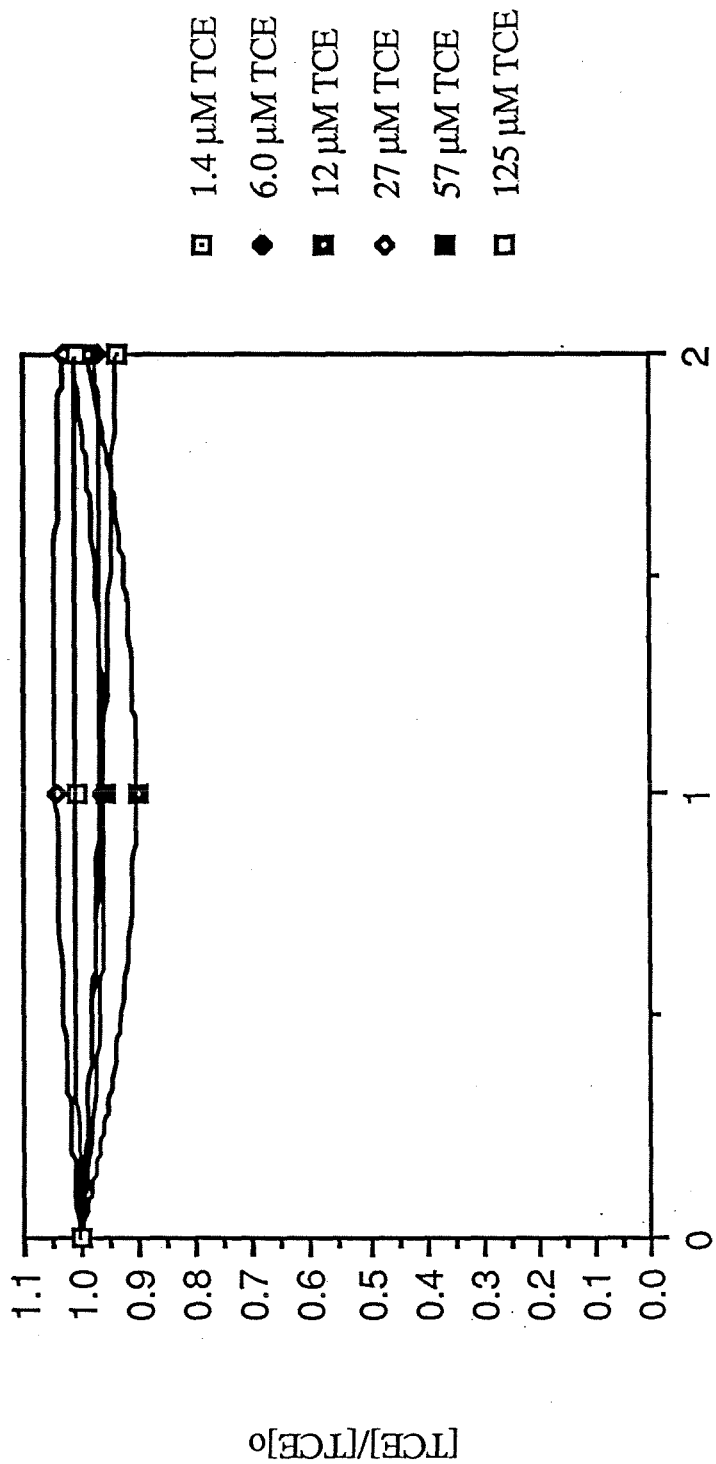

Figure 3.2. TCE degradation by *M. albus* BG8 with 2 µM copper.

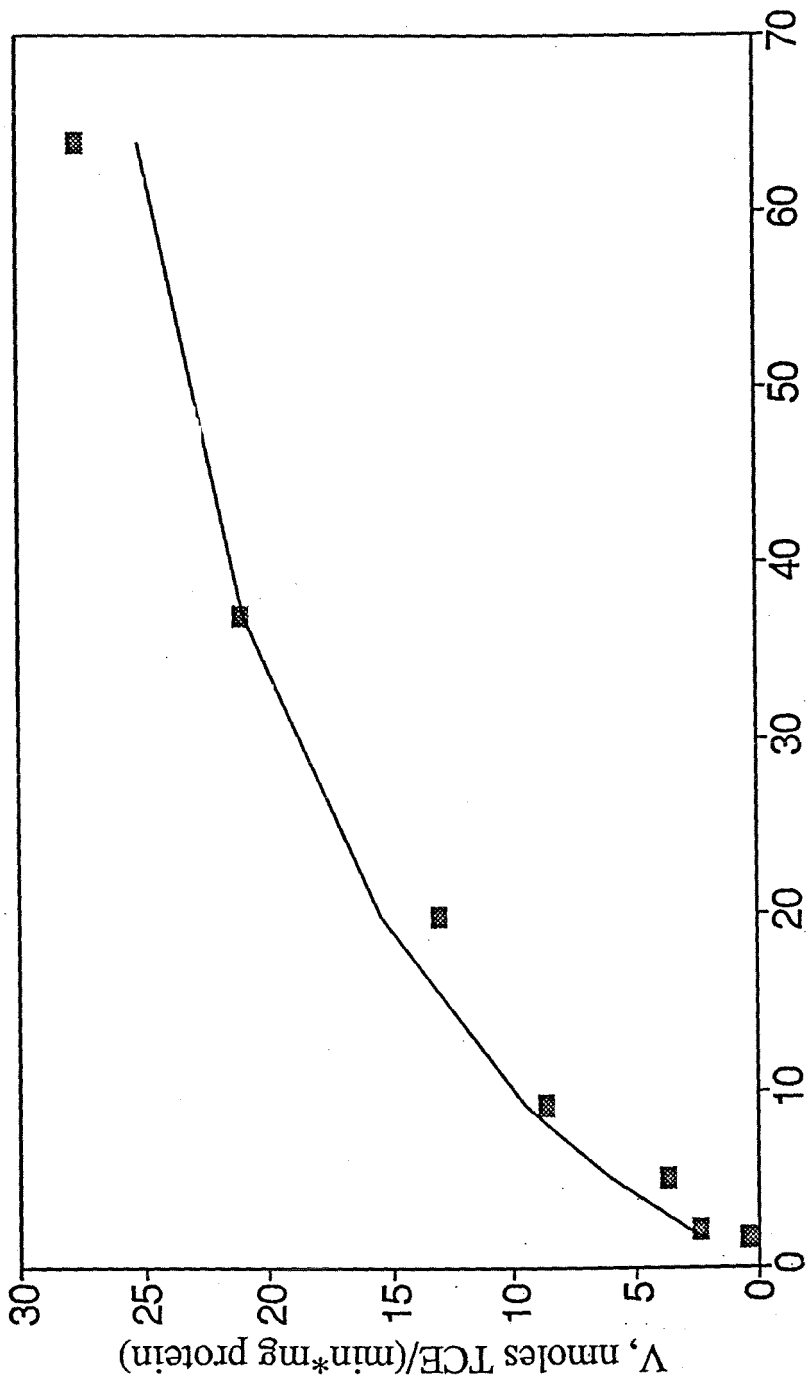

Figure 3.3. Rate of TCE degradation by *M. albus* BG8 grown with 2 µM copper and incubated with 20 mM formate as a function of TCE concentration.

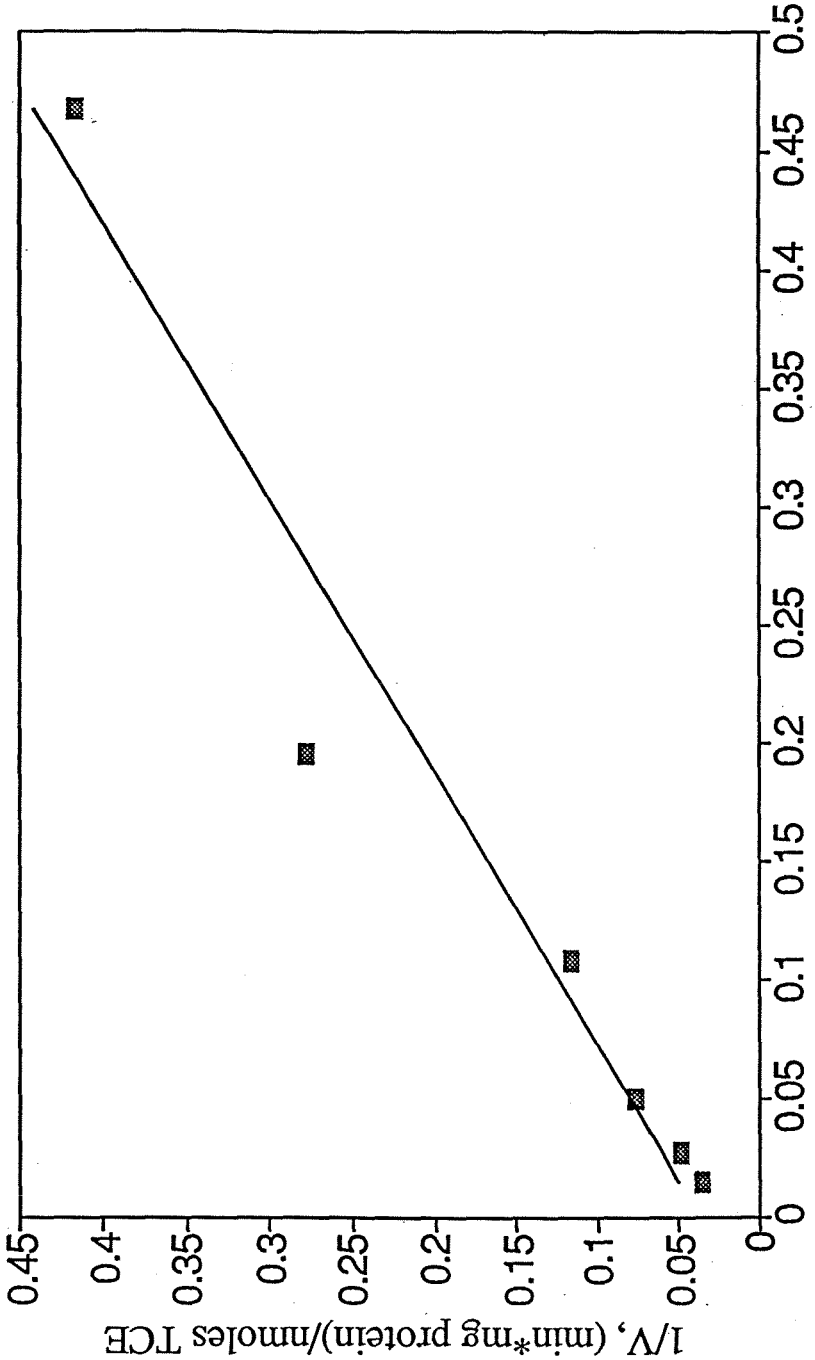

Figure 3.4. Double reciprocal plot of TCE degradation by *M. albus* BG8 grown with 2 µM copper and incubated with 20 mM formate during the assay.

$r^2 = .96$

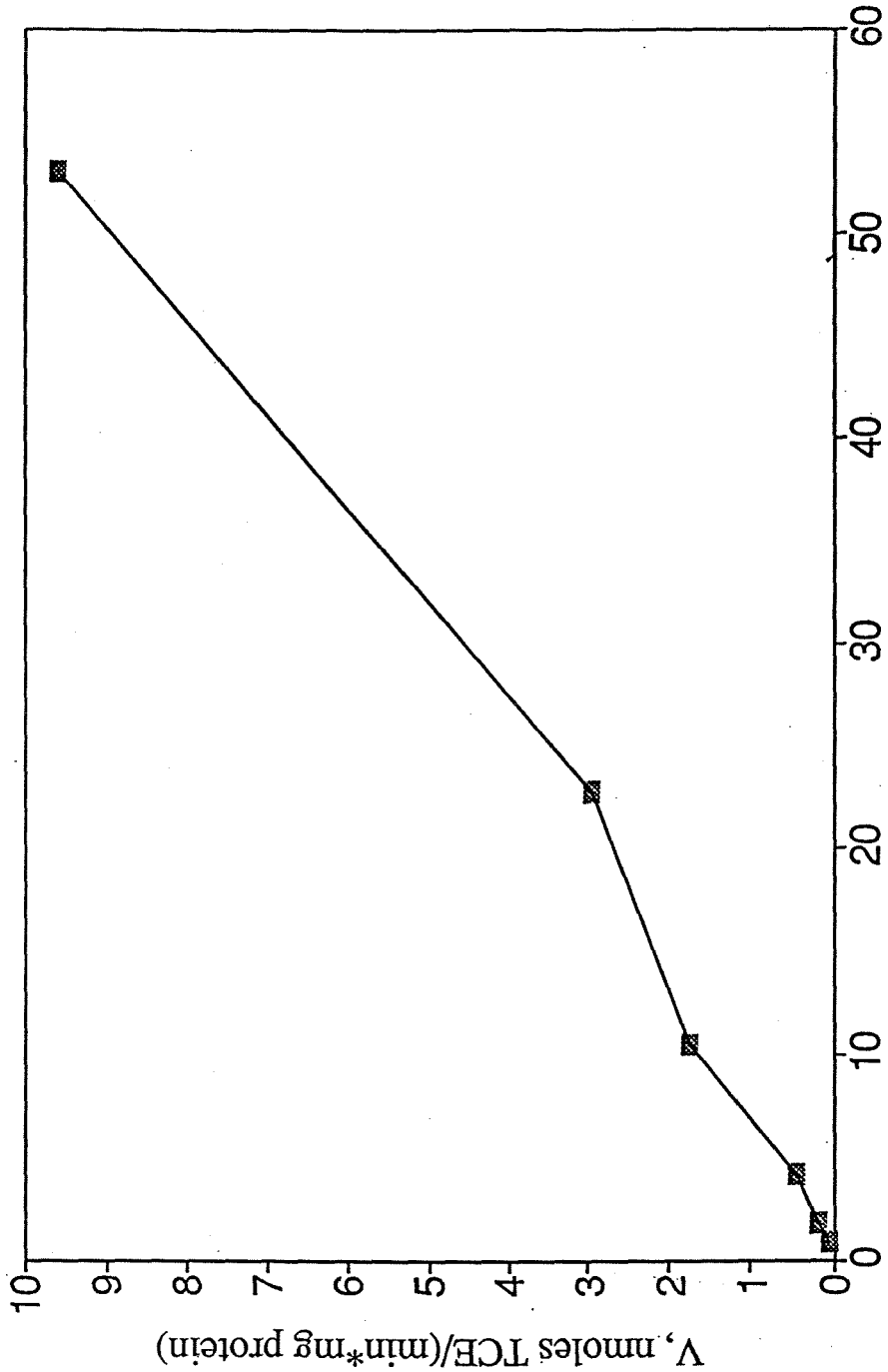

Figure 3.5. Rate of TCE degradation by *M. albus* BG8 grown with 20 µM copper as a function of TCE concentration.

linearly with the initial TCE concentration up to 53 μM of TCE. In this case, V_{max} can be estimated from the double-reciprocal plot in Figure 3.6 to be 37 nmol/(min•mg protein). Unfortunately the maximal uptake rate measured in the experiments was 9.8 nmol/(min•mg protein), much less than $V_{max}/2$. Therefore the K_S value can not be accurately determined in this study. It can only be said that the K_S for TCE for *M. albus* BG8 grown with 20 μM copper is greater than 53 μM. The double-reciprocal plot in Figure 3.6 also shows some curvature, indicating that some sort of cooperativity is present (33). If the degradation data are linearized using the Hill equation (eqn. 2.14), an n value of 1.3 is calculated.

Adding formate to the assay mixture of cells grown with 20 μM copper enhanced TCE degradation. As shown in Figure 3.7, the plot of velocity of TCE degradation vs. the initial TCE concentration exhibits an asymptotic, sigmoidal shape. The maximal uptake rate was determined to be 45 nmol/(min•mg protein). Since the plot is sigmoidal, the Hill equation was used to determine the n value. As shown in Figure 3.8, the n value was determined to be 2.2. The corresponding K_h value is then the TCE concentration at half the maximal degradation rate raised to the 2.2 power. This gives a K_h value of 1190 $\mu M^{2.2}$. The results of all TCE uptake experiments are compiled in Table 3.2.

3.5 DISCUSSION

From the TCE degradation assays, it is apparent that copper not only affects the uptake of methane by cells expressing the pMMO, it also affects the degradation of TCE. Analysis of the data from the TCE assays is more complicated than for the methane consumption assays because of the possible problems of limitation of reducing equivalents, substrate toxicity and product toxicity. To avoid problems associated with product toxicity, the time course of the experiments was designed to

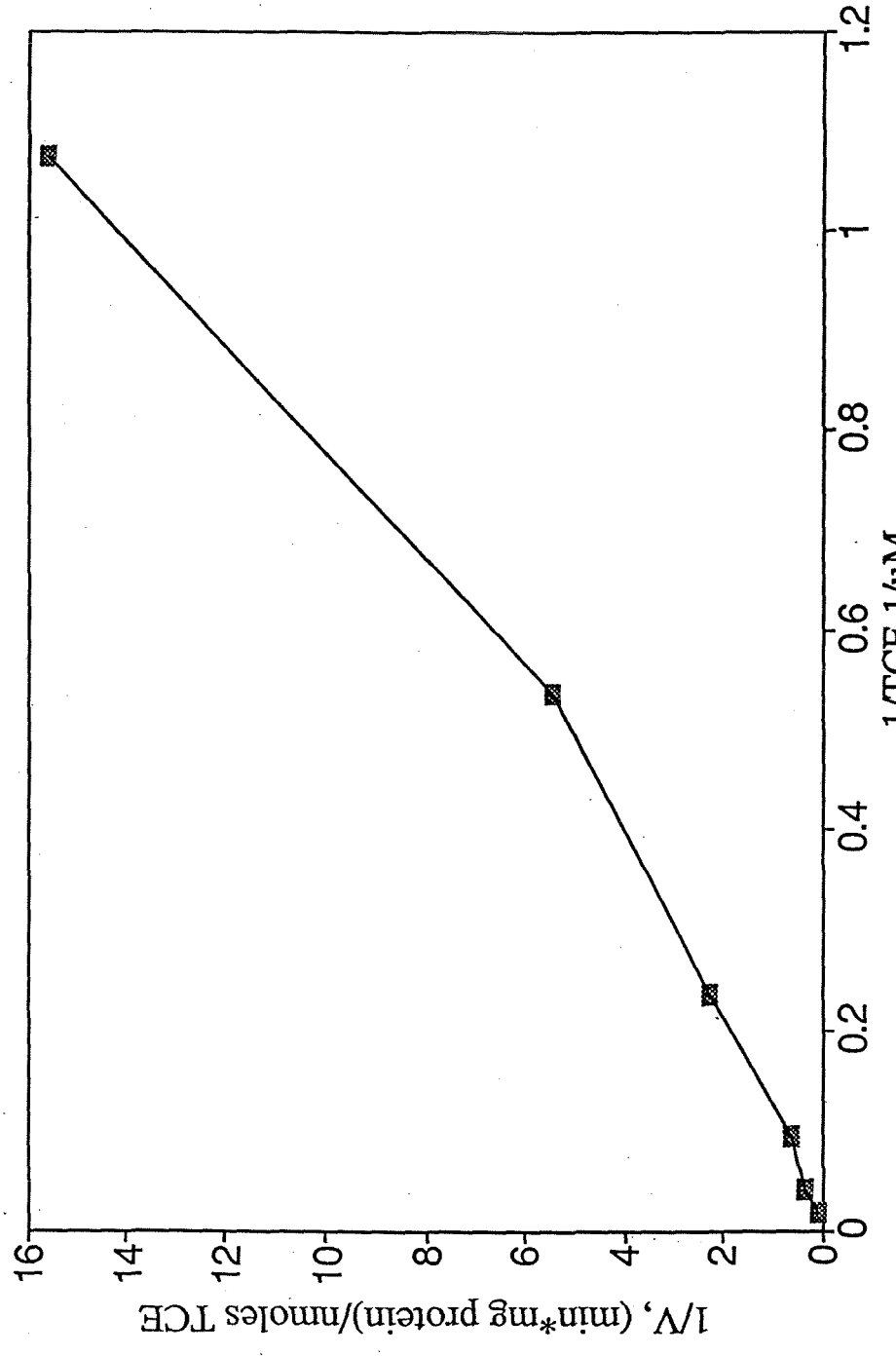

Figure 3.6. Double reciprocal plot of TCE degradation by *M. albus* BG8 grown with 20 µM copper.

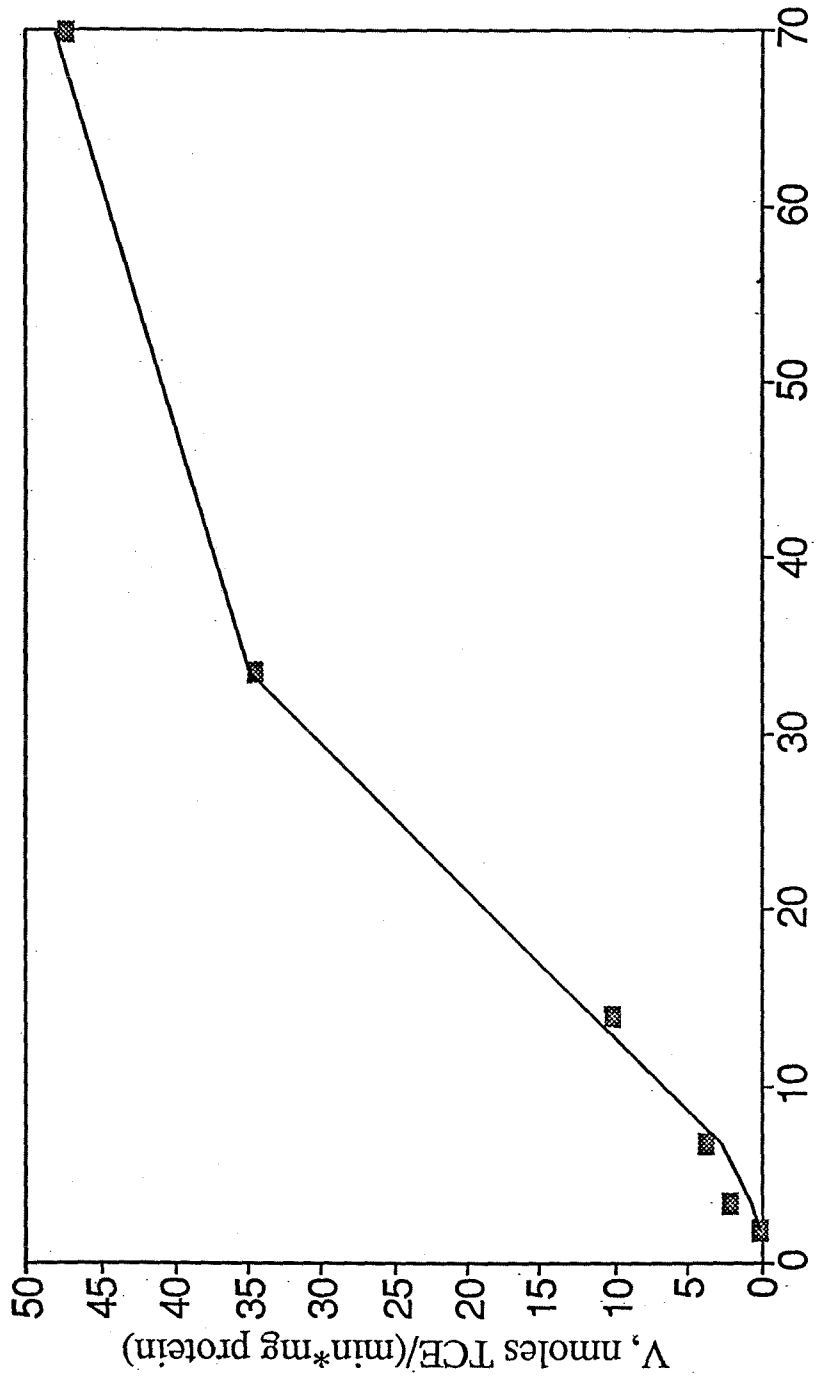

Figure 3.7. Rate of TCE degradation by *M. albus* BG8 grown with 20 µM copper and incubated with 20 mM formate as a function of TCE concentration.

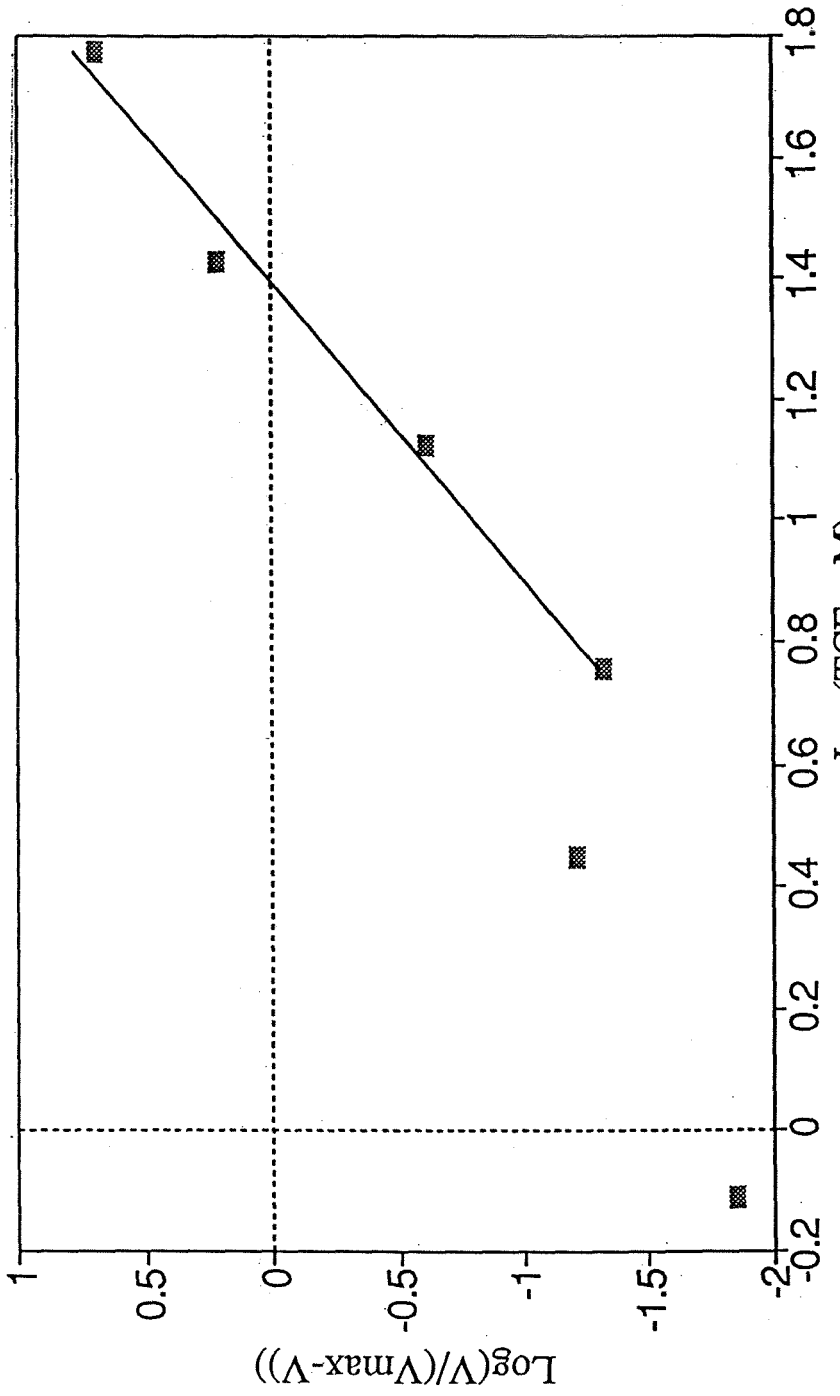

Figure 3.8. Hill plot of TCE degradation by *M. albus* BG8 grown with 20 µM copper and incubated with 20 mM formate.

$r^2 = .99$

Table 3.2. Kinetic parameters of TCE degradation by *M. albus* BG8.

Copper μM	Formate mM	K_S μM	K_h uM^n	V_{max} nmol/min/mg protein	n
2	0	NM[a]	NM	NM	NM
2	20	25	-	35	1
20	0	>53	66	~37	1.3
20	20	25	1190	53	2.2

[a]NM - No measurable TCE uptake.

be sufficient to obtain initial degradation rates, but not long enough to build up oxidation products to toxic levels. Since linear kinetics were always obtained over the two-hour time period, it was clear that product toxicity did not occur. To avoid substrate toxicity, TCE concentrations were kept at levels below that found to be toxic (34). Since the TCE degradation rate generally increased with increasing TCE concentrations up to a calculated V_{max} and never decreased with increasing TCE concentrations, substrate toxicity was in fact not encountered under these conditions (up to 75 μM). Therefore, the effect of copper and reducing equivalents, however, could be directly assessed.

If formate was added to the assay mixtures in order to provide a source of NADH, TCE degradation was stimulated at both high and low growth copper concentrations. As shown in Figure 3.2, cells grown with 2 μM copper showed no detectable TCE degradation over two hours. If formate was added to the incubation, TCE degradation was detected and a plot of V vs. S could be approximated with the Michaelis-Menten model (Figure 3.3). It is possible that in cells grown at 2 μM copper the endogenous reserves of reducing equivalents are low and that TCE degradation can be enhanced by providing an exogenous supply of reducing equivalents.

When *M. albus* BG8 was grown with 20 μM copper, but with no formate added to the assay mixture, TCE degradation was again detected. The degradation of TCE as shown in Figure 3.5, however, was linear with no upper limit being approached. It is possible that at the higher growth concentrations of copper the pMMO has greater affinity for in vivo reducing equivalents, therefore even though formate was not provided, TCE degradation occurred. The low endogenous supply of reducing equivalents, however, may limit the degradation of TCE. From these data only an estimate of V_{max} can be made from the double-reciprocal plots. The V_{max}

obtained from the double-reciprocal plots, 37 nmol/(min•mg protein) is over three times as great as the highest degradation rate measured, therefore the K_S value can also only be estimated to be greater than 53 μM. If formate is added to the assay mixtures, TCE degradation is greatly stimulated and an asymptotic plot of V vs. S is seen in Figure 3.7. The plot is sigmoidal in shape, suggesting that multiple active sites exist on the pMMO. Furthermore the V_{max} of 53 nmol/(min•mg protein) is about 1.5x greater than the other measured maximal rates. The asymptotic shape of the degradation rate vs. TCE concentration indicates that for this set of conditions, TCE is indeed the limiting substrate for TCE oxidation and meaningful kinetic data can be obtained. It is interesting to note that for cells grown at 20 μM copper and incubated with formate, the substrate concentration at the half-maximal degradation rate is 25 μM. It appears that as the cells are grown with higher copper, the degradation rate of TCE increases by a factor of 1.5, but the affinity for TCE remains about the same as measured by the substrate concentration at half-maximal degradation rate. As shown in Chapter 2, the affinity for methane by *M. albus* BG8 increased as the growth copper concentration increased. It is possible that the inclusion of more copper in the pMMO may cause a structural change in the pMMO, causing the affinity for the primary substrate to increase. For the remediation of contaminated sites, it is necessary to keep the ratio of K_{SCH4}/K_{STCE} to be as low as possible to have maximal co-metabolism of TCE. It may be advantageous to provide the cells with low copper concentrations and an endogenous supply of reducing equivalents.

Table 3.1 and 3.2 compile the kinetic data from this study and from other researchers. A comparison of these tables shows that the sMMO has a much greater V_{max} for TCE than the pMMO. Furthermore, the maximal degradation rates of TCE by the pMMO reported here are 100x greater than the values reported by DiSpirito et al (11). It is unknown why such a large discrepancy exists, but it may be because the

previous study only examined the degradation of TCE at one TCE concentration, typically around 100 μM. It is possible that this concentration of TCE is toxic to the cells, thereby limiting their ability to oxidize TCE. Furthermore, it is difficult to obtain accurate kinetic data by measuring the disappearance of TCE at one initial concentration. The values of V_{max} reported here are an order of magnitude less than those for the sMMO, which agrees well with the results of Hanson, et al. (14). In this study, *M. trichosporium* OB3b was grown at copper concentrations ranging from 0 to 1 mM. The oxidation of TCE was highest at 0 μM copper and decreased by an order of magnitude as the copper concentration increased. Although the form of the MMO expressed was not determined, it is likely that at low copper concentrations the sMMO was expressed, but at the high copper concentrations only the pMMO was expressed.

The affinity of cells expressing the pMMO for TCE is reported for the first time in this chapter. As can be seen in Table 3.2, the affinity of *M. albus* BG8 expressing the pMMO for TCE was similar at both high and low growth concentrations of copper with formate provided as an exogenous source of reducing equivalents. The K_S value of 25 μM under these conditions is 5-9x lower than the values reported for the sMMO. It may be advantageous to use methanotrophs expressing the pMMO to degrade TCE in situ because of the greater affinity of the pMMO for TCE, allowing biodegradation to remove TCE closer to EPA standards. Although the degradation rates are an order of magnitude less than the sMMO, it may be more desirable necessary to obtain more complete removal of TCE on longer time-scales rather than to obtain fast initial degradation that does not remove TCE to mandated levels.

As was observed with methane uptake, the TCE data support the idea that there are two kinetically different forms of the pMMO that change their relative

expression depending on the available copper. It is still unknown whether multiple active sites are created on the pMMO, thereby changing its structure and kinetics, or if two sets of genes encode slightly different forms of the pMMO and the expression of these two forms is regulated by the amount of bioavailable copper. Biochemical and genetic analyses of the pMMO are needed to address these questions.

3.6 CONCLUSIONS

Varying copper in the growth medium of *M. albus* BG8 affects the degradation of TCE as well as methane uptake. As shown in Chapter 2, the whole-cell affinity of *M. albus* BG8 for the primary substrate, methane increased with increasing copper, and it was proposed that the conformation of the pMMO may change with more copper to become more specific for methane. Since we have shown that under similar conditions the affinity of the cells for TCE does not change, it suggests that as the cells are grown in higher copper, the pMMO becomes more specific for methane. From these results it appears that the use of the pMMO for TCE degradation is optimal when the cells are grown at low copper concentrations with a exogenous supply of reducing equivalents. This could be advantageous for TCE degradation in situ because of the difficulty in providing copper in bioavailable forms to natural populations. Finally, as with methane oxidation, the data support the hypothesis that two kinetically different forms of the pMMO exist. From the whole-cell analysis it is still unclear if there is one form of the pMMO that has varying amounts of copper, and possibly varying numbers of active sites, or if there are two forms of the pMMO whose expression is regulated by the amount of bioavailable copper. Genetic and biochemical analysis of the pMMO are necessary to address these questions and are discussed in the next two chapters.

3.7 REFERENCES

1. The Merck Index, Centennial Edition. 1989. Merck and Co., Inc. Rahway, N. J.

2. Westrick, J. J., J. W. Mello, and R. F. Thomas. 1984. The groundwater supply survey. J. AWWA. **5**:52-59.

3. Travis, C. C. 1992. Toxic waste in groundwater: can it be removed? J. NIH Res. **4**:49-51.

4. Trvais, C. C. and C. B. Doty. 1990. Can contaminated aquifers at Superfund sites be remediated? Environ. Sci, Technol. **24:** 1464-1466.

5. Vertsraete, W. and E. Top. 1992. Holistic environmental biotechnology, in Microbial control of pollution, Ed. by J. C. Fry, G. M. Gadd, R. A. Herbert, C. W. Jones, and I. A. Watson-Carik. Cambridge University Press. Great Britain.

6. Alvarez-Cohen, L., and P. L. McCarty. 1991. Effects of toxicity, aeration, and reductant supply on trichloroethylene transformation by a mixed methanotrophic culture. Appl. Environ. Microbiol. **57**:228-235.

7. Alvarez-Cohen, L. and P. L. McCarty. 1991. Product toxicity and cometabolic competitive inhibition modeling of chloroform and trichloroethylene transformation by methanotrophic resting cells. Appl. Environ. Microbiol. **57**:1031-1037.

8. Alvarez-Cohen, L., P. L. McCarty, E. Boulygina, R. S. Hanson, G. A. Brusseau, and H. C. Tsien. 1992. Characterization of a methane-utilizing bacterium from a bacterial consortium that rapidly degrades trichloroethylene and chloroform. Appl. Environ. Microbiol. **58**:1886-1893.

9. Broholm, K., T. H. Christensen, and B. K. Jensen. 1993. Different abilities of eight mixed cultures of methane-oxidizing bacteria to degrade TCE. Wat. Res. **27**:215-224.

10. Brusseau, G. A., H-C. Tsien, R. S. Hanson, and L. P. Wackett. 1990. Optimization of trichloroethylene oxidation by methanotrophs and the use of a colorimetric assay to detect soluble methane monooxygenase activity. Biodeg. **1**:19-29.

11. Dispirito, A. A., J. Gulledge, A. K. Shiemke, J. C. Murrell, M. E. Lidstrom, and C. L. Krema. 1992. Trichloriethylene oxidation by the membrane-associated methane monooxygenase in type I, type II, and type X methanotrophs. Biodeg. **2**:151-164.

12. Eng, W., A. V. Palumbo, S. Sriharan, and G. W. Strandberg. 1991. Methanol suppression of trichloroethylene degradation by *Methylosinus trichosporium* (OB3b) and methane-oxidizing mixed cultures. Appl. Biochem. Biotech. **28**:887-899.

13. Fliermans, C. B., T. J. Phelps, D. Ringelberg, A. T. Mikell, and D. C. White. 1988. Mineralization of trichloroethylene by heterotrophic enrichment cultures. Appl. Environ. Microbiol. **54**:1709-1714.

14. Hanson, R. S., H. C. Tsien, K. Tsuji, G. A. Brusseau, and L. P. Wackett. 1990. Biodegradation of low-molecular weight halogenated hydrocarbons by methanotrophic bacteria. FEMS Microbiol. Rev. **87**:273-278.

15. Henry, S. M. and D. Grbic-Galic. 1991. Infuence of endogenous and exogenous electron donors and trichloroethylene oxidation toxicity on trichloroethylene oxidation by methanotrophic cultures from groundwater aquifers. Appl. Environ. Microbiol. **57**:236-244.

16. Henrysson, T. and P. L. McCarty. 1993. Influence of the endogenous storage lipid poly-β–hydroxybutryate on the reducing power availability during cometabolism of trichloroethylene and napthelene by resting methanotrophic mixed cultures. Appl. Environ. Microbiol. **59**:1602-1606.

17. Koh, S-C., J. P. Bowman, and G. S. Sayler. 1993. Soluble methane monooxygenase production and trichloroethylene degradation by a type I methanotroph, Methylomonas methanica 68-1. Appl. Environ. Microbiol. **59**:960-967.

18. Little, C. D., A. V. Palumbo, S. E. Herbes, M. E. Lidstrom, R. L. Tyndall, and P. J. Gilmer. 1988. Trichloroethylene biodegradation by a methane-oxidizing bacterium. Appl. Environ. Microbiol. **54**:951-956.

19. Nakajima, T., H. Uchiyama, O. Yagi, and T. Nakahara. 1992. Novel metabolite of trichloroethylene in a methanotrophic bacterium, *Methylocystis* sp. M, and hypothetical degradation pathway. Biosci. Biotech. Biochem. **56**:486-489.

20. Oldenhuis, R., J. Y. Oedzes, J. J. van der Waarde, and D. B. Janssen. 1991. Kinetics of chlorinated hydrocarbon degradation by *Methylosinus trichosporium* OB3b and toxicity of trichloroethylene. Appl. Environ. Microbiol. **57**:7-14.

21. Strandberg, G. W., T. L. Donaldson, and L .L. Farr. 1989. Degradation of trichloroethylene and trans-1,2-dichloroethylene by a methanotrophic consortium in a fixed-film, packed-bed bioreactor. Environ. Sci. Technol. **23**:1422-1425.

22. Taylor, R. T., M. L. Hanna, N. N. Shah, D. R. Shonnard, A. G. Duba, W. B. Durham, K. J. Jackson, R. B. Knapp, A. M. Wijesinghe, J. P. Knezoich, and M. C. Jovanivich. 1993. In situ bioremediation of trichloroethylene-contaminated water by a resting-cell methanotrophic microbial filter. Hydrolog. Sci. J. **38**:323-342.

23. Tsien, H-C., G. A. Brusseau, R. S. Hanson, and L. P. Wackett. 1989. Biodegradation of trichloroethylene by *Methylosinus trichosporium* OB3b. Appl. Environ. Microbiol. **55**:3155-3161.

24. Uchiyama, H., T. Nakajima, O. Yagi, and T. Tabuchi. 1989. Aerobic degradation of trichloroethylene by a new type II methane-utilizing bacterium, strain M. Agric. Biol. Chem. **53**:2903-2907.

25. Uchiyama, H., K. Oguri, O. Yagi, and E. Kokufuta. 1992. Trichloriethylene degradation by immobilized resting-cells of *Methylocystis* sp. M in a gas-solid bioreactor. Biotech. Lett. **14**:619-622.

26. Uchiyama, H. T. Nakajima, O. Yagi, and T. Tabuchi. 1989. Aerobic degradation of trichloroethylene at high concentration by a methane-utilizing mixed culture. Agric. Biol. Chem. **53**:1019-1024.

27. Fox, B. G., J. G. Borneman, L. P. Wackett, and J. D. Lipscomb. 1990. Haloalkene oxidation by the soluble methane monooxygenase from *Methylosinus trichosporium* OB3b: mechanistic and environmental implications. Biochem. **29**:6419-6427.

28. Newman, L. M. and L. P. Wackett. 1991. Fate of 2,2,2-trichloroacetaldehyde (chloral hydrate) produced during trichloroethylene oxidation by methanotrophs. Appl. Environ. Microbiol. **57**:2399-2402.

29. Miller, R. E. and F. P. Guengerich. 1982. Oxidation of trichloroethylene by liver microsomal cytochrome-P-450: evidence for chlorine migration in a transition state not involving trichloroethylene oxide. Biochemistry **21**:1090-1097.

30. Sittig, M. 1991. Handbook of toxic and hazardous chemical and carcinogens, Third Edition. Noyes Publications. Park Ridge, N. J.

31. Whittenbury, R. K., K. D. Philips, and J. F. Wilkinson. 1970. Enrichment, isolation and some properties of methane-utilizing bacteria. J. Gen. Microbiol. **61**:205-218.

32. Gossett, J. M. 1987. Measurement of henry's law constants for C_1 and C_2 chlorinated hydrocarbons. Environ. Sci. Technol. **21**:202-208.

33. Segel, I. H. 1975. Enzyme kinetics: behavior and analysis of rapid equilibrium and steady-state enzyme systems. John Wiley & Sons, Inc. New York.

34. Strand, S. E., M. D. Bjelland, and H. D. Stensel. 1990. Kinetics of chlorinated hydrocarbon degradation by suspended cultures of methane-oxidizing bacteria. J. Res. J. Water Pollut. Control Fed. **62**:124-129.

Chapter 4

The Role for Copper in the pMMO of *Methylococcus capsulatus* Bath: a Structural *vs.* Catalytic Function

(Submitted to *Journal Of Biological Chemistry*)

4.1 ABSTRACT

Methanotrophs convert methane to methanol by the methane monooxygenase (MMO). It is well known that two forms of the MMO can be expressed: one form is found in the cytoplasm, or in the soluble fraction (sMMO); the other is associated with the membranes, or particulate fraction (pMMO). The sMMO has been extensively examined, and much is known about its structure and mechanism of dioxygen activation. The pMMO, however, is less well understood: the enzyme has proven difficult to purify as it loses activity once the membranes become solubilized. Furthermore, although copper is known to be important for the stability and activity of the pMMO, its role is still unclear. In a recent study, we reported the use of electron paramagnetic resonance (EPR) spectroscopy to probe the nature of the copper ions in these membranes. Two EPR signals were uncovered for the highly oxidized membranes: one set of signals arises from the type 2 Cu(II) centers, and the other has been assigned to trinuclear copper (Cu(II)) clusters (H-H. Nguyen et al *J. Biol. Chem.*, in press). Here, we attempt to correlate the EPR spectra of the membrane fraction of *Methylococcus capsulatus* Bath with the amount of copper present in the membranes and to the activity of the pMMO as measured by the production of propylene oxide from propene by the pMMO. From these studies we conclude that the primary role of copper is in the active site of the pMMO rather than simply a structural one.

4.2 INTRODUCTION

Methanotrophs are a group of gram-negative bacteria that utilize methane as their sole carbon and energy source. Three general categories of methanotrophs have been identified based on their pattern of internal membranes, carbon assimilation pathway, 16s rRNA sequence, mole percent G + C, and predominant fatty acid chain length (1). In particular, type I methanotrophs (γ-proteobacteria) have stacks of membranes throughout the cytoplasm, while type II strains (α-proteobacteria) have intracytoplasmic membranes in rings around the periphery of the cell membrane. Type X strains have characteristics of both type I and type II, although they contain type I membranes and class phylogenetically with the type I strains in the γ-proteobacteria (1).

The total oxidation of methane by methanotrophs is initiated by the enzyme methane monooxygenase (MMO), which catalyzes the conversion of methane to methanol. In the *Methylococcus* (type X) and *Methylosinus* (type II) strains, MMO can be expressed in two forms, a cytoplasmic or soluble form (sMMO) and a membrane bound or particulate form (pMMO) (2-5). Two other strains, *Methylomonas methanica* 68-1, and *Methylocystis* M, have also been shown to express both forms (6,7). All other strains have only been shown to express the pMMO. The sMMO has been extensively studied. It consists of three protein components: the hydroxylase; the reductase; and a regulatory subunit. The hydroxylase component contains a binuclear iron cluster which is the putative center

for dioxygen reduction (8-10). The crystal structure of the sMMO hydroxylase from *Methylosinus trichosporium* OB3b has recently been reported (11). The pMMO has been less well characterized due to the lack of a reproducible procedure for purification of this protein in active form. Study of the pMMO is important, however, because of the potential applications of the pMMO for commercial use, including the degradation of small halogenated hydrocarbons (12), because of the importance of methanotrophs in the global methane budget and global warming (13), and because of the industrial importance of the methane to methanol conversion (14). As the majority of known methanotrophic strains express only the pMMO, it is crucial to gain more fundamental knowledge of the biochemistry of this enzyme.

Copper has recently been shown to be an important factor in MMO expression and activity. In the strains *M. capsulatus* Bath and *M. trichosporium* OB3b, expression of sMMO versus pMMO has been shown to be controlled primarily by the amount of copper in the growth medium, sMMO being the dominant form expressed under conditions of copper limitation (15,16). Addition of copper to the growth medium has also been shown to increase pMMO activity in cell free extracts and membrane fractions of *M. capsulatus* Bath and in whole cells of *Methylomonas albus* BG8 (a type I methanotroph) up to a limiting concentration of copper (various values) beyond which the activity decreases (17-20). Addition of copper to cell free extracts (17) and membrane fractions of *M. capsulatus* Bath (16) during assay has also been shown to further increase *in vitro* pMMO activity. In addition copper has been shown to affect the membrane and lipid content of *M. capsulatus* Bath (17, 21). In particular,

addition of copper to the growth medium results in formation of tightly packed arrays of intracytoplasmic membranes up to a limiting concentration of copper, at which larger lumenal spacings appear between the membrane (3). In *M. albus* BG8, copper has also been shown to affect cell yield (20).

Although the role of copper in pMMO activity is still not fully understood, some important insights have been recently obtained. In a recent study, we reported an electron paramagnetic resonance (EPR) study of the copper ions in highly oxidized membrane fractions of *M. capsulatus* Bath grown under varying copper concentrations in the growth medium. Two overlapping signals were uncovered: one signal appears to be due to normal type 2 copper centers; the second has been attributed to a copper cluster, and its intensity has been shown to correlate with pMMO activity. This has led to the preliminary hypothesis that the latter center is the active site of the pMMO (18,19). In this earlier study, however, copper ions were added to the isolated membranes prior to pMMO activity assays and EPR analysis. It is conceivable then that the type 2 copper EPR signals have origin in adventitiously bound copper ions, incompletely assembled copper sites, or assembled copper sites that are otherwise distorted so that weak exchange coupling between the copper ions no longer prevail. This scenario seems rather likely since there are indications that a large number of clusters are associated with each protein molecule and they appear to be dispersed heterogeneously throughout the protein structure. Therefore, it is still unclear whether copper plays a secondary, structural role on the tertiary folding of the protein, in addition to serving directly as active sites for dioxygen activation. Toward addressing

this issue, we have now carefully prepared membrane samples of *M. capsulatus* Bath under more controlled conditions, with and without copper added to the isolated membranes prior to pMMO activity assays and EPR analysis, and have compared the EPR spectra, copper/protein ratio, and pMMO activity under both sets of experimental conditions. From these studies we have been able to conclude that copper plays a role in the active site of the pMMO rather than a simple structural one.

4.3 METHODS AND MATERIALS

M. capsulatus Bath was grown on NMS medium (22) with an additional vitamin mixture (23). Copper in the form of a sterile stock of $CuSO_4 \bullet (H_2O)_5$ was added to the autoclaved medium at varying concentrations immediately prior to inoculation. Samples with 2 and 10 μM $CuSO_4$ added to the medium were grown in flasks with 250 mL medium and utilized for propylene epoxidation assays and EPR studies. Samples with 5 μM $CuSO_4 \bullet (H_2O)_5$ added to the medium were grown in flasks for EPR studies, and in an 8 L fermentation system for propylene epoxidation assays and metal assays. Samples with 20 μM $CuSO_4 \bullet (H_2O)_5$ were grown in flasks for propylene epoxidation assay and EPR, and in an 8 L fermentation system for metal assays.

Membrane fractions were obtained from whole cell preparations as follows. The cells were harvested by centrifugation (7000 rpm, 25 minutes) and then washed three times in 10 mM Pipes buffer. The pellet was resuspended and cells were lysed by passing through a French pressure cell (SLM Aminco, Silver Spring, MD) three

times at 20,000 psi. At this point the cell preparation was split in half and the copper concentration was increased in one of the fractions by adding $CuSO_4 \bullet (H_2O)_5$ to a concentration of 200 μM. Unlysed cells were removed by centrifugation at 13000 rpm for 15 minutes, and the resultant supernatant was ultracentrifuged at 65000 rpm for one hour to pellet out the membrane fraction. The membrane fraction was then washed once by resuspending it in 10 mM Pipes buffer and repeating ultracentrifugation. This procedure differs from that in previous studies in which excess copper was added directly to the purified membrane extract for activity assays and EPR analysis (18, 19). With that procedure, the effect of added excess copper on the activity of the pMMO can be measured, but the corresponding EPR spectra could be complicated by large amounts of adventitious and unbound copper. The extra steps in the procedure used in the present experiments should remove loosely-bound copper. For direct comparison, membrane extracts were also purified according to the method of Nguyen et al (19). In both purifications, the resultant pellets were resuspended in 1 mL of 10 mM Pipes.

The pMMO activity of the resultant membrane fractions was determined immediately after harvest by the propylene epoxidation assay described by Colby, Stirling and Dalton (24) with the following modification: the membrane activity was assayed at room temperature with 5 mM NADH added as an external source of reducing equivalents. Propylene oxide formation was monitored by injection of 2 mL

liquid samples into a Hache Carle (Oklahoma City, OK) gas chromatograph with a Haysep A column at 140° C.

Protein concentration was determined by Bio Rad Protein Concentration Assay (Bio Rad, Hercules, CA). Metal analysis was performed by Gordon Bradford at the Department of Soil and Environmental Sciences of U.C. Riverside by the method of inductively coupled plasma optical emission spectroscopy (ICP-OES), and by the authors by the method of inductively coupled plasma mass spectroscopy (ICP-MS). EPR studies were performed on an E-line Century X-band Spectrometer (Varian, Palo Alto, CA) equipped with an ESR-900 liquid helium cryostat (Oxford Instruments, Oxford, UK) for low temperature observations.

4.4 RESULTS AND DISCUSSION

Activity data obtained in this and previous studies are compared in Table 4.1. In the present study, addition of copper to membrane fractions after cell lysis increased pMMO activity as measured by the propylene epoxidation assay for all samples regardless of the amount of copper added to the cell growth medium. The additional copper increased activity by a factor of 1.1 to 2.5. This ratio is in good agreement with previous work done on cell free extracts of *M. capsulatus* Bath (15), but is lower than the results reported in a previous study of membrane fractions (18, 19). In addition, the specific activities obtained in the present study are lower than the specific activities reported previously for the cell-free extracts and membrane fractions. Different procedures were used, however, in all these studies. In the first, activities were measured in cell-free extracts, not membranes (15). In the study on membrane

Table 4.1. Comparison of the effects of copper added after cell lysis on pMMO activity.

Source	($CuSO_4$) in growth medium (μM)	pMMO specific activity without excess $CuSO_4$ (nmol/min/mg)	pMMO specific activity with excess $CuSO_4$ (nmol/min/mg)	Ratio of activity with and without excess $CuSO_4$
Cell-free extract study of (15) (400 μM excess copper)	0	0	4.1	∞
	1.3	3.9	7.3	1.9
	3.8	10.5	18.7	1.8
	6.3	44.7	75.4	1.7
	7.6	110.1	175.6	1.6
	13	58.2	92.1	1.6
Membrane study of (19) (150 μM excess copper)	<0.3	0.68	19.5	29
	2.0	9.6	27.3	2.8
	5.0	17.6	27.7	1.6
	10.0	26.8	30.2	1.1
	20.0	53.7	22.1	0.41
Present study (200 μM excess copper)	0.0	0.18	0.25	1.4
	0.0[A]	0.52[A]	1.3[A]	2.5[A]
	2.0	2.2	3.4	1.5
	5.0	2.1	3.6	1.7
	10.0	5.3	5.9	1.1
	20.0	3.0	4.6	1.5
	20.0[A]	9.0[A]	23.0[A]	2.6[A]

[A] Based on analysis of membranes purified in this study according to the procedure of (19).

fractions, copper was added directly to the assay mixture (19). Since one of our objectives of the present study is to determine the effects of added copper on the EPR spectra and pMMO activity, in the present experiments copper was added after cell lysis and any excess and loosely-bound copper, which might complicate the EPR spectrum, was subsequently washed away (see Experimental).

To determine whether the discrepancy between previous results and those obtained in the current study were due to procedural differences, cells grown at 0 and 20 μM $CuSO_4•(H_2O)_5$ were harvested and membrane extracts purified according to the procedure of Nguyen *et al* (19). As shown in Table 4.1, higher activities were indeed, obtained using this procedure than with the procedure developed in this paper, suggesting that at least part of the difference was due to the extra copper associated with the membranes in the procedure of Nguyen, *et al* (19). Metal analysis in Table 4.2 shows that the copper/protein ratio in the membranes is greater in our experiments using the method of Nguyen *et al.* (19) though still substantially less than the values reported in that previous study. It seems likely that the procedure used in the previous study (19) resulted in higher residual copper in the membrane preparations, which may have enhanced pMMO activity except in the case of high (20 μM) copper, where it inhibited activity. The lower activity obtained with our present procedure in comparison to the study with cell extracts (15) was probably due to a loss of activity during membrane purification. These comparisons emphasize the relationship between copper content in the membranes and pMMO activity.

Table 4.2. **Results of copper analysis of membrane fractions with and without copper added after cell lysis[A].**

($CuSO_4$) in growth medium, μM	(μg Cu)/(mg protein)	(μg Cu)/(mg protein) with 200 μM additional $CuSO_4$	Ratio of copper content with and without added $CuSO_4$
0	0.065	0.60	10
0[B]	0.11[B]	C	C
5	0.22	0.36	1.6
10	0.66	0.84	1.3
20	1.6	1.7	1.1
20[B]	5.2[B]	C	C

[A] Samples from cells grown with 5 and 20 μM copper in the medium were analyzed by ICP-OES; samples with 0 and 10 μM copper were analyzed by ICP-MS. [B] Metal analysis performed on membranes purified according to the procedure of (19). [C] Not measured.

As shown in Table 4.2, as the ratio of copper/protein increased in the current study, the activity of the pMMO also increased. Furthermore, these results show unequivocally that samples grown under high copper concentration incorporated less additional copper into their membranes after cell lysis than samples grown at low copper concentrations using the procedure developed in this study. Assuming all of the copper measured is in the pMMO, that the pMMO is the bulk of the measured protein, and that the mass of the pMMO is approximately 100,000 kDa, we estimate the maximum number of copper atoms per protein molecule to approach 8 in present experiments. Until the pMMO can be purified in its active state, however, the amount of copper and the exact size of the pMMO cannot be accurately measured.

To assess whether the additional copper incorporated into the membranes is associated with type 2 copper sites or with the reported "cluster" signal, X-band EPR spectra of the membrane preparations were taken. Figure 4.1 shows the results for membranes collected from cells grown with 0, 2, 5, 10 and 20 μM copper using the procedure outlined in this paper. As can be seen in Figure 4.1, as the growth concentration of copper increased, only the putative copper cluster signal increased. Furthermore, in Figure 4.2, the EPR spectra of membrane preparations from cell grown with 0 and 20 μM copper with and without additional copper in the purification procedure are shown. Because any unbound and loosely-bound copper should have been removed in subsequent washings in these experiments, meaningful comparison

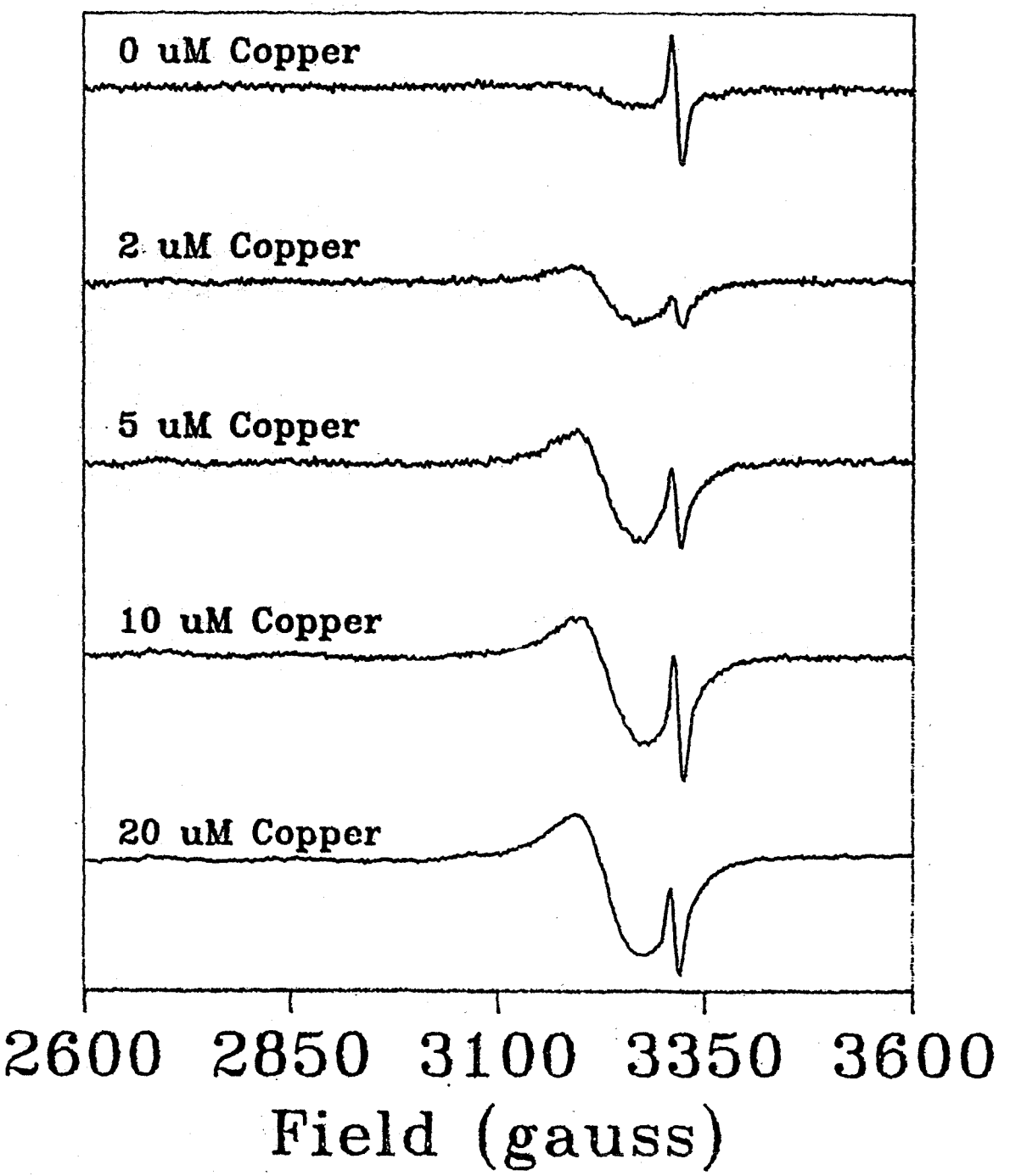

Figure 4.1. EPR spectra of membranes of *M. capsulatus* Bath cells grown with varying copper concentrations.

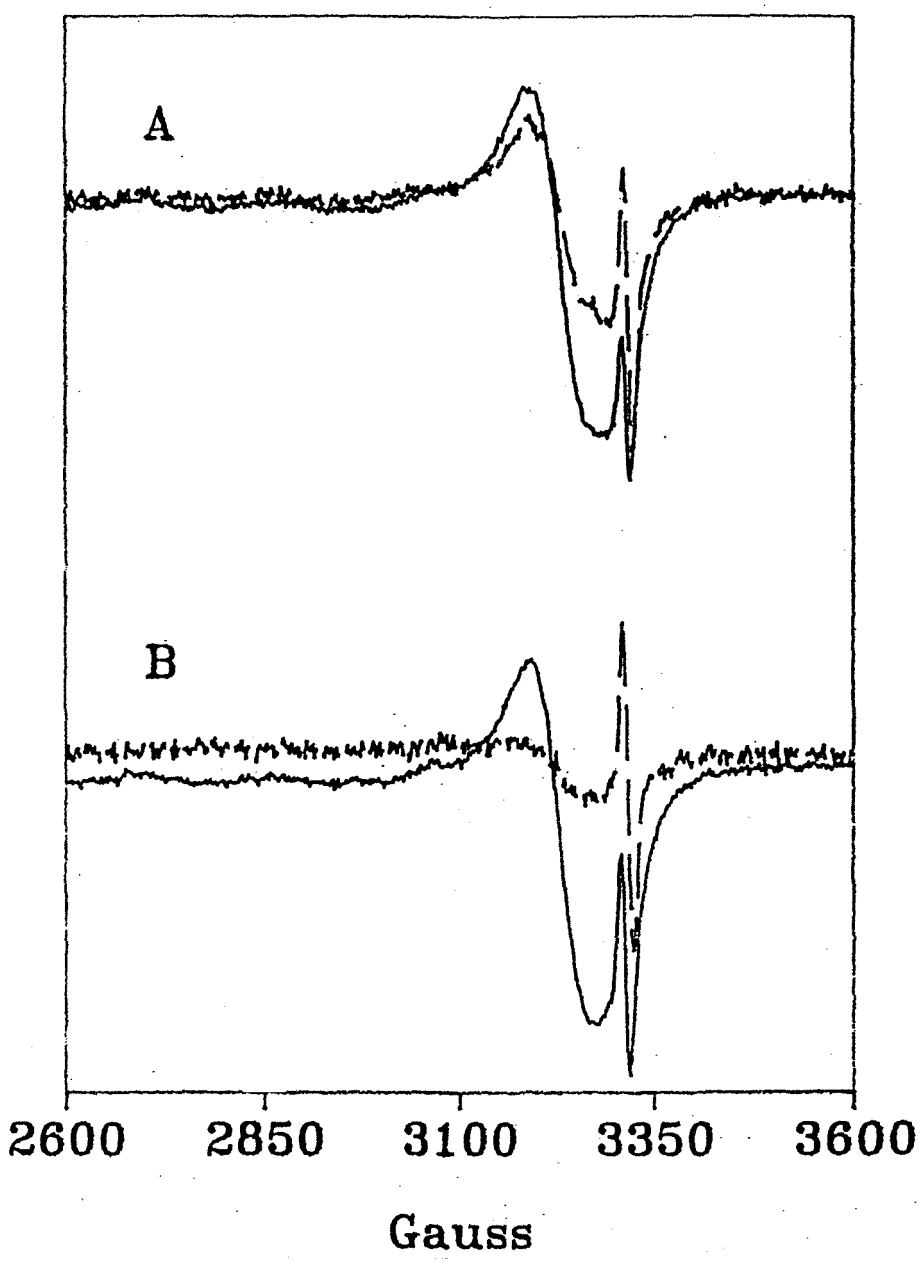

Figure 4.2. EPR spectra of membranes of *M. capsulatus* Bath. A. Membrane samples with excess copper. B. Membranes samples with no excess copper added during purification. Initial growth conditions: membranes purified from cells grown with 0 μM copper (----); membranes purified from cells grown with 20 μM copper (——).

can be made of the EPR spectra taken both with and without added copper. As seen in Figure 4.2, type 2 copper signals are weak in the membranes with and without excess copper. The "cluster" signal around g = 2.0, however, is apparent in membranes from cells grown with 20 μM copper, but not for cells grown with 0 μM copper. Figures 4.1 and 4.2 also show that for samples to which excess copper was not added, only the putative copper cluster signal increased proportionally to the activities reported in Table 4.1, suggesting that this cluster signal and not the type 2 may represent part of the pMMO active site. Previous work has hypothesized that this signal is due to a copper cluster with an odd number of copper atoms, most likely three (19).

Figure 4.3 shows the relationship between the copper/protein ratio and the activity of the pMMO. As can be seen, the expected hyperbolic trend is present with one notable exception. For membranes purified from cells grown with 0 μM copper to which extra copper had been added, the activity did not increase significantly although the copper/protein ratio did. This is especially interesting as Figure 4.2 also shows that the EPR spectra of samples with extra copper are very similar, regardless of the initial growth concentration of copper. The discrepancy between measured activity and what would be expected from EPR spectra and metal analysis may be explained as follows.

The current hypothesis for oxygen activation of the pMMO requires a fully reduced form of the copper cluster. Copper was added, however, as Cu(II) in the

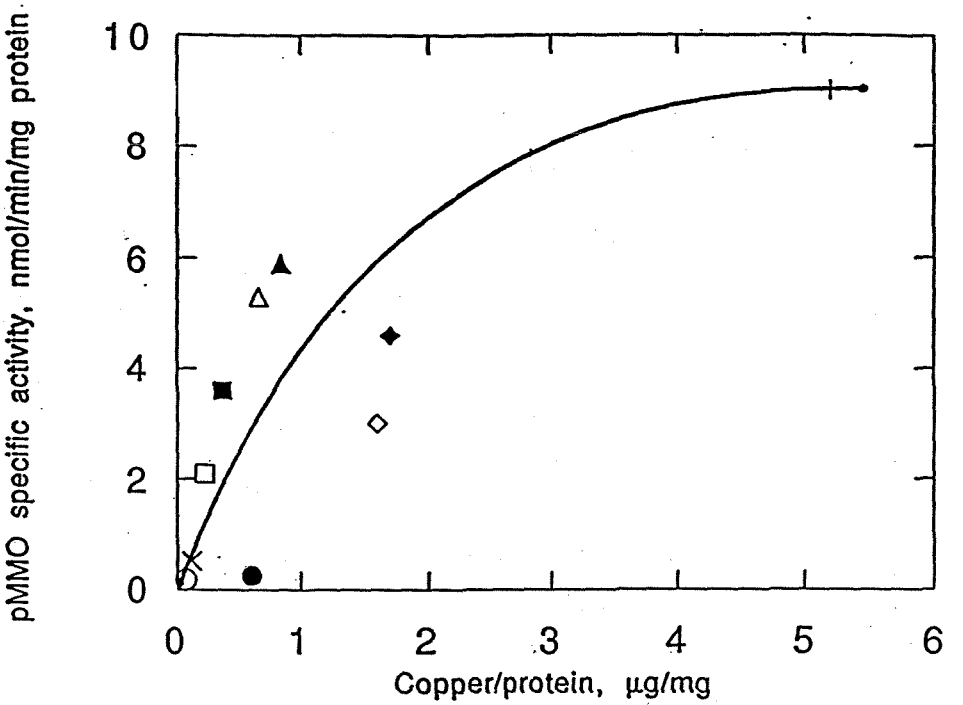

Figure 4.3. Dependence of the pMMO specific activity on copper/protein ratio in *M. capsulatus* Bath. Open symbols are for samples to which no excess copper was added during membrane purification. Closed symbols indicate samples to which excess copper was added. Initial growth conditions - (○, ●): membranes purified from cells grown with 0 µM copper; (□, ■): membranes purified from cells grown with 5 µM copper; (Δ, ▲): membranes purified from cells grown with 10 µM copper; (◊, ♦): membranes purified from cells grown with 20 µM copper; (×): membranes purified from cells grown with 0 µM copper using the method of Nguyen, et al (19); (+): membranes purified from cells grown with 20 µM copper using the method of Nguyen, et al (19).

form of $CuSO_4 \bullet (H_2O)_5$. Any cluster formed from the addition of copper after cell lysis would initially be fully oxidized and require reduction before activity could be assayed. If this is true, some lag after NADH has been added to the assay mixture should be seen in membrane preparations from cells grown with low copper. In Figure 4.4, the production of propylene oxide over time is shown for samples prepared from cells grown with 0 and 20 μM copper. The data showed that membrane preparations from cells grown at a low copper concentration (0 μM) have at least a 40 minute lag before any propylene oxide is measured. Figure 4.4 also shows that for samples taken from cells grown with 20 μM copper there was no lag before activity was seen. The sites formed during growth may therefore exist in a fully or partially reduced state that are more easily activated through the addition of reducing equivalents in the form of NADH than those sites created after cell lysis with the addition of excess copper.

Another possible reason for the lack of significant activity increase from cells grown with 0 μM copper is that the addition of excess copper to the purified membranes may not create the full complement of copper atoms required for formation of the trinuclear copper clusters. Depending on the amount of copper present in the membranes during growth and the amount of the excess copper available to the sites, the copper may be monomeric (type 2 sites); copper dimers may also be formed that are inactive and EPR silent. This suggests that the additional copper plays an active site role, rather than the structural role that the type 2 site, which has not been correlated to pMMO activity, would suggest. Since the putative cluster signal

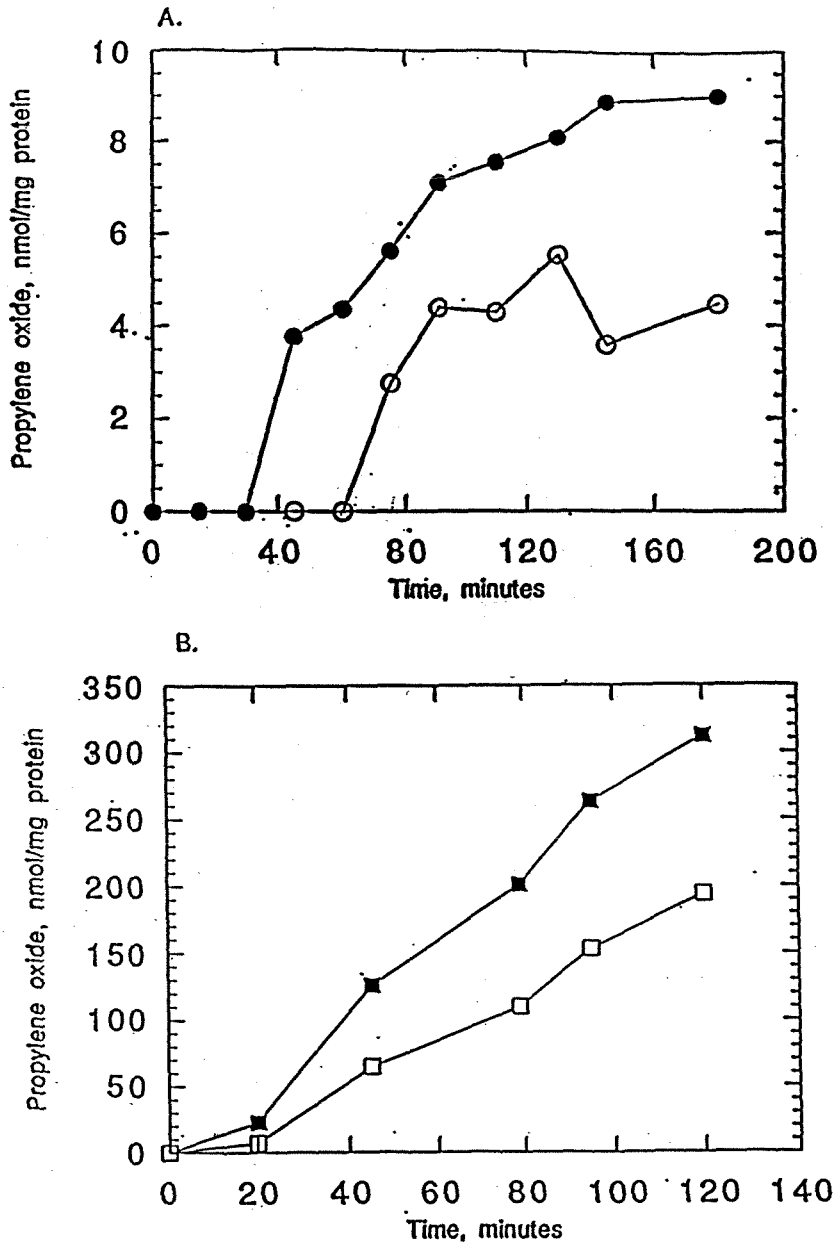

Figure 4.4. Propylene oxide formation by membrane preparations of *M. Capsulatus* Bath. A. Propylene oxide formation from membranes purified from cells grown with 0 μM copper. B. Propylene oxide formation from membranes purified from cells grown 20 μM copper. Closed symbols are for membrane preparations to which excess copper has been added. Open symbols are for membrane preparations with no excess copper.

increased more significantly for samples grown with low copper concentrations to which excess copper was added during membrane purification than for cells grown under high copper concentrations, it is possible that at higher copper growth concentrations more of the active sites are approaching saturation with copper.

The current results suggest the following scenario. Cell lysis either disrupts an extremely labile set of copper active sites in the pMMO or exposes pMMO with incompletely filled copper active sites. Addition of copper to this system then supplies copper to these deficient active sites, restoring or increasing assayed pMMO activity. This conclusion seems particularly reasonable in light of recent results on ammonia monooxygenase (AMO). This enzyme is similar to pMMO in substrate range and inhibitors, and its activity has been shown to be dependent on copper (25). Recently it has been shown that addition of copper to cell extracts restores AMO activity lost upon cell lysis. No increase in activity is seen with addition of copper to whole cells, nor do other metal ions increase AMO activity in the cell extracts, as might be expected if the copper played a structural rather than a catalytic role. The conclusion drawn from this study is that copper is lost from the membranes after cell lysis, yielding inactive enzymes which are reactivated by addition of catalytically important copper (25). This conclusion is extremely similar to that drawn here for the pMMO. In the current study, in addition to observing the increased activity seen in the AMO and previously in the pMMO, we have used EPR results to show that the added copper likely plays an active site role. Although we have shown here that the primary role of copper in the pMMO is in the activation of dioxygen, it is a misrepresentation

to state that copper involved in the active site can not also play as structural role in the folding of the pMMO. The creation of the active site may be necessary for the correct tertiary structure for optimal activity of the enzyme.

4.5 CONCLUSIONS

The present study provides specific evidence that copper added to membrane fractions after lysis is incorporated into sites hypothesized in previous work to be a constituent of the pMMO active site. This study also shows that some of the copper added is loosely bound, as indicated by the removal of much of the added copper with washing. Furthermore, the study presents strong evidence for a catalytic role for copper in the pMMO. Although copper is believed to be primarily involved in the activation of dioxygen, the copper clusters may play a secondary role in the folding the protein to the correct structure. The copper cluster(s), however, must be in a fully reduced state for activity to be apparent, therefore addition of Cu(II) need not significantly increase activity. The results are in good agreement with recent studies on the closely related AMO, and suggest that copper plays an important active site role in both systems.

4.6 REFERENCES

1. Hanson, R. S., A. I. Netrusov, and K. Tsuji. 1992. in *The Prokaryotes,* Balows, A., Truper, H. G., Dworkin, M., Harder, W., and Schleifer, K-H. Ed., Springer-Verlag, New York Vol. I, Chap. 118.

2. Green, J., and H. Dalton. 1989. Substrate specificities of soluble methane monooxygenase: mechanistic implications. J. Biol. Chem. **264**:17698-17703.

3. Higgins, I. J., D. J. Best., R. C. Hammond, and D. Scott. 1981. Methane-oxidizing microorganisms. Microbiol. Rev. **45**:556-590.

4. Woodland, M. P., and H. Dalton. 1984. Purification and characterization of component A of the methane monooxygenase from *Methylococcus capsulatus* (Bath). J. Biol. Chem. **259**:53-59.

5. Pilkington, S. J., and H. Dalton. 1991. Purification and cahracterization of the soluble methane monooxygeanse from *Methylosinus sporium* 5 demonstrates the highly conserved nature of this enzyme in methanotrophs. FEMS Microb. Lett. **78**:103-108.

6. Koh, S-C, J. P. Bowman, and G. S. Sayler. 1993. Soluble methane monooxygenase production and trichloroethylene degradation by a type I methanotroph, *Methylomonas methanica* 68-1. Appl. Environ. Microbiol. **59**:960-967.

7. Nakajima, T., H. Uchiyama, O. Yagi, and T. Nakahara. 1992. Purification and properties of a soluble methane monooxygenase from *Methylocystis* sp. M. Biosci. Biotech. Biochem. **56**:736-740.

8. Fox, B. G., K. K. Surerus, E. Munck, and J. D. Lipscomb. 1988. Evidence for a μ-oxo-bridged binuclear iron cluster in the hydroxylase component of methane monooxygenase: mossbauer and electron paramagnetic resonance studies. J. Biol. Chem. **263**:10553-10556.

9. Ericson, A., B. Hedman, K. O. Hodgson, J. Green, H. Dalton, J. G. Bentsen, R. H. Beer, and S. J. Lippard. 1988. Structural chracterization by EXAFS spectroscopy of the binuclear iron center in proteinA of methane monooxygenase from *Methylococcus capsulatus* (Bath). J. Am. Chem. Soc. **110**:2330-2332.

10. Dewitt, J. G., J. G. Bentsen, A. C. Rosenzweig, B. Hedman, J. Green, S. Pilkington, G. C. Papaefthymion, H. Dalton, K. O. Hodgson, and S. J. Lippard. 1991. X-ray absorption, mossbauer, and epr studies of the dinuclear iron center in the

hydroxylase component of methane monooxygenase. J. Am. Chem. Soc. **113**:9219-9235.

11. Rosenzweig, A. C., C. A. Frederick, S. J. Lippard, and P. Nordlund. 1993. Crystal structure of a bacterial nonheme iron hydroxylase that catalyzes the biological oxidation of methane. Nature **366**:537-543.

12. DiSpirito, A. A., J. Gulledge, A. K. Shiemke, J. C. Murrell, M. E. Lidstrom, and C. L. Krema. 1992. Trichloroethylene oxidation by the membrane-associated methane monooxygenase in type I, type II, and type X methanotrophs. Biodeg. **2**:151-164.

13. Oremland, R. S., and C. W. Culbertson. 1992. Importance of methane-oxidizing bacteria in the methane budget as revealed by the use of a specific inhibitor. Nature **356**:421-423.

14. Higgins, I. J., D. J. Best, and R. C. Hammond. 1980. New findings in methane-utilizing bacteria highlight thier importance in the biosphere and their commercial potential. Nature **286**:561-564.

15. Stanley, S. H., S. D. Prior, D. J. Leak, and H. Dalton. 1983. Copper stress underlies the fundamental change in the intracellular location of methane

monooxygenase in methane-oxidizing organisms - studies in batch and continuous culture. Biotech. Lett. **5**:487-492.

16. Burrows, K. J., A. Cornish, D. Scott, and I. J. Higgins. 1984. Substrate specificities of the soluble and particulate methane monooxygenases of *Methylosinus trichosporium*. OB3b J. Gen Microbiol. **130**:3327-3333.

17. Prior, S. D., and H. Dalton. 1985. The effect of copper ions on membrane content and methane monooxygenase activity in methanol-grown cells of *Methylococcus capsulatus* (Bath). J. Gen. Microbiol. **131**:155-163.

18. Chan, S. I., H-H. T. Nguyen, A. K. Shiemke, and M. E. Lidstrom. 1993. in *Bioinorganic Chemistry of Copper*, K. D. Karlin and Z. Tyeklar, Ed., Chapman & Hall, New York, pp. 184-195.

19. Nguyen, H-H., A. K. Shiemke, S. J. Jacobs, B. J. Hales, M. E. Lidstrom, and S. I. Chan. 1994. The nature of the copper-ions in the membranes containing the particulate methane monooxygenase from *Methylococcus capsulatus* (Bath). J. Biol. Chem. (in press).

20. Collins, M. L. P., L. A. Bulchholz, and C. C. Remsen. 1991. Effect of copper on *Methylomonas albus* BG8. Appl. Environ. Microbiol. **57**:1261-1264.

21. Peltola, P., P. Priha, and S. Laakso. 1993. Effect of copper on membrane lipids and methane monooxygenase activity of *Methylococcus capsulatus* Bath. Arch. Microbiol. **159**:521-525.

22. Whittenbury, R., and H. Dalton. 1981. in *The Prokaryotes*, Starr, M. P., Stolp, H., Truper, H. G., Balows, A., and Schlegel, H. G., Ed., Springer-Verlag, New York, 1981, Vol. I, Chap. 71.

23. Lidstrom, M. E. 1988. Molecular approaches to problems in biogeochemical cycling. Ant. v. Leeuw. **54**:189-199.

24. Colby, J., D. I. Stirling, and H. Dalton. 1977. The soluble methane monooxygenase of *Methylococcus capsulatus* (Bath): its ability to oxygenate *n*-alkanes, *n*-alkenes, ethers, alicyclic, aromatic and heterocyclic compounds. Biochem. J. **165**:395-402.

25. Ensign, S. A., M. R. Hyman, and D. J. Arp, D. J. 1993. In vitro activation of ammonia monooxygenase from *Nitrosomonas europaea* by copper. J. Bacteriol. **175**, 1971-1980.

Chapter 5

Particulate Methane Monooxygenase Genes in Methanotrophs

(Submitted to *Journal of Bacteriology*)

5.1 ABSTRACT

A 45-kDa membrane polypeptide that is associated with activity of the particulate methane monooxygenase (pMMO) has been purified from three methanotrophic bacteria, and the N-terminal amino acid sequence was found to be identical in 17 out of 20 positions for all three polypeptides. DNA from a variety of methanotrophs was screened with an oligonucleotide probe designed from the N-terminal sequence of the 45-kDa polypeptide from *Methylococcus capsulatus* Bath, and in most cases, two gene copies were identified. A DNA fragment containing a portion of one of the copies of this gene (*pmoB*) was cloned from *M. capsulatus* Bath, and the predicted amino acid sequence revealed high identity with the gene product of *amoB*, the 40-kDa subunit of the ammonia monooxygenase from *Nitrosomonas europaea*. The gene encoding the 27-kDa acetylene-binding subunit of the ammonia monooxygenase (*amoA*) was used as a second probe to screen DNA from methanotrophs and in most cases two gene copies were identified. These results suggest that the 45- and 27-kDa pMMO-associated polypeptides of methanotrophs are subunits of the pMMO and are present in duplicate gene copies in methanotrophs.

5.2 INTRODUCTION

Methanotrophs are a group of gram-negative bacteria that utilize methane as their sole source of carbon and energy. The initial transformation involves the conversion of methane into methanol by methane monooxygenase (MMO)

$$CH_4 + O_2 + NADH + H^+ \rightarrow CH_3OH + H_2O + NAD^+ \qquad (5.1)$$

Methanol is then further oxidized to formaldehyde, which is either assimilated into biomass or oxidized to carbon dioxide. The MMO exists in two forms, a cytoplasmic or soluble form (sMMO) and a membrane-bound or particulate form (pMMO). The sMMO has been purified from several methanotrophs and is known to have three components; the hydroxylase, containing polypeptides of 61-kDa, 45-kDa and 20kDa in an $\alpha_2\beta_2\gamma_2$ configuration, the reductase, a 39-kDa flavoprotein, and a small component of 15.5-kDa apparently involved in regulation (8, 15, 36). The purified sMMO has been shown to contain a μ-oxo bridged diiron cluster in the active site (16) and the crystal structure of the hydroxylase has recently been published (36). The genes for these polypeptides have been cloned from two methanotrophs and are found to cluster together in both cases (29, 40, 41). The sMMO has been found to oxidize a wide range of substrates, including aromatic and aliphatic hydrocarbons, ammonia, and halogenated solvents (17, 44). The sMMO, however, is only present in six described species, which include most of the a-proteobacteria methanotrophs and only some of the γ-proteobacteria strains (8, 15, 18, 21, 30, 33, 42). The pMMO is present in all known methanotrophs (18).

The pMMO is less well studied than the sMMO and has never been reproducibly purified to homogeneity (35, 39, 46), possibly due to the instability of the pMMO upon removal of the polypeptides from the membrane lipids. Therefore much is still unknown about the structure of the pMMO, with the current information having

been obtained from whole-cell, cell-free extract, and membrane studies (9, 10, 12, 31, 35, 43). The substrate range of the pMMO is more limited than the sMMO; the pMMO has been shown to oxidize short-chain aliphatic compounds, ammonia and small halogenated hydrocarbons. Although much is unknown about the pMMO, it is important to obtain a more fundamental understanding of this enzyme because of the importance of methanotrophs in the global methane cycle (32) and the fact that the majority of known methanotrophs contain only the pMMO. Furthermore, methanotrophs have been proposed for the in situ bioremediation of sites contaminated with small halogenated solvents (28, 45) and the pMMO can degrade halogenated hydrocarbons including trichloroethylene (12).

It is known that for cells which are able to express both forms of the MMO, the ratio of copper to biomass is significant in controlling the relative expression of the sMMO and pMMO (6, 35, 43). Under low copper/biomass ratios, the sMMO is the predominant MMO expressed, while at high copper/biomass ratios MMO activity is associated with the membrane fractions. When the soluble and particulate fractions of cells grown under increasing copper/biomass ratios are analyzed by SDS-PAGE gels, the known sMMO polypeptides decrease in intensity in the soluble fraction while two polypeptides of approximately 45-kDa and 27-kDa appear in the particulate fractions, concomitant with the appearance of pMMO activity (6, 9, 10, 12). Polypeptides of similar size were found as major species in a partially purified pMMO preparation from *M. capsulatus* Bath (39), providing further evidence that these polypeptides may be pMMO subunits. Acetylene has been shown to be a suicide substrate for both the sMMO and the pMMO (2, 17, 19, 34). In cells containing the sMMO, [^{14}C]acetylene specifically labels the alpha subunit of the hydroxylase (34). In cells containing the pMMO, [^{14}C]acetylene specifically labels a membrane polypeptide of approximately 27-kDa, which is assumed to be the 27-kDa polypeptide mentioned above (12). pMMO activity has been obtained in purified membrane preparations (31) and in a

partially purified preparation extracted from membranes (39) using an assay based on the ability of MMO to oxidize propene. For these assays, NADH is commonly used as a source of reducing equivalents, but the electron donor *in vivo* is not known (31, 33).

Recent studies of another enzyme, the ammonia monooxygenase (AMO) have provided information relevant to the pMMO. The AMO shares many characteristics with the pMMO. Both enzymes have similar substrate ranges including their primary substrates, methane and ammonia, both are inhibited by acetylene, and in both enzymes, [^{14}C]acetylene labels a membrane polypeptide of approximately 27-kDa (20). In addition, a 40-kDa polypeptide copurifies with the 27-kDa acetylene-binding polypeptide in *Nitrosomonas europaea* (26) and these are thought to be analogous to the 27- and 45-kDa polypeptides associated with the pMMO. Substantial evidence suggests the 27- and 40-kDa polypeptides are subunits of the AMO (20, 26). Both enzymes are highly unstable after cell lysis, but activity in vitro is stabilized by copper for both the AMO (14) and the pMMO (31), and copper has been suggested to be part of the active site of both enzymes (14, 31). It has been recently reported that the pMMO may contain copper clusters that are responsible for the activation of oxygen (31). Although nothing was known about the genetics of the pMMO prior to the current study, the gene encoding the acetylene-binding subunit of the AMO (*amoA*) has been cloned from *N. europaea* and sequenced (26). The sequence predicts the actual size of AmoA to be 32-kDa. A second gene encoding the 40-kDa AMO subunit was discovered downstream and labeled *amoB* (26). In the same study it was shown that *N. europaea* contains two gene copies for the AMO. In this paper, we report the presence in methanotrophs of two copies of genes similar to *amoA* and *amoB* of *N. europaea*. Furthermore, we have cloned and sequenced a portion of one of the genes for the 45-kDa putative pMMO subunit and have obtained N-terminal

amino acid sequence for this polypeptide from three methanotrophs.

5.3 MATERIALS AND METHODS

5.3.1 Growth of Methanotrophs.

Methanotrophs were grown on nitrate mineral salts medium (NMS) in batch culture with copper added as $CuSO_4 \cdot (5H_2O)$ (47). For *Methylobacter marinus* A45 (previously called *Methylomonas* sp. strain A45 (4, 23) a sterile solution of NaCl was added for a final concentration of 1% (w/v). The cells were shaken at 200 rpm under a methane-air headspace (approximately 1:3 vol/vol) at one atmosphere of pressure. *Methylobacter albus* BG8 (previously called *Methylomonas albus* BG8), *Methylocystis parvus* OBBP, *Methylosinus trichosporium* OB3b, "*Methylobacter capsulatus*" Y, *Methylobacter agile* (Azo), *Methylosinus sporium* 5 (4, 47), and *Methylomonas* MM2 and *Methylomonas* MN (12) were grown at 30°C, while *Methylococcus capsulatus* Bath (47) was grown at 45°C, and *M. marinus* A45 was grown at 37°C. The cells were grown to late-exponential phase and then harvested.

5.3.2 DNA Purification and Hybridization.

Chromosomal DNA was isolated from the methanotrophs using a modified version of the Marmur technique (25). Cells were first pelleted by centrifugation at 5000 rpm. The cells were then washed once with saline-EDTA (0.15M NaCl, 0.1 M EDTA, pH 8.0) and resuspended in 10 ml of saline-EDTA to which 10 mg/ml of lysozyme was added. The suspensions were then frozen at -70°C. Before thawing 10 ml of Tris-sodium-dodecyl sulfate (Tris-SDS) (0.1 M Tris, 1% w/v SDS, and 0.1 M NaCl, pH 9.0) with 1 mg/ml of proteinase K was added and the solution placed in a 50°C waterbath for 30 min or until the solution became translucent. DNA was then extracted using a phenol-saline-EDTA solution. The DNA was then precipitated with isopropanol and resuspended in TE buffer (10 mM Tris, 1 mM EDTA, pH 8.0).

Plasmid DNA was isolated from *M. albus* BG8 as follows. Cells were washed once and then resuspended in TE. The cells were then lysed with 4% SDS (w/v) in TE (pH 12.4). After 30 min incubation at room temperature, a neutral buffer (2M Tris, pH 7.0) and a salt solution (5M NaCl) were added. The resulting suspension was then placed on ice overnight. The samples were then centrifuged at 18,000 rpm for 20 min at 4 °C. The supernatant was removed and 0.6 vol. isopropanol was added. The solution was centrifuged at 12,000 rpm for 20 min at 23 °C, and the pelleted plasmid DNA was resuspended in TE and analyzed on 0.7% agarose gels in a Tris Acetate (TA) buffering system.

Both chromosomal and plasmid DNA were digested with restriction enzymes as recommended by the supplier (New England Biolabs, Inc, Beverly, MA). The digested DNA was separated using standard procedures on TA 0.7% gels, and these were prepared for hybridization as described by Meinkoth and Wahl (27).

The oligonucleotide probe, AC10, 5' -ATG-CG(A,G,C,T)-AC(A,G,C,T)-AT(A,C,T)-CA(C,T)-TGG-TA(C,T)-GA-3' was based on the amino acid sequence MRTIHWY of the N-terminal region of the 45-kDa polypeptide from methanotrophs (see Table 1), and had 192-fold redundancy. It was end-labelled with T4 polynucleotide kinase and 5'-[g - ^{32}P]ATP as described in Sambrook et al. (37). The probe was then hybridized to dried gels overnight at 42°C using a standard hybridization solution (0.5% (w/v) SDS, 1M NaCl, 0.1M sodium citrate, and 0.5% (w/v) powdered milk). Excess probe was removed using a wash solution of 0.1% SDS, 75 mM NaCl, and 7.5 mM sodium citrate at 42°C. The dried gels were then exposed to X-ray film.

Hybridizations were also performed with a fragment of the *amoA* gene by J. Murrell of the University of Warwick, Coventry, England. Polymerase chain reaction (PCR) was used to amplify a 693 bp internal fragment of the gene. Primers used were

AMO1 (GCACTTTATGCTGCTGGC) and AMO2 (GATCCCCTCTGGAAAGCC) which correspond to regions of *amoA* at positions 380–398 and 1073–1056, respectively of the published sequence (26). Amplification was carried out on a Hybaid thermal cycler (Combi TR-2) in 50 ml volumes. Each tube contained 0.1% Triton (w/v), 1.5 mM $MgCl_2$, 50 mM KCl, 10 mM Tris-HCl (pH 9.0) 100 mM each dNTP, 50 pmol of each primer, 1 unit Taq polymerase (Promega, Madison, WI) and approximately 1 ng template DNA. Reaction conditions were denaturation: 94°C for 1 min, annealing: 50°C for 1 min, polymerization: 72°C for 1 min; 30 cycles. The *amo*A gene was cloned from DNA of *Nitrosomonas europaea* (NCIMB11850), kindly supplied by Dr. J. Prosser, University of Aberdeen, with the T/A cloning kit (Invitrogen, San Diego, CA) using the vendor's instructions. Plasmids containing inserts were purified by the method of Saunders and Burke (38) and the insert size was checked after digestion with *Eco*RI. The identity of the 693 bp *amoA* gene fragment was confirmed by sequencing. Hybridizations with *amoA* were carried out as outlined in Sambrook et al. (37) with hybridizations performed in 6x SSC at 65°C and subsequent washes in 2x SSC at 50°C.

5.3.3 Protein Purification and Sequencing.

Membrane fractions of *M. capsulatus* Bath, *M. albus* BG8, and *M. marinus* A45 were collected as follows. Cells were centrifuged at 7500 rpm for 10 min and then washed with 10 mM PIPES buffer, pH 7.0. The cells were then passed three times through a French Pressure cell at 137 MPa. Any remaining whole-cell debris was then removed by centrifugation at 10,000 rpm for 15 min. The supernatant was then poured off and re-centrifuged at 45,000 rpm for 90 min. The resulting membrane pellets were then resuspended in a sample buffer solution (50% w/v urea, 0.2% w/v bromophenol blue, 4% w/v SDS, and 100 mM Tris, pH 6.8).

SDS-polyacrylamide gel electrophoresis (PAGE) was performed using the

Novex Xcell II gel system (Novex, Inc., San Diego, CA). Pre-packaged 1.0 mm thick tris-glycine gels with 10-27% polyacrylamide gradients were used for protein separation. The gels were pre-run with SDS-urea gel loading buffer to remove any free radicals that may modify the N-terminus of desired polypeptides. The running buffer contained 25 mM Tris, 250 mM glycine, 0.1% w/v SDS and 0.1 mM thioglycolate. The system was operated at 125V for 90 min. After electrophoresis, the polypeptides were transferred to Immobilon P membranes (Millipore Corp., Bedford MA) using a Biorad Trans-Blot cell. The polypeptides were transferred to the membranes overnight at 100V in a transfer buffer containing 12 mM Tris, 96 mM glycine, 10% v/v methanol and 0.5 mM dithiothreitol. The membranes were then soaked in water overnight to remove residual glycine. Bands of approximately 45-kDa were then excised. N-termini were sequenced using Edman degradation on ABI 476 and 477 pulsed liquid protein sequencers (Applied Biosystems, Inc., Foster City, CA.) by the Biopolymer Synthesis & Analysis Resource Center at the California Institute of Technology. From the sequence found from *M. capsulatus* Bath, the oligonucleotide probe AC10 was synthesized at the Microchemical Facility at the California Institute of Technology.

5.3.4 Cloning of a Portion of the pMMO Large Subunit Gene from *M. capsulatus* Bath.

Fractions of the restriction endonuclease digested *M. capsulatus* Bath chromosome that hybridized with the AC10 oligonucleotide were isolated from agarose gels as described by Sambrook et al. (37). Each fraction was ligated with the vector (pRK310; 13) to generate partial clone libraries. These were used to transform *E. coli*, and approximately 1000 colonies of each were screened by hybridization to the AC10 probe. Only one of these libraries, that was made using chromosomal DNA digested with *Pst*I (0.8 - 1.5 kb), resulted in colonies that hybridized to the probe. Plasmids

were isolated from four separate colonies, and all contained the same 0.9 kb insert. The 0.9 kb *Pst*I fragment was recloned in pAYC63 (7) and sequenced on both strands at the Sequencing Core Facility at UCLA.

5.3.5 Homology Searches.

The Wisconsin Genetics Computer Group Program (11) and PC/GENE (Genofit SA, Geneva, Switzerland) were used to search for genes and polypeptide sequences with similarity to the cloned gene for the 45-kDa polypeptide. The Wisconsin package was also used for calculating the hydrophilicity of the primary sequence of the 45-kDa polypeptide using the Kyte-Doolittle algorithm over a span of seven residues.

5.4 RESULTS

5.4.1 Purification and Sequencing of the 45-kDa Polypeptide.

Two major polypeptides of 45-kDa and 27-kDa are consistently associated with the pMMO (1, 10, 12, 31), and we have observed that the major band on SDS-PAGE gels around 45-kDa contains two polypeptides of approximately 45-kDa and 46-kDa. The polypeptides from three methanotrophs, *M. capsulatus* Bath, *M. albus* BG8, and *M. marinus* A45 were transferred to Immobilon P membranes and the areas containing the 45- and 46-kDa polypeptides were sequenced. The 27-kDa polypeptide did not transfer well and sequencing was not possible. The sequences for the first 20 residues of the 45- and 46-kDa polypeptides were identical for the strain from which they were isolated. The sequences between strains were identical with the exception of the fourth and eighteenth residues (Fig. 5.1). For *M. capsulatus* Bath, the fourth residue was lysine, while in *M. marinus* A45, the fourth amino acid was unidentified. For *M. albus* BG8, the fourth residue coeluted with tyrosine, but did not have a typical tyrosine spectral shape, suggesting that this residue is an unusual amino acid. In *M. capsulatus*

```
MC      HGEKSQAAFMRMRTIHWYDL
        ||| ||||||||||||||•||
A45     HGEXSQAAFMRMRTIHWFDL
        ||| ||||||||||||||•||
BG8     HGEXSQAAFMRMRTIHWYDL
        ||| ||  | ||||• ||||
AmoB    HGERSQEPFLRMRTVQWYDL
```

X = unknown amino acid

MC, *M. capsulatus* Bath; A45, *M. marinus* A45; BG8, *M. albus* BG8.

Figure 5.1. N-terminal amino acid sequence for the 45-kDa polypeptide from methanotrophs and for AmoB of *N. europaea* (26). Vertical bars indicate identical amino acids and and dots denote conserved substitutions.

Bath and *M. albus* BG8, the eighteenth residue was tyrosine, while in *M. marinus* A45, it was phenylalanine.

Using both the Wisconsin Genetics Computer Group program and PC/GENE to search for polypeptides similar to the portion of the 45-kDa polypeptide sequenced in this study, only one match was identified. As shown in Fig. 5.1, the N-terminus of the gene product of *amoB*, the 40-kDa subunit of the AMO has 14 out of 20 residues identical to the N-terminus of the 45-kDa polypeptide sequenced from *M. capsulatus* Bath and *M. albus* BG8, and 13 out of 20 residues identical for the polypeptide from *M. marinus* A45.

5.4.2 Hybridization with an Oligonucleotide Probe.

The N-terminal sequence of the 45-kDa polypeptide found in *M. capsulatus* Bath was used to design an oligonucleotide probe, AC10 (see Methods). Chromosomal DNA from several methanotrophs was digested with *Hin*dIII and *Bst*YI, separated on gels and probed with AC10. Hybridization to specific DNA fragments was observed for all methanotrophs except *M. parvus* OBBP. In one strain, *M. marinus* A45, only one DNA fragment was identified in each digest. However, for *M. capsulatus* Bath, *M. albus* BG8, *Methylomonas* sp. MN, *Methylomonas* sp. MM2 and *M. trichosporium* OB3b, two DNA fragments were identified for both restriction digests (data not shown). Two of these strains, *M. capsulatus* Bath and *M. albus* BG8, were chosen for more detailed study. DNA from these strains was digested with five restriction enzymes and then probed with AC10. For both strains, two bands were observed in all five digests (Fig. 5.2, Table 5.1).

The presence of two hybridizing bands in *M. capsulatus* Bath and *M. albus* BG8 suggested that duplicate gene copies exist for the 45-kDa polypeptide. This raised the possibility that one gene might be plasmid-encoded. Although no plasmids have

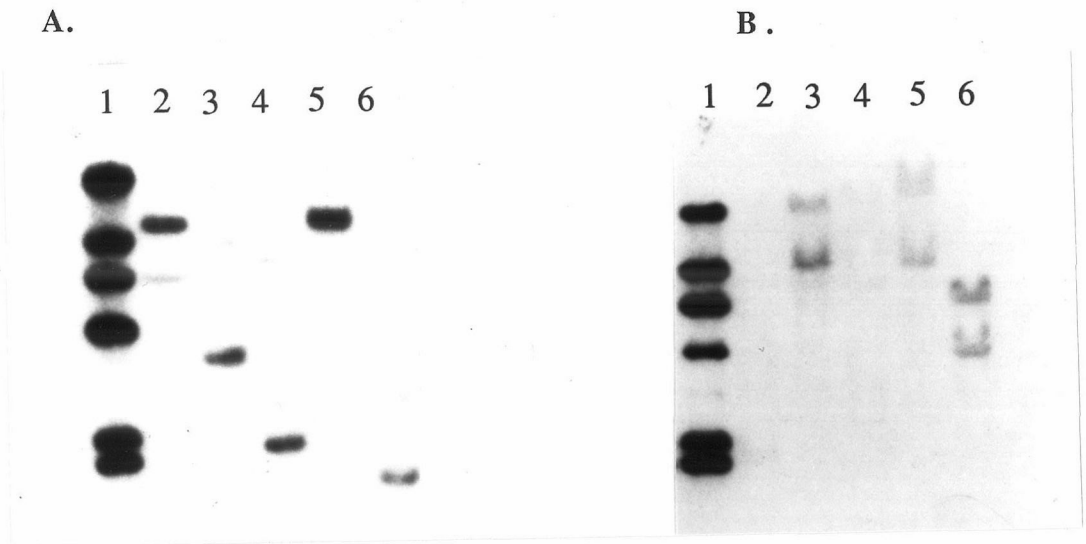

Figure 5.2. Hybridization of AC10 to restriction enzyme digests of *M. albus* BG8 (**A**) and *M. capsulatus* Bath (**B**) chromosomal DNA. **A.** 1. Molecular weight standards (lambda DNA digested with *Hin*dIII; sizes 23 kb, 9.0 kb, 6.0 kb, 4.0, kb, 2.3 kb, and 2.0 kb); 2. *Pst*I digest; 3. *Hin*dIII digest 4. *Eco*RI digest; 5. *Bgl*II digest; 6. *Bst*YI digest. **B.** 1. Molecular weight standards (same as above); 2. *Pst*I digest; 3. *Bam*HI digest; 4. *Sal*I digest; 5. *Hin*dIII digest; 6. *Eco*RI digest. Lanes 2-6 contain approximately 10 μg DNA.

Table 5.1. Sizes of DNA fragments of methanotrophs that hybridized to the probes, AC10 and *amoA*.

Strain	AC10 (kb)		*amoA* (kb)(A)	
M. albus BG8	*Pst*I -	14		
		7.3		
	*Hin*dIII -	9.5		
		4.0		
	*Eco*RI -	4.7		
		2.1		
	*Bgl*II -	23		
		14		
	*Bst*YI -	2.6		
		1.6		
M. capsulatus Bath				
	*Pst*I -	2.2	*Pst*I -	4.7
		0.9		2.7
	*Bam*HI -	23	*Bam*HI -	11
		11		6.0
	*Sal*I -	1.2	*Sal*I -	4.7
		0.9		1.7
	*Hin*dIII -	~25	*Hin*dIII -	~25
		12		
	*Eco*RI -	8.0	*Eco*RI -	5.3
		5.0		4.2

A. Probing performed by J. C. Murrell, University of Warwick, Coventry, England.

been detected in *M. capsulatus* Bath, a plasmid has been noted in *M. albus* BG8 (22). To determine whether one of the hybridizing fragments was part of the 65 kb plasmid of *M. albus* BG8, this plasmid was isolated, digested with *Hin*dIII, *Bst*YI, and *Bam*HI and separated on gels. Membranes containing the plasmid DNA were hybridized to the AC10 probe, but no hybridization was observed. When the procedure was repeated with intact plasmid DNA that had been denatured using a solution of 150 mM NaCl and 0.5N NaOH, AC10 did not hybridize to the circular DNA (data not shown).

5.4.3 Cloning and Sequencing of the Gene Encoding the 45-kDa Polypeptide of *M. capsulatus* Bath.

The high identity between *amoB* and the 45-kDa polypeptides from three methanotrophs supported the hypothesis that this 45-kDa polypeptide is a pMMO subunit. Therefore a portion of this gene was cloned and sequenced. It was not possible to clone large fragments containing this gene, presumably due to a toxic effect in *E. coli*, as reported for cloning of the *amoAB* region (26). We were successful, however, in cloning a 0.9 kb *Pst*I fragment from *M. capsulatus* Bath that had been identified in the genomic blots (Table 5.1). The sequence revealed an open reading frame of 265 amino acids that extended to one end of the fragment, and which contained the N-terminal sequence determined for the 45-kDa polypeptide (Fig. 5.3). The cloned DNA fragment therefore contains about two-thirds of this gene, which we propose to call *pmoB*, in analogy to *amoB*. This sequence could be aligned with the translated *amoB* sequence with no gaps and showed 43% identity over the 235 amino acid overlap, excluding the proposed leader sequences (Fig. 5.3). When the PmoB sequence was analyzed on a hydropathy plot using the Kyte-Doolittle algorithm, it was revealed to be hydrophobic and contained two potential membrane-spanning segments in addition to a hydrophobic hypothesized leader sequence (Fig. 5.4). The pattern observed was very similar to that for AmoB, although in AmoB only one of the two

```
     MKTIKDRIAKWSAIGLLSAVAATAFYAPSASAHGEKSQAAFMRMRTIHWYDLSWSKE
                                          |||| ||  | ||||• |||• |  |
MGIKNLYKRGVMGLYGVAYAVAALAMTVTLDVSTVAAHGERSQEPFLRMRTVQWYDIKWGPE

KVKINETVEIKGKFHVFEGWPETVDEPDVAFLNVGMPGPVFIRKESYIGGQLVPRSVRLEIG
  |•||   | ||||• | ||      ||  | ||| | ||| |    | |      |  | ||
VTKVNENAKITGKFHLAEDWPRAAAQPDFSFFNVGSPSPVFVRLSTKINGHPWFISGPLQIG

KTYDFRVVLKARRPGDWHVHTMMNVQGGGPIIGPGKWITVEGSMSEFRNPVTTLTGQTVDLE
  | | | | || ||  | | | ||   ||| ||| | • ||   | ||•  ||| |•| |
RDYEFEVNLRARIPGRHHMHAMLNVKDAGPIAGPGAWMNITGSWDDFTNPLKLLTGETIDSE

NYNEGNTYFWHAFWFAIGVAWIGYWSRRPIFIPRLLMVDAGRADELVSATDRKVAMGGLAAT
 •|  |  ||| | ||• |||    || |•||  • |  | |    | |•       |
TFNLSNGIFWHVVWMSIGIFWIGVFTARPMFLPRSRVLLAYGDDLLMDPMDKKITWVLAILT

ILIVVMAMSSANSKYPITIPLQ
• •|          | | |•
LALVWGGYRYTENKHPYTV
```

Figure 5.3. Comparison of predicted amino acid sequence of *pmoB* from *M. capsulatus* Bath (upper) and *amoB* (lower; 26). Identical amino acids are marked with a vertical line and conserved substitutions are marked with dots, and the N-terminal sequence of the 45-kDa polypeptide is underlined.

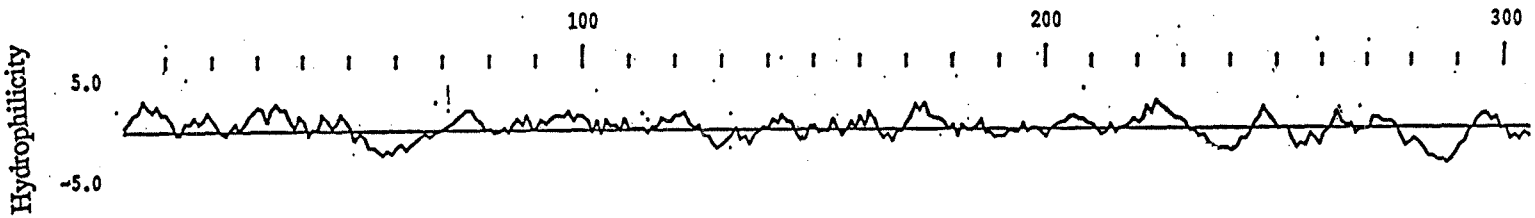

Figure 5.4. Predicted hydropathy plot of the *pmoB* gene product using the Kyte-Doolittle algorithm over a span of seven residues.

potential membrane-spanning segments was indicated (26).

5.4.4 Hybridization with *amoA*.

Chromosomal DNA from several methanotrophs were also hybridized with a second probe, a 693 bp PCR product containing an internal segment of *amoA*. (by J. Murrell of the University of Warwick, Coventry, England). Negative controls showed no hybridization, and included *E. coli, Klebsiella pneumoniae, Micrococcus luteus, Rhodobacter sphaeroides* and *Methylobacterium extorquens* AM1 (data not shown). Specific fragments of DNA digested with *Pst*I hybridized to *amoA* for all tested methanotrophs, including *M. capsulatus* Bath, *M. albus* BG8, *M. parvus* OBBP, *M. trichosporium* OB3b, *"M. capsulatus"* Y, *M. agile* (Azo), *M. methanica* S1, and *M. sporium* 5 (data not shown). For *M. methanica* S1 and *"M. capsulatus"* Y, only one band was detected, while in all other methanotrophs tested, two bands were identified. *M. capsulatus* Bath was studied in more detail. As shown in Fig. 5.5, *M. capsulatus* Bath DNA digested with five different restriction enzymes showed two bands that hybridized to the *amoA* sequence in four of the five digests. These data show that a gene is present in *M. capsulatus* Bath with significant similarity to *amoA*, and that it appears to also be present in duplicate copies. A comparison of the hybridization data for *amoA* and *pmoB* shows that for each enzyme except *Pst*I, one of the fragments identified by both probes was the same size and one was not (Table 5.1).

5.5 DISCUSSION

The pMMO that oxidizes methane to methanol in methanotrophs is not well-understood biochemically. Although some information is available concerning substrate range and inhibitors (8, 9, 24, 30), the pMMO is unstable and has never been reproducibly purified to homogeneity (39). Therefore, the structure of the enzyme is

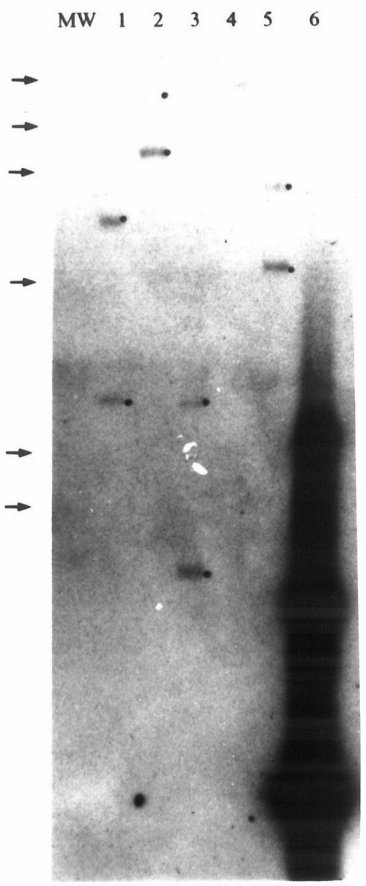

Figure 5.5. Hybridization of *amoA* to restriction enzyme digests of *M. capsulatus* Bath chromosomal DNA. Lanes: MW, size standards (lambda DNA digested with *Hin*dIII; sizes 23 kb, 9.0 kb, 6.0 kb, 4.0, kb, 2.3 kb, and 2.0 kb) 1. *Pst*I digest; 2. *Bam*HI digest; 3. *Sal*I digest; 4. *Hin*dIII digest; 5. *Eco*RI digest. 6. PCR product of *amoA* from *Nitrosomonas europaea.* Lanes 1-5 contain approximately 10 mg DNA.

uncertain and details concerning assembly and maturation processes are completely unknown. In this paper, we describe the first steps towards a genetic approach to studying the pMMO

We have shown that the 45-kDa membrane polypeptide that is associated with pMMO activity is highly conserved at the N-terminus in three different methanotrophs. Hybridization experiments using an oligonucleotide probe based on this N-terminal amino acid sequence support the hypothesis that this conservation is widespread in methanotrophs. We have cloned and sequenced a portion of a gene encoding the 45-kDa polypeptide (*pmoB*), and have shown that this part of PmoB has high identity with the corresponding part of the gene product of *amoB*. *AmoB* encodes the 40-kDa subunit of the ammonia monooxygenase, an enzyme that shares many characteristics with the pMMO. These data strongly suggest that the gene product of *pmoB* (the 45-kDa membrane polypeptide associated with pMMO activity) is analogous to the 40-kDa subunit of the AMO, and that it is a subunit of the pMMO. Neither sequence shows substantial identity to any other protein or gene sequences in Genbank.

The 27-kDa membrane polypeptide that is associated with pMMO activity binds acetylene (12), a suicide inhibitor of the pMMO (2, 19). An apparently analogous acetylene-binding polypeptide, the 27-kDa AMO subunit has been suggested to contain the active site of the AMO (14, 20). DNA fragments containing the gene encoding the acetylene-binding subunit of AMO (*amoA*) have been cloned from *N. europaea* and sequenced (26), and we have now shown that an *amoA* probe hybridizes to specific DNA fragments of methanotrophs, but not to DNA from a variety of other bacteria. We have not yet been successful in cloning a gene that hybridizes to *amoA*, which we propose to call *pmoA*. This may be due to toxicity of the gene product in *E. coli*, since a similar problem was encountered in the cloning of *amoA* (26). In that case, it was not possible to obtain a single DNA fragment containing the complete *amoA*, but rather,

two overlapping fragments that each contained a portion of *amoA* were cloned separately and sequenced (26). The similarities between the two 27-kDa acetylene-binding polypeptides and between *pmoA* and *amoA* suggest that the 27-kDa acetylene-binding polypeptide of methanotrophs is a subunit of the pMMO.

The genes *amoA* and *amoB* have been found to exist in two copies in *N. europaea* (26). Our evidence suggests that in several methanotrophs, *pmoA* and *pmoB* are also present as two gene copies. The data for this assertion are especially convincing in *M. capsulatus* Bath, in which two DNA fragments were identified with the *amoA* probe in four out of five restriction digests tested, and with the *pmoB* probe in all five restriction digests tested. The sole exception for the *amoA* probe, the *Hin*d III digest, showed one large band, which may have been two that were not resolved. Since the *pmoB* probe is an oligonucleotide that does not contain sites for any of the restriction enzymes tested, only one DNA fragment would be expected in each case. The *amoA* probe is larger and might in some cases hybridize to two DNA fragments split by a restriction enzyme, but it is unlikely that all five restriction enzymes would cut within this gene. In those methanotrophs in which only one DNA fragment was identified by hybridization, it is not known whether only one gene copy exists, or alternatively, whether the second gene copy is too divergent to detect.

It is not known whether both gene copies are expressed. It has recently been shown that the pMMO exists in two kinetically and spectroscopically distinct forms, depending upon the copper concentration in the growth medium (24). At high copper, a low K_m form is expressed that has a specific EPR signature, while at low copper, a high K_m form is present that lacks this EPR signature (24). Our data suggest the possibility that these two forms of the pMMO might be separate gene products. If so, the N-terminal amino acid sequence of PmoB isolated from cells grown at the two copper regimes might be different. However, although two membrane polypeptides

from *M. capsulatus* Bath of approximately 45- and 46-kDa can be resolved on gels, the first 20 amino acids of each were identical in PmoB from cells grown under both high and low copper. Therefore, if the two forms of the pMMO are different gene products, their N-termini are highly conserved. This might be expected from the probing experiments, since in the case of *M. capsulatus* Bath, both DNA fragments hybridized equally well to the oligonucleotide probe designed from N-terminal amino acids of PmoB.

The finding that the pMMO may be closely related to the AMO is not surprising, in light of the many common characteristics known for these enzymes. However, the finding that structural genes for both of these enzymes are present in two copies is more unexpected. It is relatively rare to find duplicate gene copies in prokaryotes, but in one case it is common. The genes involved in carbon dioxide fixation (*cfx*) in facultative autotrophic bacteria are usually found in two sets (3). In those cases in which it has been studied, the duplicate sets of *cfx* genes are closely related in DNA sequence and are apparently functionally equivalent (3). In order to determine the significance of these two gene copies of pMMO in the methanotrophs, it will be necessary to clone and sequence both sets of genes from a methanotroph and to generate and characterize mutants in each gene set. Due to the difficulties of carrying out genetic manipulations in methanotrophs (29), this will be a lengthy process. However, the results presented here raise the intriguing possibility that two different pMMOs might be present in methanotrophs, and might be differentially expressed depending upon cellular needs.

In *N. europaea*, one of the copies of *amoA* is located immediately upstream of *amoB* (26), but the relative position of *pmoA* and *pmoB* in *M. capsulatus* Bath is not yet known for either gene set. The sequence of the 0.9 kb *Pst*I fragment containing the 5' portion of *pmoB* revealed two possible open reading frames of 4 and 14 amino acids, at a distance of 107 and 77 bp respectively, upstream of *pmoB*. However,

neither sequence showed any identity with the C-terminal sequence of the gene product of *amoA*, and so it is not known whether this is the 3' end of *pmoA*. The hybridization results showed that in *M. capsulatus* Bath, for each restriction digest except *Pst*I, one of the restriction fragments that hybridized to *amoA* was the same size as one that hybridized to the AC10 *pmoB* probe. Therefore it is possible that in one of the gene sets, *pmoA* and *pmoB* are adjacent. The sequence results show that if *pmoA* and *pmoB* are adjacent, *Pst*I must separate *pmoB* from the major portion of *pmoA*, which would explain why there is no overlap in fragments detected in the *Pst*I digests. However, since in most cases a second fragment was identified by each probe that was of a different size, it is not certain whether *pmoA* and *pmoB* are adjacent in either gene copy. It appears that the sMMO genes are not closely linked to any of the *pmo* genes detected here, since the restriction fragments are different sizes in all cases (42).

The similarities between the AMO and pMMO polypeptides and genes strongly suggest that PmoA and PmoB are subunits of the pMMO. Definitive proof for this hypothesis would require either the development of a procedure for reproducibly purifying active pMMO, or the generation of mutants in both copies of *pmoA* and *pmoB*, and analysis of their phenotype. Efforts are underway to attempt to purify active pMMO from *M. capsulatus* Bath (31). However, generating pMMO mutants from inactivated cloned genes is not possible in *M. capsulatus* Bath, due to the lack of suitable markers and the limited substrate range of this strain (29). Other methanotrophs, such as *M. albus* BG8 and *M. trichosporium* OB3b are more amenable to genetic analysis (29), and the apparent conservation of pMMO genes in these methanotrophs suggests that it will be possible to continue studies of pMMO genetics in these strains.

5.6 REFERENCES

1. Anthony C. 1986. Bacterial oxidation of methane and methanol. Adv. Microb. Physiol. **27**:113-210.

2. Bedard, C. and R. Knowles. 1989. Physiology, biochemistry, and specific inhibitors of CH_4, NH_4^+, and CO oxidation by methanotrophs and nitrifiers. Microbiol. Rev. **53**:68-84.

3. Bowien, B., R. Bednarski, B. Kusian, U. Windhövel, A. Freter, J. Schäferjohann, and J-G. Yoo. 1993. Genetic regulation of CO_2 assimilation in chemoautotrophs. p. 481-492. *In* J. C. Murrell and D. P. Kelly (ed.) Microbial Growth on C_1 compounds. Intercept, Ltd., Andover, U.K.

4. Bowman, J., L. I. Sly, P. D. Nichols, and A. C. Hayward. 1993. Revised taxonomy of the methanotrophs: Description of *Methylobacter* gen. nov., emendation of *Methylococcus*, validation of *Methylosinus* and *Methylocystis* species, and a proposal that the family *Methylococcaceae* include only the group I methanotrophs. Int. J. Syst. Bact. **43**:735-753.

5. Brusseau, G. A., E. S. Bulygina and R. S. Hanson. 1994. Phylogenetic analysis of methylotrophic bacteria based on 16S rRNA sequence. Appl. Environ. Microbiol. **60**:626-636.

6. Burrows, K. J., A. Cornish, D. Scott and I. J. Higgins. 1984. Substrate specificities of the soluble and particulate methane monooxygenases of *Methylosinus trichosporium* OB3b. J. Gen. Microbiol. **130**:3327-3333.

7. Chistoserdov, A. Y., J. Boyd, F. S. Matthews, and M. E. Lidstrom. 1992. The genetic organization of the *mau* gene cluster of the facultative autotroph *Paracoccus denitrificans*. Biochem. Biophys. Res. Comm. **184**:1226-1234.

8. Colby, J., and H. Dalton. 1976. Some properties of a soluble methane mono-oxygenase from *Methylococcus capsulatus* strain Bath. Biochem. J. **157**:495-497.

9. Dalton, H. 1992. Methane oxidation by methanotrophs: physiological and mechanistic implications. p.85-113. *In* J. C. Murrell and H. Dalton (ed.), Methane and methanol utilizers. Plenum Press, New York.

10. Dalton, H., and D. J. Leak. 1985. Methane oxidation by microorganisms, p. 173-200. *In* S. R. K. Poole and C. S. Dow (ed.), Microbial gas metabolism. Academic Press, Ltd., London.

11. Devereux, J., P. Haeberli, and O. Smithies. 1984. A comprehensive set of sequence analysis programs for the VAX. Nucl. Acids Res. **12**:387-395.

12. DiSpirito, A. A., J. Gulledge, J. C. Murrell, A. K. Shiemke, M. E. Lidstrom, and C. L. Krema. 1992. Trichloroethylene oxidation by the membrane associated methane monooxygenase in type I, type II and type X methanotrophs. Biodeg. **2**:151-164.

13. Ditta, G., T. Schmidhauser, F. Yakobson, P. Lu, X. Liang, D. Finley, D. Guiney, and D. Helinski. 1985. Plasmids relating to the broad host range vector, pRK290, useful for gene cloning and monitoring gene expression. Plasmid **13**:149-153.

14. Ensign, S. A., M. R. Hyman, and D. J. Arp. 1993. In vitro activation of ammonia monooxygenase from *Nitrosomonas europaea* by copper. J. Bacteriol. **175**:1971-1980.

15. Fox, B. G., W. A. Froland, J. E. Dege, and J. D. Lipscomb. 1989. Methane monooxygenase from *Methylosinus trichosporium* OB3b. Purification and properties of a three-component system with high specific activity from a type II methanotroph. J. Biol. Chem. **264**:10023-10033.

16. Fox, B. G., K. K. Surerus, E. Münck, and J. D. Lipscomb. 1988. Evidence for a m-oxo-bridged binuclear iron cluster in the hydroxylase component of methane monooxygenase. Mössbauer and EPR studies. J. Biol. Chem. **263**:10553-10556.

17. Green, J. and H. Dalton. 1989. Substrate specificity of soluble methane monooxygenase: mechanistic implications. J. Biol. Chem. **264**:17698-17703.

18. Hanson, R. S., A. I. Netrusov, and K. Tsuji. 1990. The obligate methanotrophic bacteria *Methylococcus, Methylomonas*, and *Methylosinus. In* A. Balows, H. G. Truper, M. Dworkin, W. Harder, and K-H. Schleifer (eds), The Prokaryotes, 2nd edition. Springer-Verlag, New York.

19. Hubley, J. H., A. W. Thomson, and J. F. Wilkinson. 1975. Specific inhibitors of methane oxidation in *Methylosinus trichosporium.* Arch. Microbiol. **102**:199-202.

20. Hyman, M. R. and D. J. Arp. 1992. $^{14}C_2H_2$- and $^{14}CO_2$-labelling studies of the *de novo* synthesis of polypeptides by *Nitrosomonas europaea* during recovery from acetylene and light inactivation of ammonia monooxygenase. J. Biol. Chem. **267**:1534-1545.

21. Koh, S-C., J. P. Bowman, and G. S. Sayler. 1993. Soluble methane monooxygenase production and trichloroethylene degradation by a type I methanotroph, *Methylomonas methanica* 68-1. Appl. Environ. Microbiol. **59**:960-967.

22. Lidstrom, M.E. and A.E. Wopat. 1984. Plasmids in methanotrophic bacteria: isolation, characterization and DNA hybridization analysis. Arch. Microbiol. **140**:27-33.

23. Lidstrom, M. E. 1988. Isolation and characterization of marine methanotrophs. Antonie van Leeuwenhoek **54**:189-199.

24. Lidstrom, M. E. and J. Semrau. 1993. Metals and microbiology: the influence of copper on methane oxidation. *In* Advances in Chemistry: Aquatic Chemistry, C.P. Huang, Ed., American Chemical Society, Washington, D.C., pp. 123-130.

25. Marmur, J. 1961. A procedure for the isolation of deoxyribonucleic acid form micro-organisms. J. Mol. Biol. **3**:208-218.

26. McTavish, H., J. A. Fuchs, and A. B. Hooper. 1993. Sequence of the gene coding for ammonia monooxygenase in *Nitrosomonas europaea*. J. Bacteriol. **175**:2436-2444.

27. Meinkoth, J. and G. Wahl. 1984. Hybridization of nucleic acids immobilized on solid supports. Anal. Biochem. **138**:267-284.

28. Morgan, P., and R. J. Watkinson. 1989. Microbiological methods for the cleanup of soil and groundwater contaminated with halogenated organic compounds. FEMS Microbiol. Rev. **63**:277-300.

29. Murrell, J. C. 1992. Genetics and molecular biology of methanotrophs. FEMS Microbiol. Rev. **88**:233-248.

30. Nakajima, T., H. Uchiyama, O. Yagi, and T. Nakahara. 1992. Purification and properties of a soluble methane monooxygenase from *Methylocystis* sp. M. Biosci. Biotechnol. Biochem. **56**:736-740.

31. Nguyen H-H., A. K. Shiemke, S. J. Jacobs, B. J. Hales, M. E. Lidstrom, and S. I. Chan. 1994. The nature of the copper ions in the membranes containing the particulate methane monooxygenase from *Methylococcus capsulatus* (Bath). J. Biol. Chem. (in press).

32. Oremland, R. S., and C. W. Culbertson. 1992. Importance of methane-oxidizing bacteria in the methane budget as revealed by the use of a specific inhibitor. Nature. **356**:421-423.

33. Pilkington, S. J., and H. Dalton. 1991. Purification and characterisation of the soluble methane monooxygenase from *Methylosinus sporium* 5 demonstrates the highly conserved nature of this enzyme in methanotrophs. FEMS Microbiol. Lett. **78**:103-108.

34. Prior, S. D., and H. Dalton. 1985. Acetylene as a suicide substrate and active site probe for methane monooxygenase from *Methylococcus capsulatus* (Bath). FEMS Microbiol. Lett. **29**:105-109.

35. Prior, S. D., and H. Dalton. 1985. The effect of copper ions on membrane content and methane monooxygenase activity in methanol-grown cells of *Methylococcus capsulatus* (Bath). J. Gen. Microbiol. **131**:155-163.

36. Rosenzweig, A. C, C. A. Frederick, S. J. Lippard, and P. Nordlund. 1993. Crystal structure of a bacterial non-haem iron hydroxylase that catalyses the biological oxidation of methane. Nature. **366**:537-543.

37. Sambrook, J., E. F. Fritsch, and T. Maniatis. 1989. Molecular Cloning: A Laboratory Manual. Cold Spring Harbor Press. Cold Spring, New York.

38. Saunders, S. E. and J. F. Burke. 1990. Rapid isolation of miniprep DNA for double strand sequencing. Nucleic Acids Res. **18**:4948.

39. Smith, D. D. and H. Dalton. 1989. Solubilization of methane monooxygenase from *Methylococcus capsulatus* (Bath). Eur. J. Biochem. **182**:667-671.

40. Stainthorpe, A. C., V. Lees, G. P. C. Salmond, H. Dalton, and J. C. Murrell. 1990. The methane monooxygenase gene cluster of *Methylococcus capsulatus* (Bath). Gene. **91**:27-34.

41. Stainthorpe, A. C., J. C. Murrell, G. P. C. Salmond, H. Dalton, and V. Lees. 1989. Molecular analysis of methane monooxygenase from *Methylococcus capsulatus* (Bath). Arch. Microbiol. **152**:154-159.

42. Stainthorpe, A. C., G. P. C. Salmond, H. Dalton and J. C. Murrell. 1990. Screening of obligate methanotrophs for sMMO genes. FEMS Microbiol. Lett. **70:**211-216.

43. Stanley, S. H., S. D. Prior, D. J. Leak, and H. Dalton. 1983. Copper stress underlies the fundamental change in intracellular location of methane monooxygenase in methane-oxidizing organisms: studies in batch and continuous culture. Biotechnol. Lett. **5**:487-492.

44. Stirling, D. I., and H. Dalton. 1979. The fortuitous oxidation and cometabolism of various carbon compounds by whole-cell suspensions of *Methylococcus capsulatus* (Bath). FEMS Microbiol Lett. **5**:315-318.

45. Thomas, J. M., and C. H. Ward. 1989. In situ biorestoration of organic contaminants in the subsurface. Environ. Sci. Technol. **23**:760-766.

46. Tonge, G. M., D. E. F. Harrison, and I. J. Higgins. 1977. Purification and properties of the methane mono-oxygenase enzyme system from *Methylosinus trichosporium* OB3b. Biochem J. **161**:333-344.

47. Whittenbury, R., K. D. Philips, and J. F. Wilkinson. 1970. Enrichment, isolation and some properties of methane-utilizing bacteria. J. Gen. Microbiol. **61**:205-218.

Chapter 6

Conclusions and Future Work

In this thesis, the ability of methanotrophs to oxidize methane and trichloroethylene (TCE) has been examined at the whole-cell level, with further genetic and biochemical analysis of the particulate methane monooxygenase (pMMO). TCE degradation by methanotrophs expressing the pMMO has been shown here to occur, and for the first time the half-saturation constant, K_S, of the pMMO for TCE has been reported. From these studies, it has been shown that the amount of copper in the growth medium affects both methane and TCE oxidation by methanotrophs from both phylogenetic categories. In general, adding more copper caused the K_S value to decrease, indicating that the affinity of cells expressing the pMMO for methane increased. TCE oxidation by *M. albus* BG8 expressing the pMMO was also measured under varying copper concentrations. In these experiments, the affinity of the pMMO for TCE did not change, but the kinetics of oxidation shifted from hyperbolic kinetics to sigmoidal kinetics as the growth concentration of copper increased.

The role of copper in the pMMO, however, cannot be determined from these whole-cell consumption studies. By correlating activity data on the pMMO to total copper present in the membranes and electron paramagnetic resonance spectra, we have been able to conclude that copper plays a primary role in the active site of the pMMO, with a possible secondary role in controlling the tertiary structure of the pMMO. Providing extra copper in the growth medium may create extra active site(s) that cause the kinetics of methane and TCE oxidation to change at the whole-cell level.

Although copper has been shown to be involved in the active site of the pMMO, the pMMO itself may be expressed by multiple gene copies that have different kinetic

characteristics. To see if this was true, the chromosomal DNA of several methanotrophs was collected and digested with multiple enzymes. A probe based on the putative 45 kDa subunit of the pMMO was then hybridized to the chromosomal digests. For all cases with the exception of *M. parvus* OBBP, two bands were seen, indicating that two gene copies of the pMMO exist. For *M. parvus* OBBP, the probe did not hybridize at all. It is unclear why the gene(s) was not detected with the oligonucleotide probe. It is possible that the gene(s) is sufficiently different from the probe to preclude strong hybridization or that the probe is impeded from hybridizing to the chromosomal DNA in some fashion. To determine if the gene for the 45 kDa subunit is encoded on a plasmid, one plasmid was isolated from M albus BG8. The plasmid was hybridized to the oligonucleotide probe both as circular DNA and as digested DNA. In both cases, no bands were seen, indicating that the gene is not encoded on that plasmid.

From these studies, it is evident that the kinetics of methane and TCE oxidation at the whole-cell level are complicated and it is very difficult to create simple models to describe the oxidation of different substrates because of the effect of varying copper in the growth concentration and the presence of multiple gene copies that may produce proteins with different kinetic characteristics. The study here, however, is the first attempt to understand the mechanism of substrate oxidation by the pMMO at the whole-cell level by examining the genetics and biochemistry of the pMMO. This study is only the beginning in the effort to effectively utilize the pMMO for the degradation of hazardous wastes. In this thesis, the ability of pure cultures of methanotrophs to oxidize single substrates has been examined. It is now necessary to take this information and predict *a priori* the ability

of a pure methanotrophic culture to oxidize multiple substrates simultaneously. These predictions can then be compared to experimental results to see determine what other information is needed to accurately predict biodegradation of TCE. Once this step has been accomplished, artificial mixed cultures with known composition must be made and the ability of these mixed cultures to degrade multiple substrates simultaneously again predicted a priori. Any deviations of the predicted results from actual measurements will reflect competition between different strains for limiting nutrients. This information is vital for effective bioremediation.

In conclusion, bioremediation is a promising alternative for the clean-up of hazardous waste, but a great deal of research is needed. It is necessary to describe what the mechanism of degradation is, the competition between substrates for reducing equivalents and active sites on the enzyme, and competition between strains for limiting nutrients that can affect the rate and extent of biodegradation. Without this information, it will be difficult to predict when bioremediation will be effective and how to optimize biodegradation to decrease both the time and cost of clean-up.

Appendix A

Summary of Methane Consumption Experiments

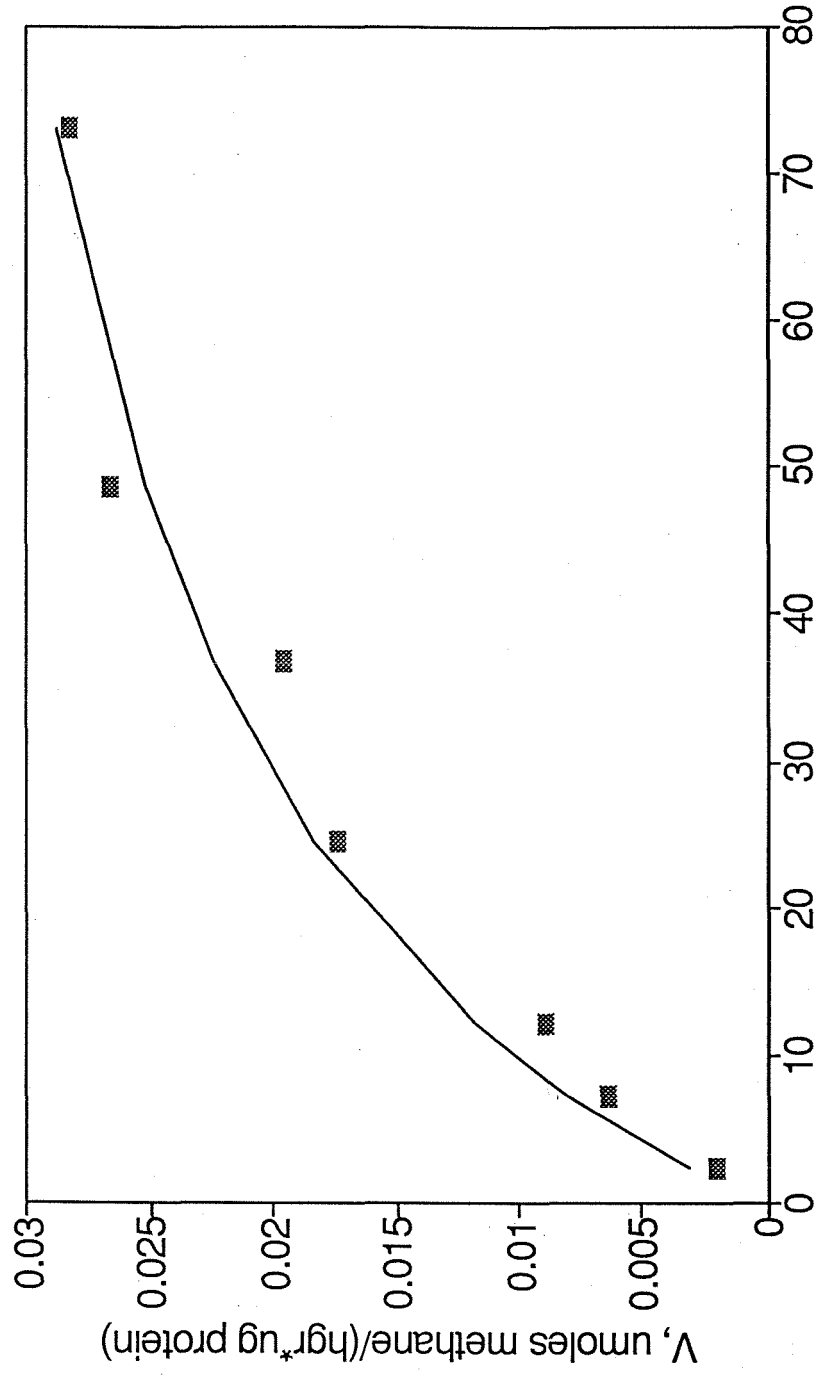

Figure A.1. Methane consumption by *M. albus* BG8 grown with 1 µM copper.

——— = Michaelis-Menten Model; V_{max} = 0.041 µmol methane/(hr•µg protein); K_S = 30 µM CH_4

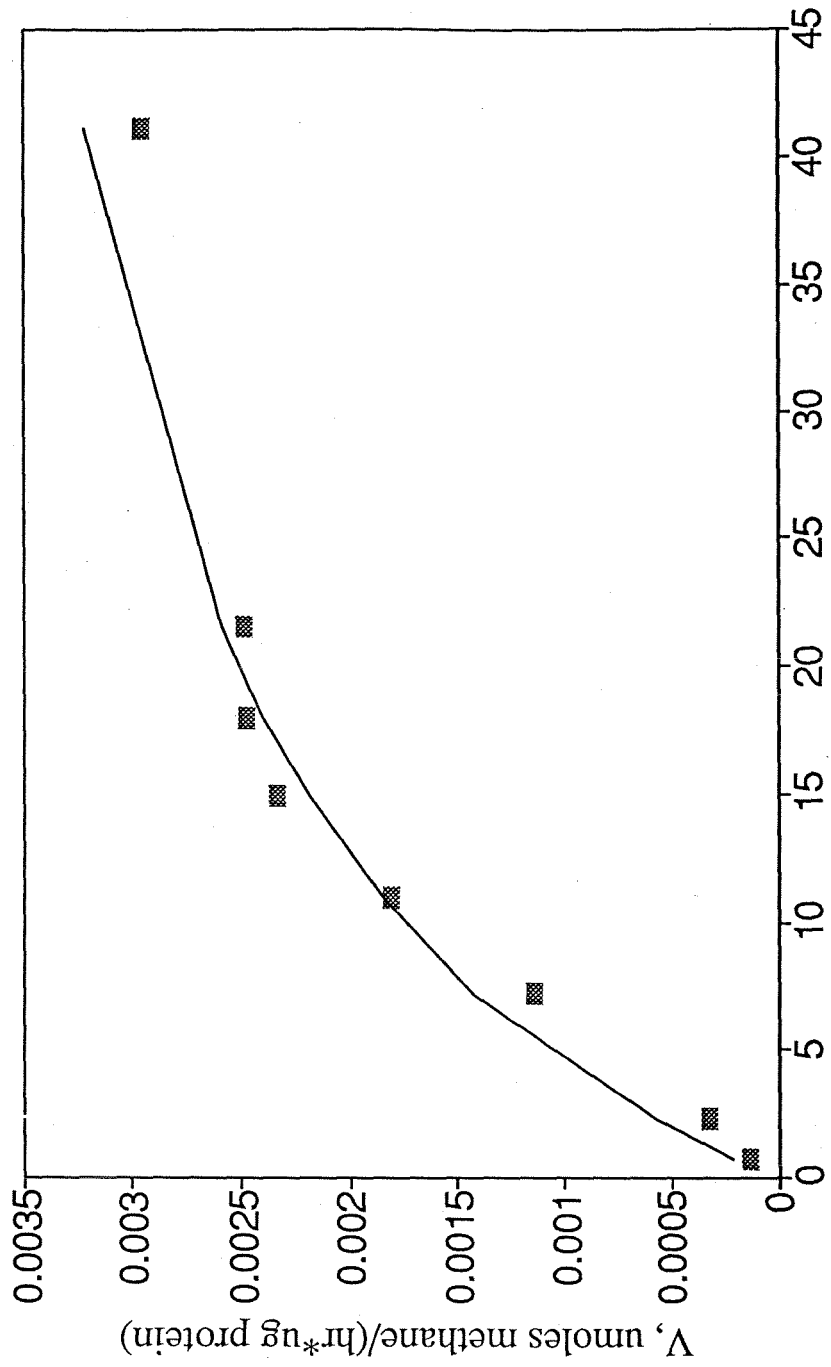

Figure A.2. Methane consumption by *M. albus* BG8 grown with 5 µM copper.

——— = Michaelis-Menten Model; V_{max} = 0.040 µmol methane/(hr•µg protein); K_S = 15 µM CH_4

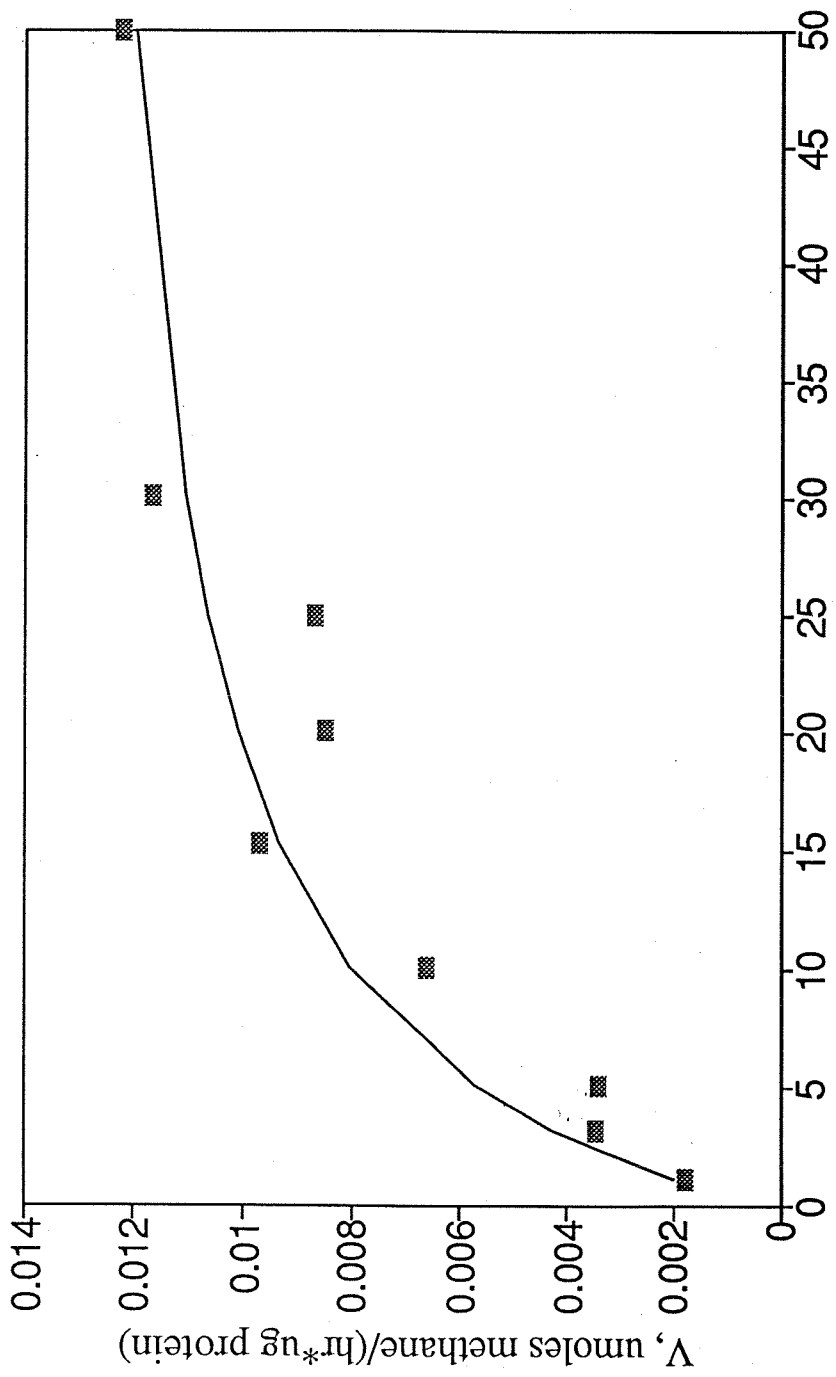

Figure A.3. Methane consumption by *M. albus* BG8 grown with 10 µM copper.

——— = Michaelis-Menten Model; V_{max} = 0.014 µmol methane/(hr•µg protein); K_S = 7 µM CH_4

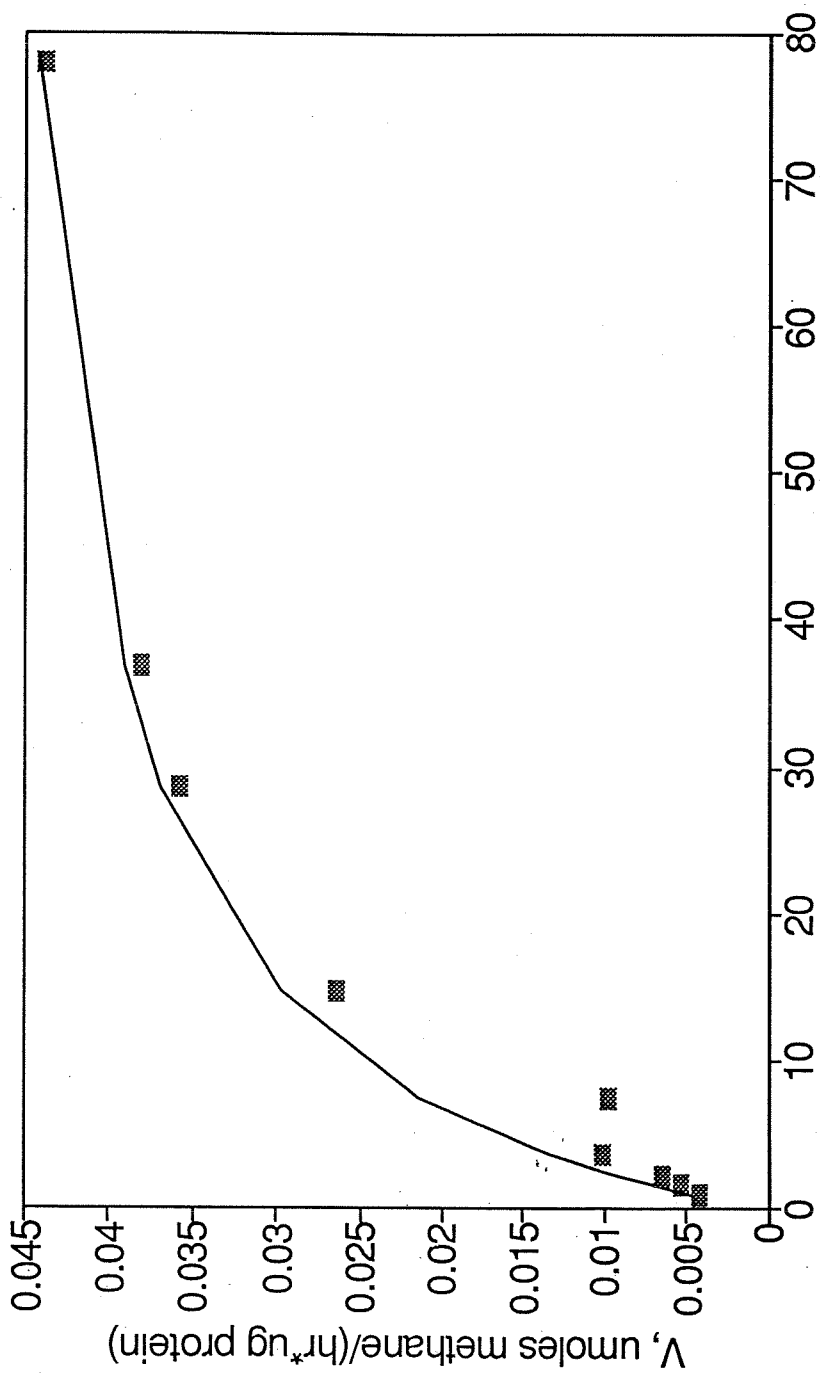

Figure A.4. Methane consumption by *M. albus* BG8 grown with 20 µM copper.

——— = Michaelis-Menten Model; V_{max} = 0.050 µmol methane/(hr•µg protein); K_S = 10 µM CH_4

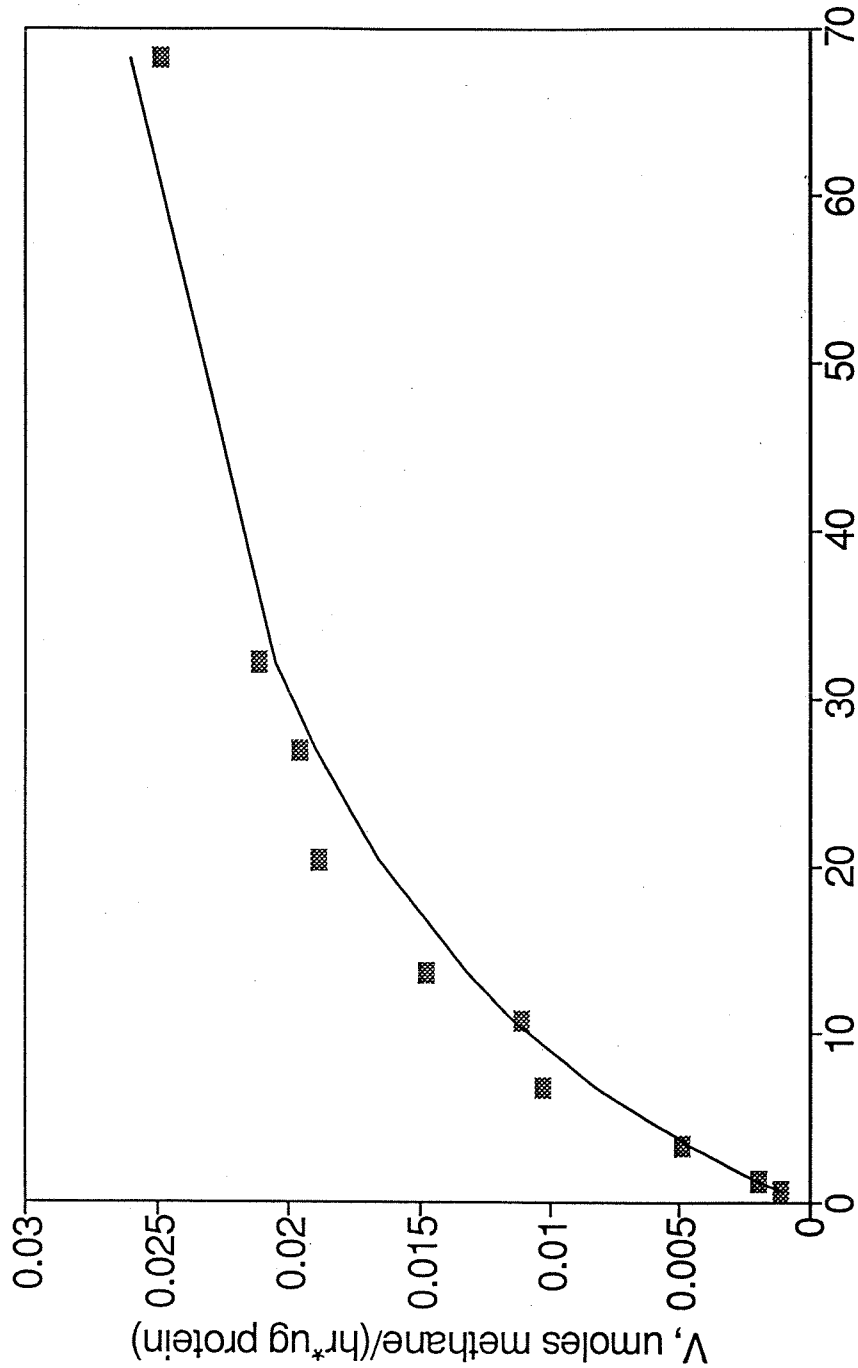

Figure A.5. Methane consumption by *M. trichosporium* OB3b grown with 2.5 µM copper.

——— = Michaelis-Menten Model; V_{max} = 0.035 µmol methane/(hr•µg protein); K_S = 22 µM CH_4

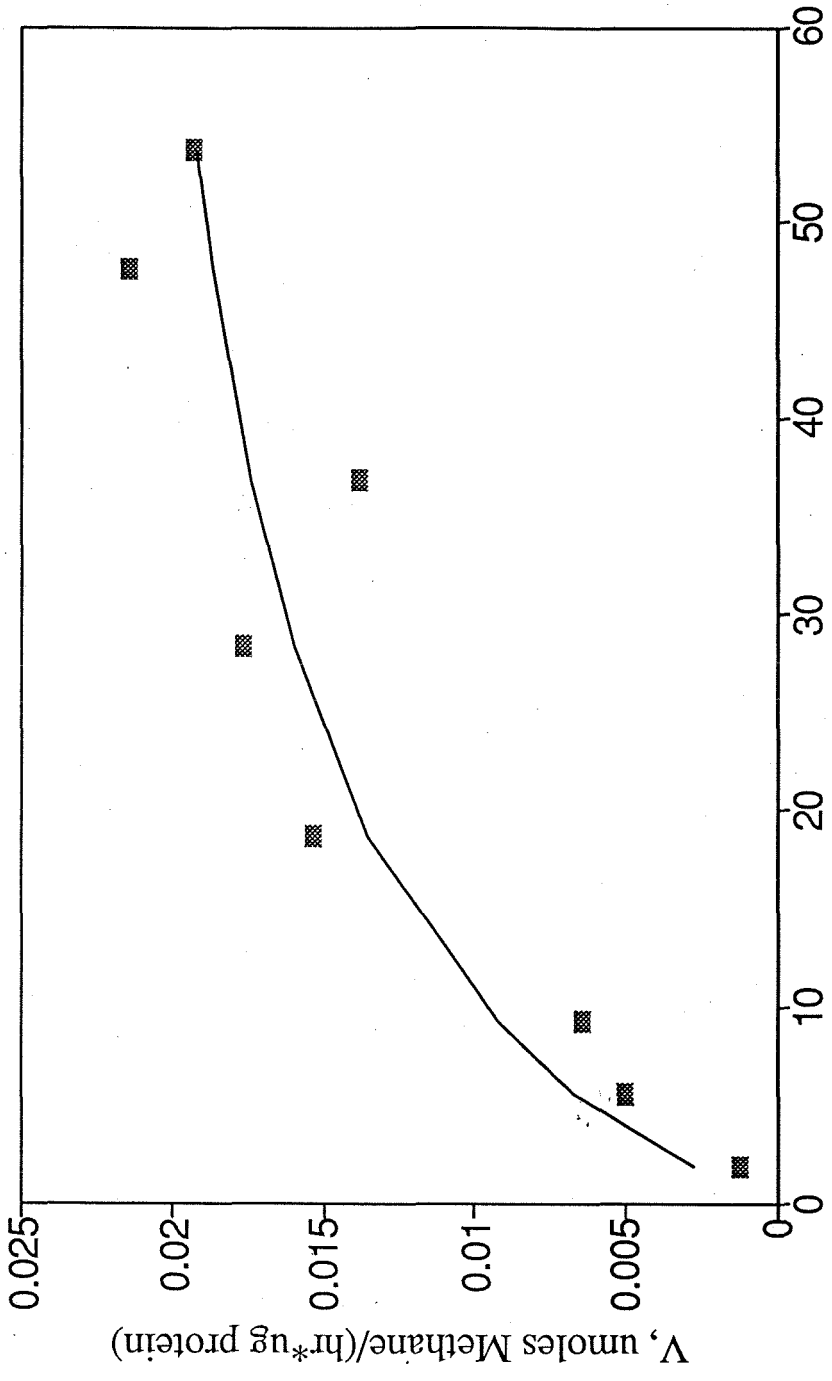

Figure A.6. Methane consumption by *M. trichosporium* OB3b grown with 5 µM copper.

——— = Michaelis-Menten Model; V_{max} = 0.025 µmol methane/(hr•µg protein); K_S = 18 µM CH_4

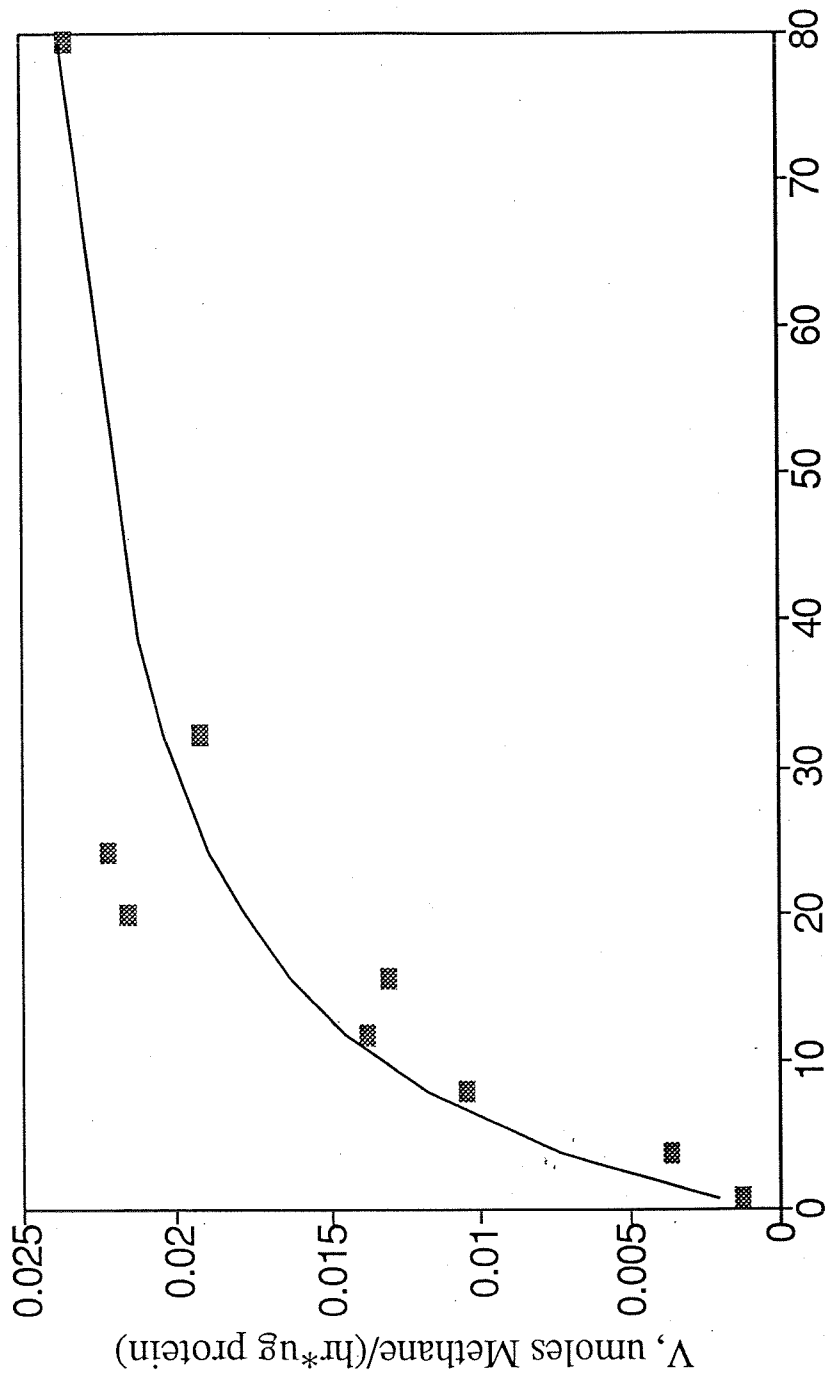

Figure A.7. Methane consumption by *M. trichosporium* OB3b grown with 10 μM copper.

——— = Michaelis-Menten Model; V_{max} = 0.027 μmol methane/(hr•μg protein); K_S = 10 μM CH_4

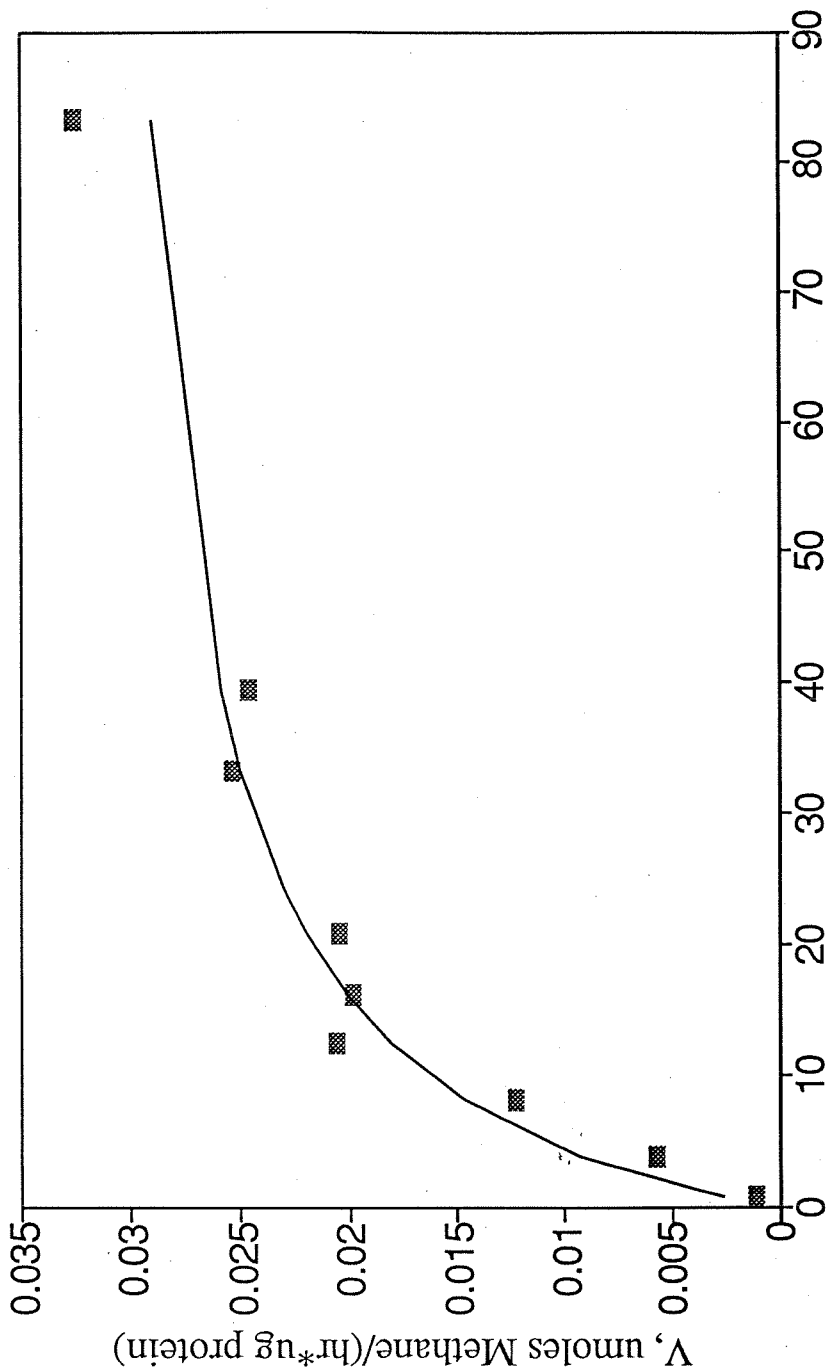

Figure A.8. Methane consumption by *M. trichosporium* OB3b grown with 20 μM copper.

——— = Michaelis-Menten Model; V_{max} = 0.036 μmol methane/(hr•μg protein); K_h = 8 μM CH_4

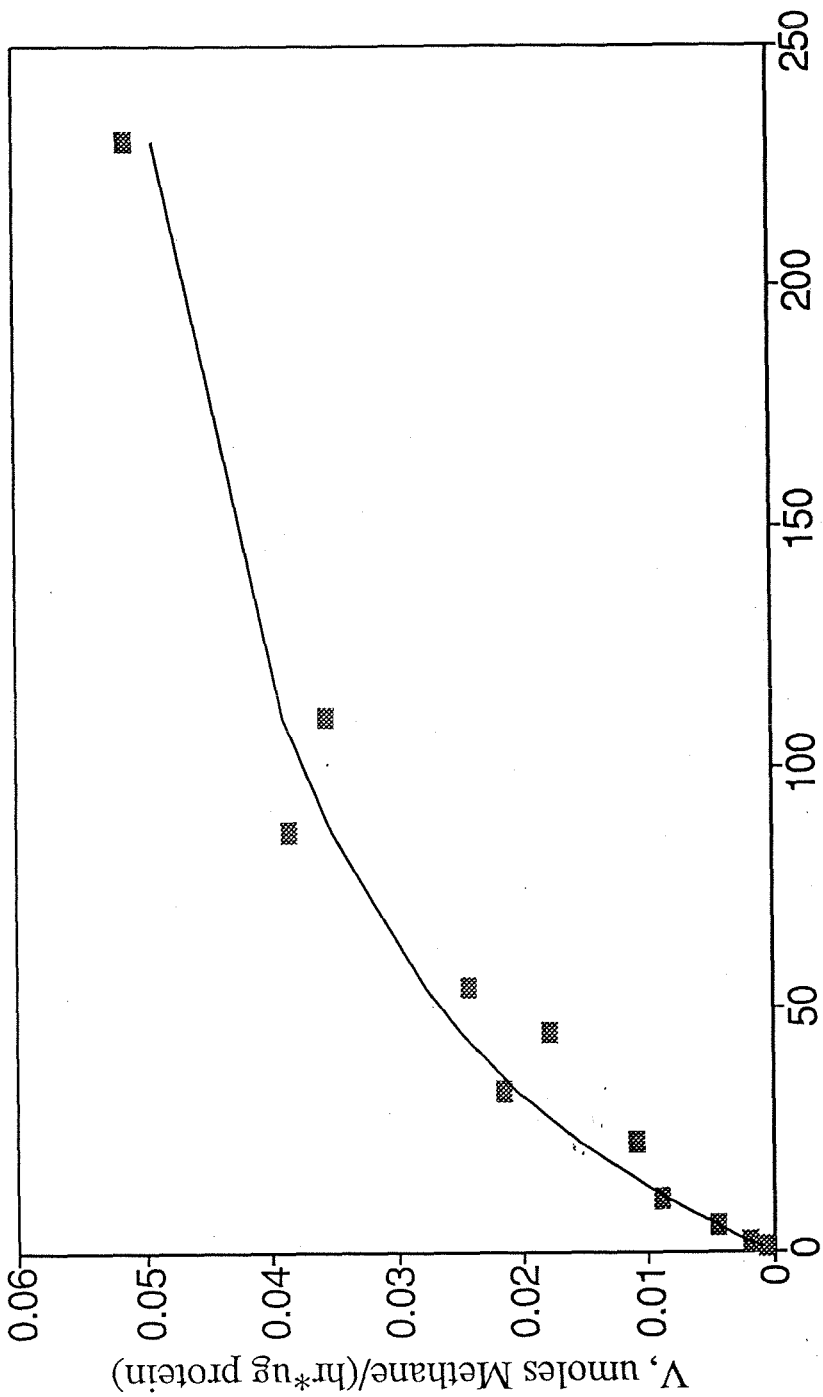

Figure A.9. Methane consumption by *M. parvus* OBBP grown with 1 μM copper.

——— = Michaelis-Menten Model; V_{max} = 0.065 μmol methane/(hr•μg protein); K_h = 75 (μM CH_4)^n

n= 1.0

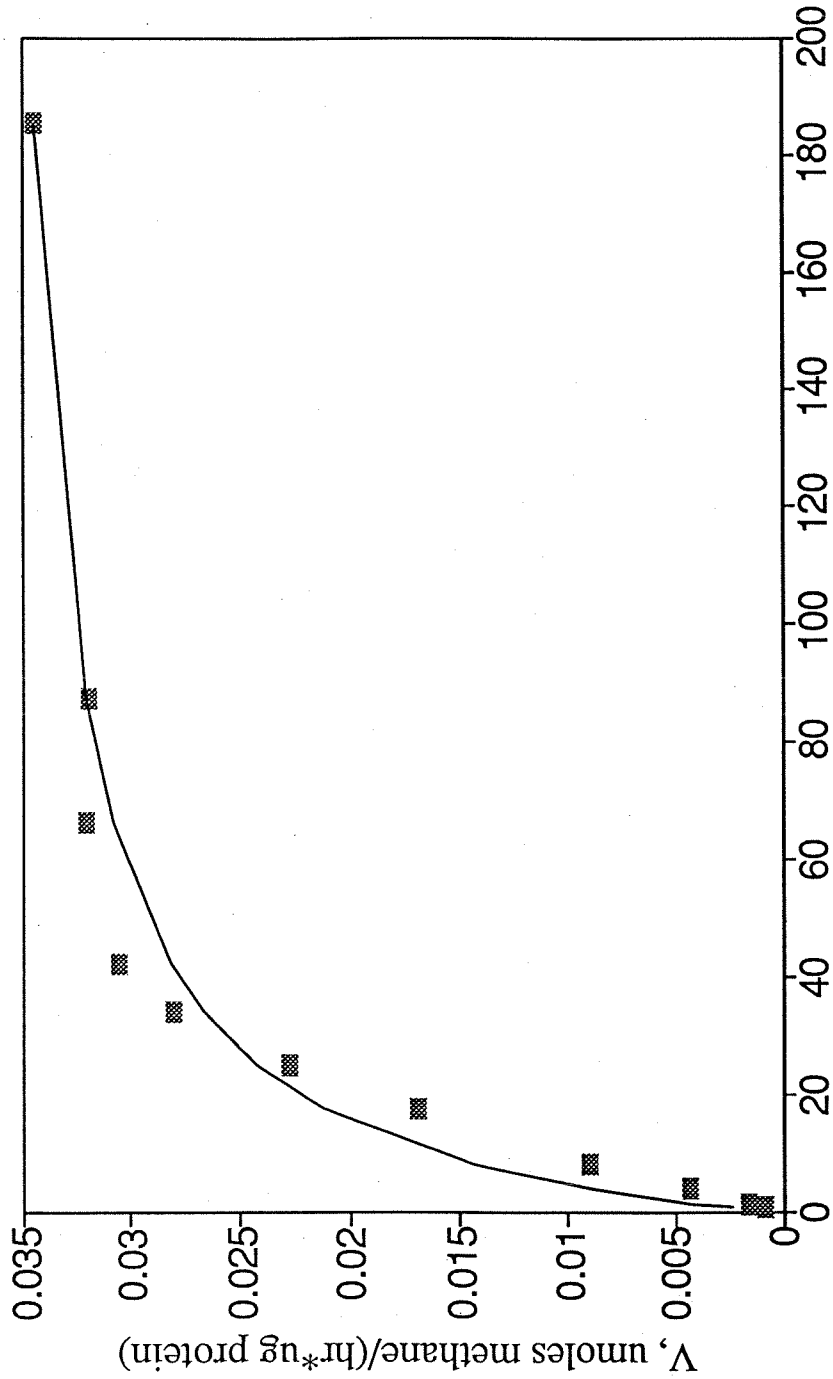

Figure A.10. Methane consumption by *M. parvus* OBBP grown with 5 µM copper.

——— = Michaelis-Menten Model; V_{max} = 0.037 µmol methane/(hr•µg protein); K_h = 13 (µM CH_4)^n

n = 1.3

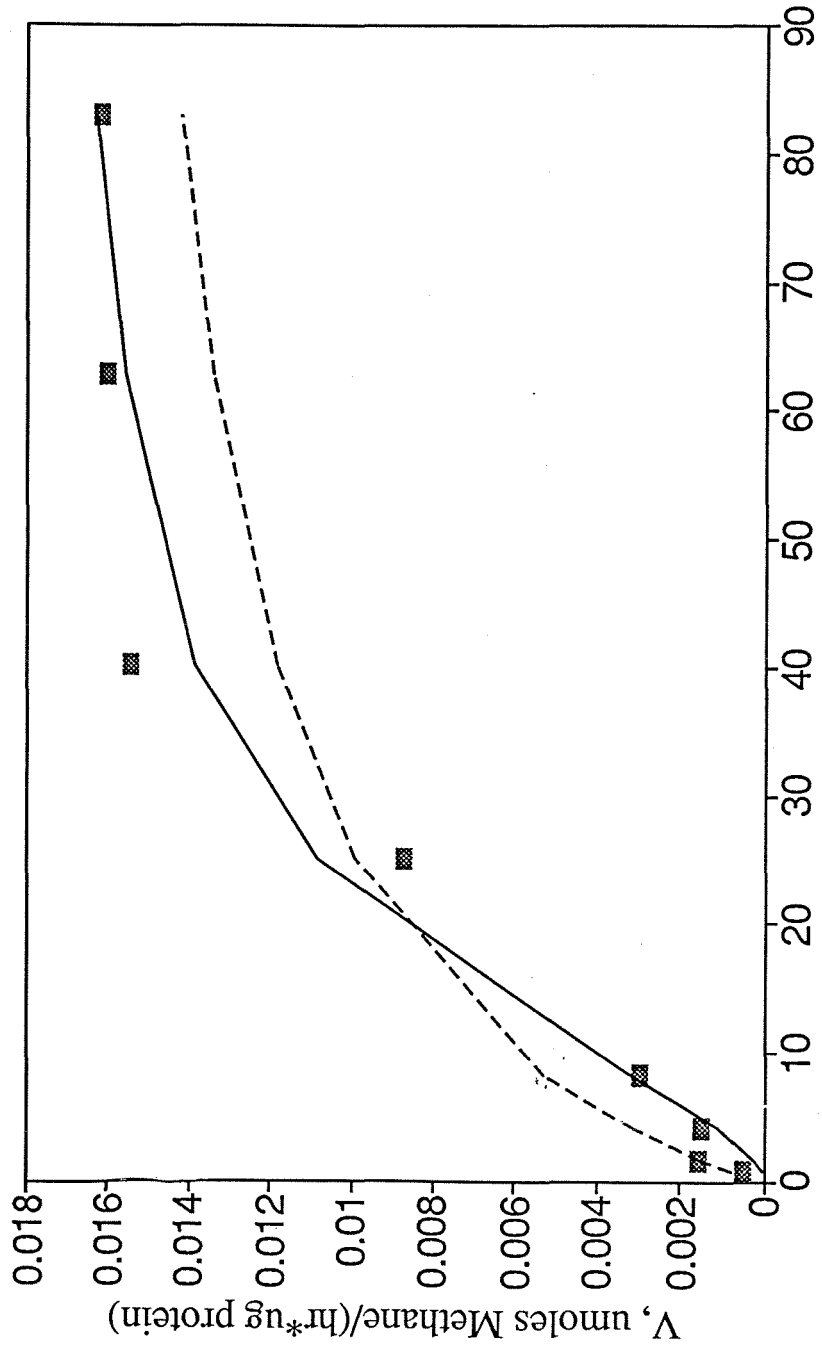

Figure A.11. Methane consumption by *M. parvus* OBBP grown with 10 µM copper.

----- = Michaelis-Menten Model; ——— = Hill Model; V_{max} = 0.017 µmol methane/(hr•µg protein);

K_h = 200 (µM CH_4)^n; n = 1.8

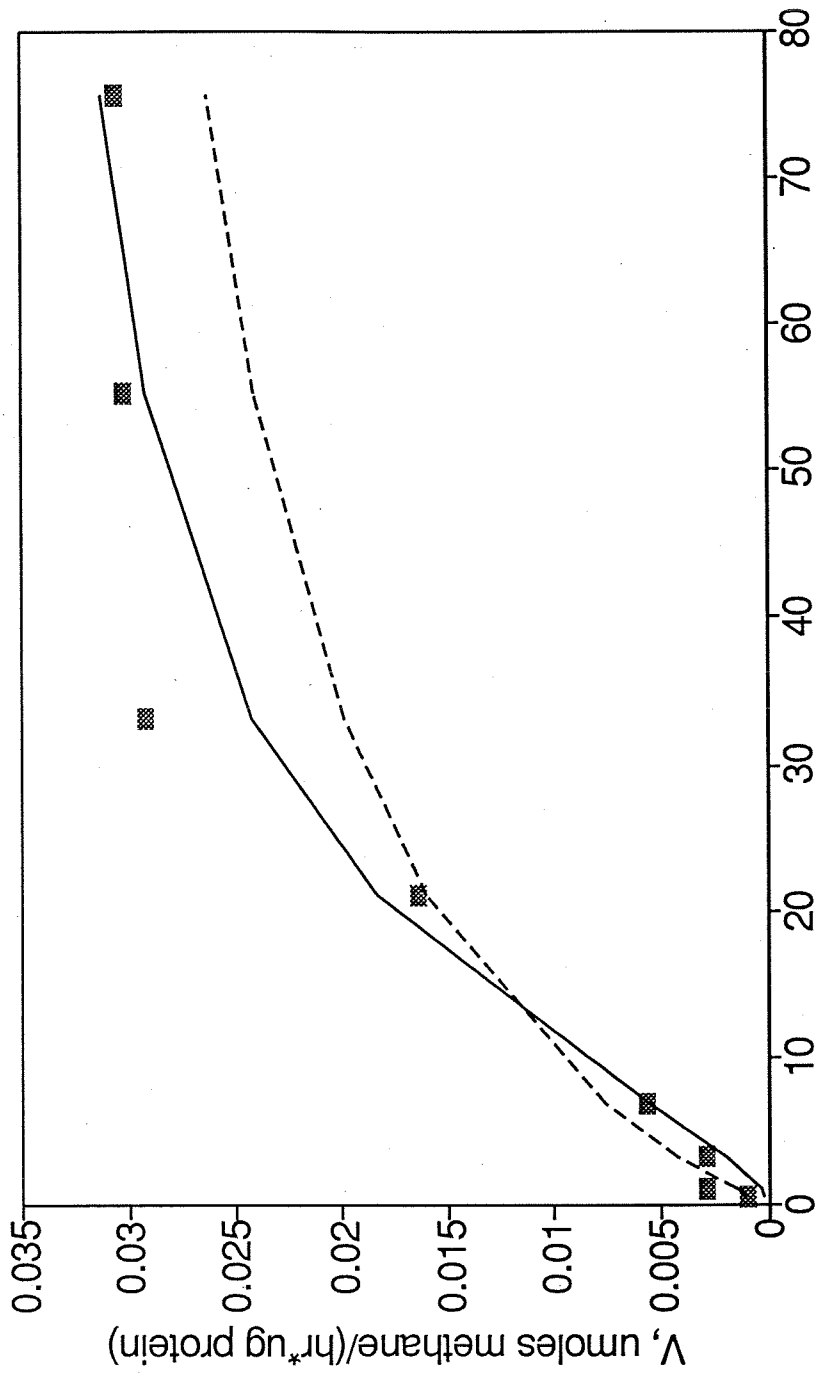

Figure A.12. Methane consumption by *M. parvus* OBBP grown with 20 μM copper.

------ = Michaelis-Menten Model; ——— = Hill Model; V_{max} = 0.035 μmol methane/(hr•μg protein);

K_h = 120 (μM CH_4)^n; n = 1.8

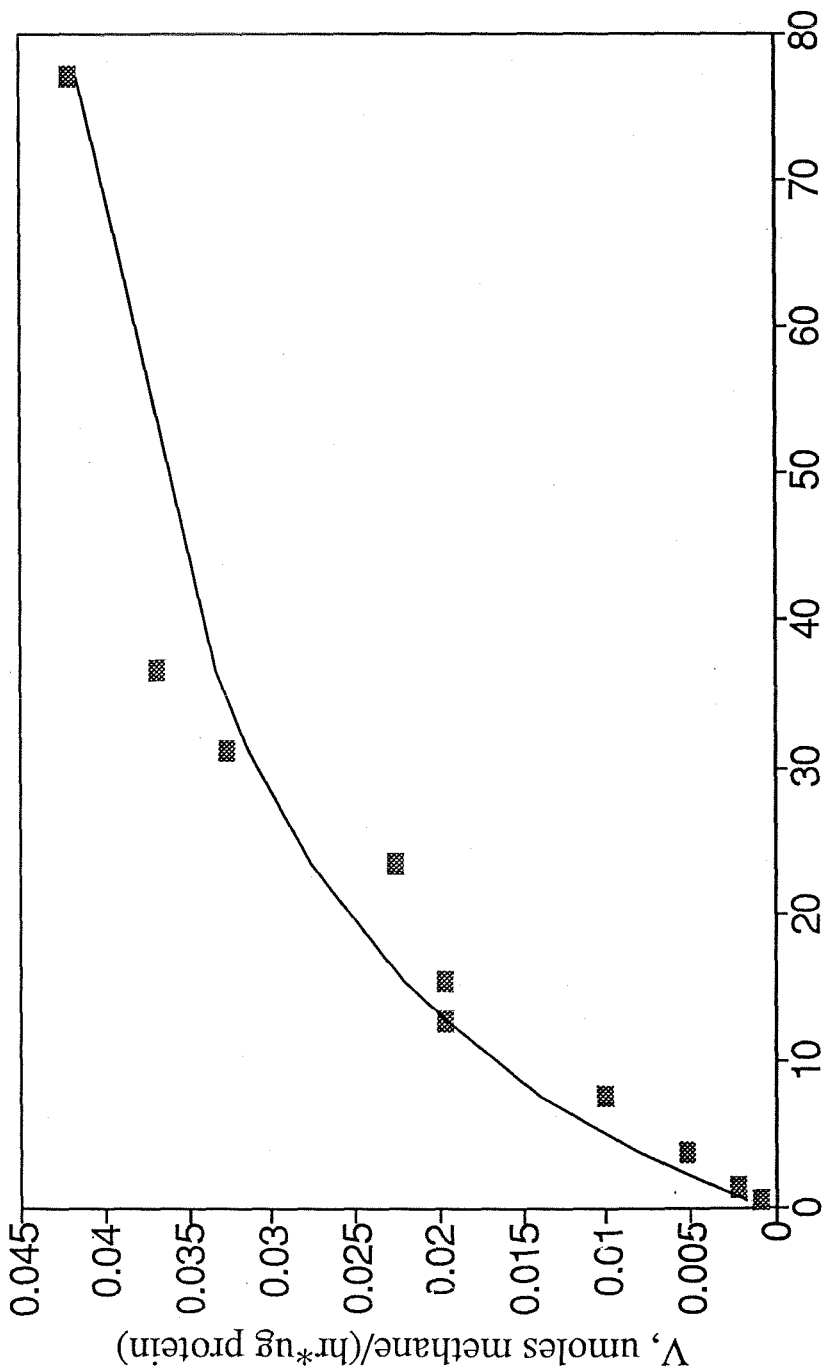

Figure A.13. Methane consumption by *M. capsulatus* Bath grown with 2.5 µM copper.

——— = Michaelis-Menten Model; V_{max} = 0.050 µmol methane/(hr•µg protein); K_h = 22 (µM CH_4)^n

n= 1.2

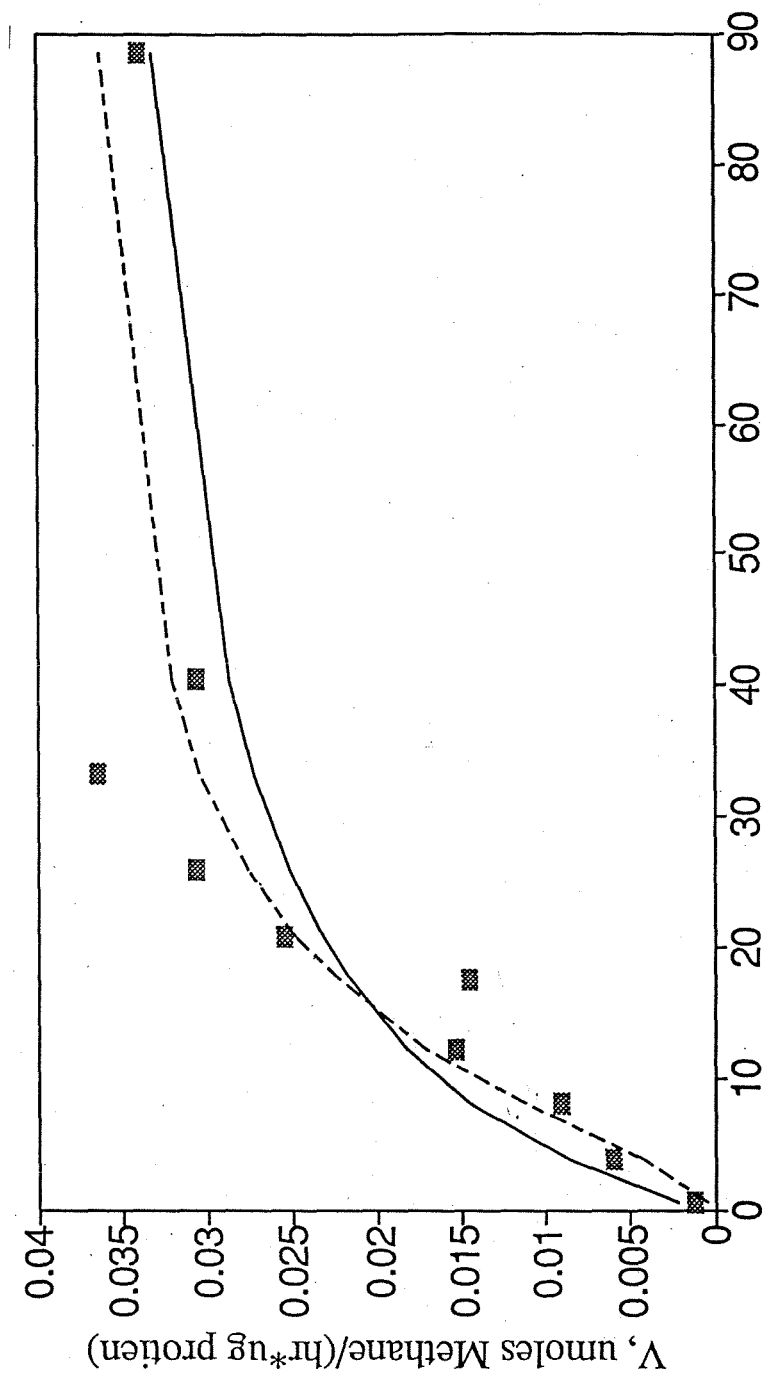

Figure A.14. Methane consumption by *M. capsulatus* Bath grown with 5 μM copper.

——— = Michaelis-Menten Model; ----- = Hill Model; V_{max} = 0.038 μmol methane/(hr•μg protein);

K_h = 70 (μM CH_4)^n; n = 2.0

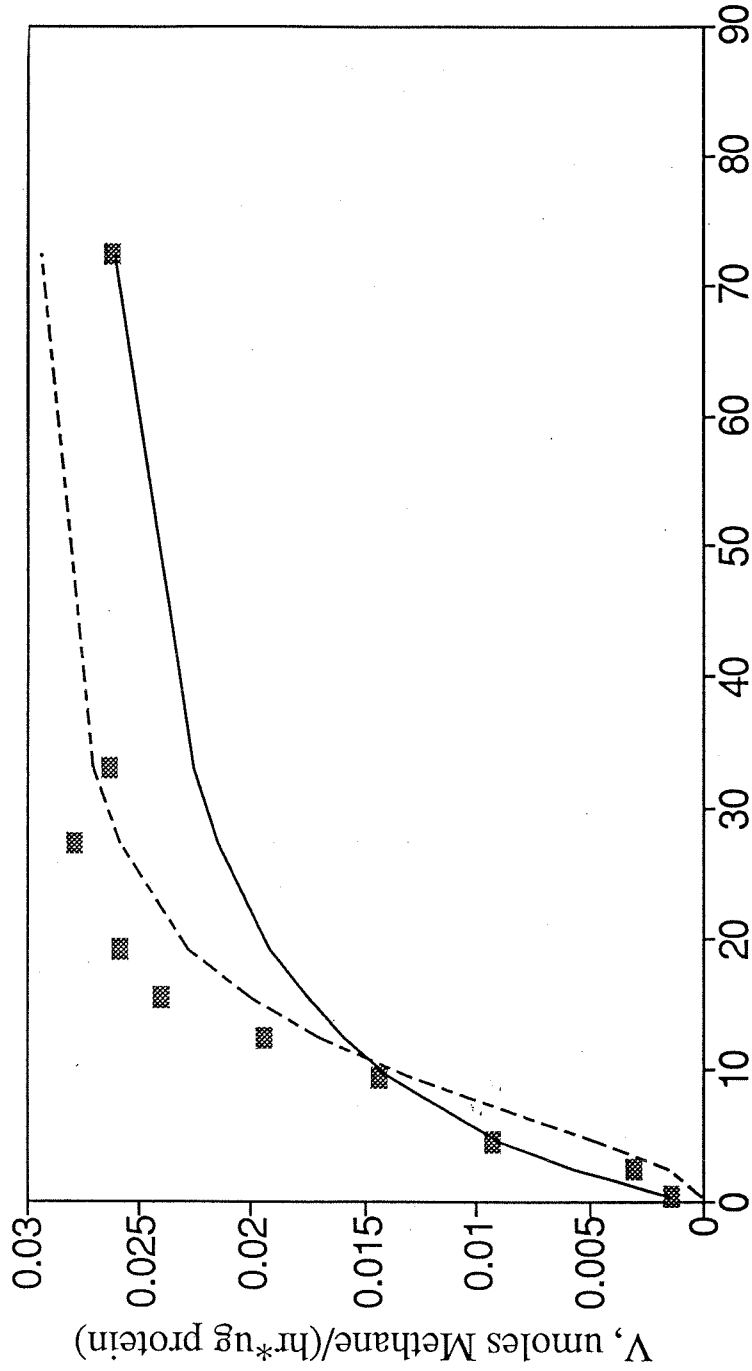

Figure A.15. Methane consumption by *M. capsulatus* Bath grown with 10 µM copper.

——— = Michaelis-Menten Model; ------ = Hill Model; V_{max} = 0.030 µmol methane/(hr•µg protein);

K_h = 120 (µM CH_4)^n; n = 1.9

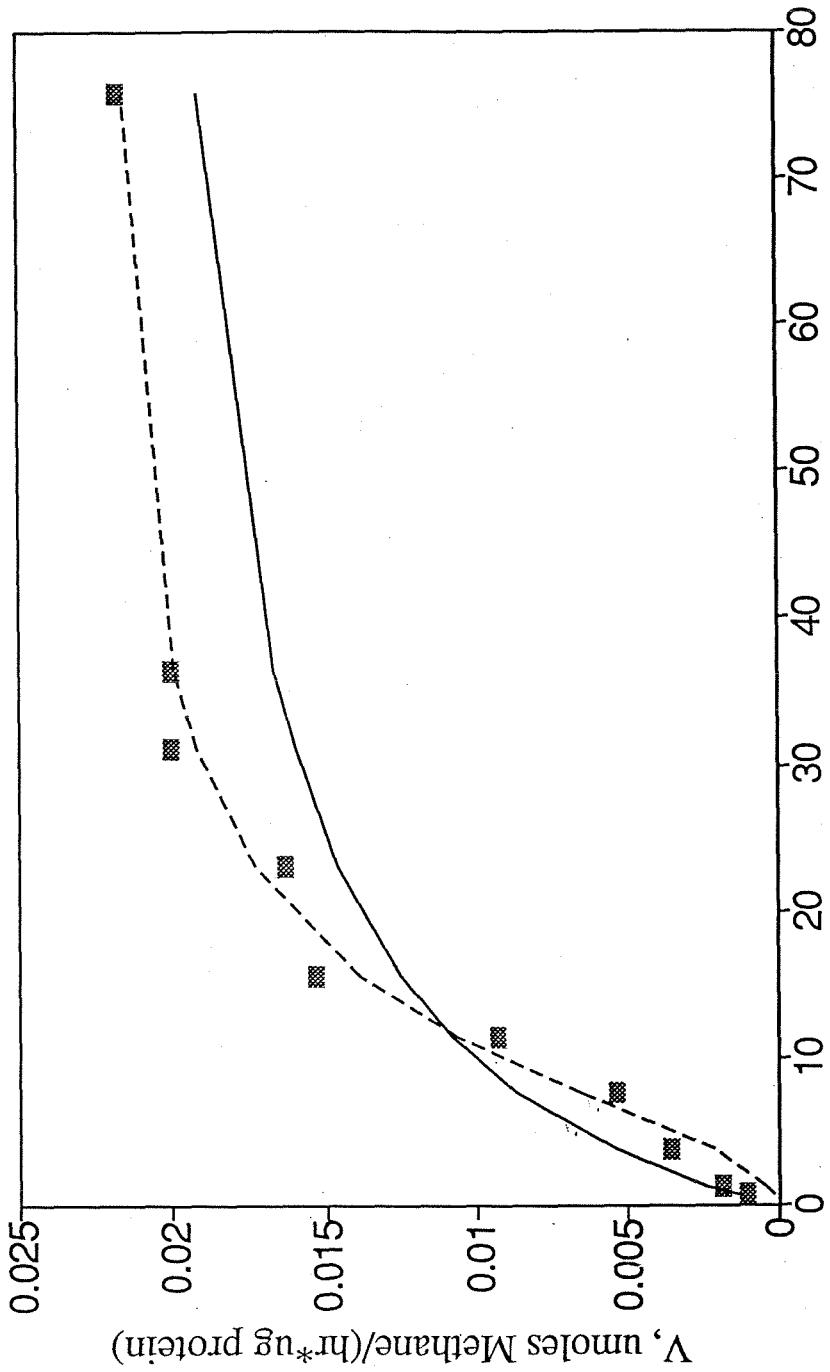

Figure A.16. Methane consumption by *M. capsulatus* Bath grown with 20 µM copper.

——— = Michaelis-Menten Model; ----- = Hill Model; V_{max} = 0.022 µmol methane/(hr•µg protein);

K_h = 130 (µM CH_4)^n; n = 2.1

Appendix B

Summary of Hybridization Results

Table B.1. Summary of Chromosomal DNA hybridization results

		AC10 (kb)	*amoA* (kb)	
Methylomonas albus BG8:	*Hin*dIII -	9.5	*Pst*I -	6.0
		4.0		3.3
	*Bst*YI -	2.6		
		1.6		
	*Eco*RI -	4.7		
		2.1		
Methylomonas MN (Menomenee):	*Hin*dIII -	14	*Pst*I -	3.3
		2.6		
	*Bst*YI -	7.8		
		3.7		
	*Eco*RI -	4.4		
		3.6		
Methylomonas MM2 -	*Hin*dIII -	2.4	*Pst*I -	3.6
	*Bst*YI -	2.5		
Methylobacter marinus A45 -	*Hin*dIII -	5.9		
	*Bst*YI -	3.6		
Methylococcus capsulatus Bath:	*Pst*I -	2.2	*Pst*I -	4.7
		0.9		2.7
	*Bam*HI -	23	*Bam*HI	11
		11		6.0
	*Sal*I -	1.2	*Sal*I	4.7
		0.9		1.7
	*Hin*dIII -	~25	*Hin*dIII	~25
		12		
	*Eco*RI -	8.0	*Eco*RI	5.3
		5.0		4.2
Methylocystis parvus OBBP: No bands detected with *Bam*HI, *Pst*I, *Bst*YI, and (*Bgl*II + *Bcl*I).			*Pst*I -	10
				2.5
Methylosinus trichosporium OB3b:	*Pst*I -	3.4	*Pst*I - 2	
		2.1	*Eco*RI -	11